NAA-SR-9033

COPY

BOILING DEPRESSURIZATION TRANSIENTS

AEC Research and Development Report

ATOMICS INTERNATIONAL

A DIVISION OF NORTH AMERICAN AVIATION, INC.

Price $2.00
Available from the Office of Technical Services
Department of Commerce
Washington 25, D. C.

NAA-SR-9033
REACTOR TECHNOLOGY
88 PAGES

BOILING DEPRESSURIZATION TRANSIENTS

By
F.J. HALFEN
F. BERGANZOLI

ATOMICS INTERNATIONAL

A DIVISION OF NORTH AMERICAN AVIATION, INC.
P.O. BOX 309 CANOGA PARK, CALIFORNIA

CONTRACT: AT(11-1)-GEN-8
ISSUED: AUG 1 1964

DISTRIBUTION

This report has been distributed according to the category "Reactor Technology" as given in "Standard Distribution Lists for Unclassified Scientific and Technical Reports" TID-4500 (29th Ed.), April 1, 1964. A total of 726 copies was printed.

ACKNOWLEDGMENT

The authors would like to thank W. H. Wickes and A. F. Lillie who conducted the experimental program and A. A. Jarrett who provided invaluable assistance and guidance during the program.

CONTENTS

TABLES

FIGURES

ABSTRACT

An analytical and experimental effort toward a better understanding of the mechanisms involved in nuclear power reactor loss-of-pressure accidents is presented. A simplified analytical model which can be used to describe the transient hydraulic and heat transfer behavior of organic-cooled reactors during depressurization accidents resulting in bulk boiling of the coolant has been developed as part of this effort. Correlations of void fraction and heat transfer and dynamic equations for the flow system are incorporated into this model. Predictions of the hydraulic and heat transfer behavior were verified experimentally to establish the applicability of the model and equations involved over the range of variables listed below.

RANGE OF EXPERIMENTAL VERIFICATION

Heat flux (Btu/hr-ft^2)	40,000 to 100,000
Inlet temperature (°F)	600 to 670
Initial outlet temperature* (°F)	705 to 780
Rate of depressurization at beginning of bulk boiling† (psi/sec)	0.05 to 2.5
Mass velocity at beginning of transients (lb/sec-ft^2)	260 to 460
Mass velocity when transients were ended (lb/sec-ft^2)	0 to 230
Direction of flow	Up and Down

*The saturation temperature of the coolant at atmospheric pressure is approximately 700 °F.

†Corresponds to flashing rate of 0.1 to 6% quality/sec.

This report contains many experimental and predicted transients plotted for direct comparison. The experimental and predicted transients are substantially in agreement. This confirms the applicability of the model and equations for prediction of the hydraulic and heat transfer effects of bulk boiling depressurization transients.

I. INTRODUCTION

An area of concern in power reactor operation is the danger of restricting the reactor coolant flow below acceptable levels. Inadequate cooling of the reactor core can lead to fuel element destruction and the subsequent potential hazard associated with release of fission products. Inadequate cooling may occur in pressurized reactors during a loss-of-pressure accident that causes bulk boiling of the coolant. When such boiling occurs in a reactor channel, the accompanying increased flow resistance in that channel causes the flow rate to decrease. This results in increased boiling which causes a further reduction in flow rate and may lead to flow-choking.

The aim of the Pressure Transients and Flow Stability Project [1] (part of the Atomics International Reactor Safety Program conducted for the USAEC) was to develop, by analytical means and with necessary experimental support, reliable models which can be used to describe the transient behavior of organic cooled reactors during depressurization accidents resulting in bulk boiling of the coolant.

In the existing organic cooled reactor, the Piqua Nuclear Power Facility, the coolant outlet temperature is substantially below the saturation temperature at atmospheric pressure. It would require a minimum of three simultaneous failures (loss of flow, loss of pressure, and protective system failure) before bulk boiling of the coolant could occur in this reactor. Simultaneous failure of more than two independent systems is extremely unlikely and is considered "incredible" in most safeguards reports. In the past few years, the trend in the advancing organic cooled reactor program has been to continue to increase the coolant temperature. In the last few organic cooled reactors proposed for the United States, POPR and OPHIR, the reactor coolant outlet temperature was approximately equal to the saturation temperature of the coolant at atmospheric pressure. Because of this trend, it has become necessary to establish reliable analytical models for use in advanced organic-cooled reactor accident analyses for prediction of the effects of depressurization accidents.[4]

Closely interrelated with an adequate evaluation of the loss-of-pressure accident is the ability to predict the transient vapor volume fraction (void fraction) in the coolant during transient boiling. To the extent to which this has been accomplished, this work may be of use in predicting void reactivity effects during reactor boiling transients although this was not among objectives of this project.

Specifically, this report presents an analytical model suitable for prediction of the hydraulic and heat transfer effects of reactor loss-of-pressure accidents resulting in bulk boiling of the coolant. The hydraulic and heat transfer effects of vapor formation were measured in an experimental apparatus, the Flow Stability Loop[3], under upflow and downflow conditions with two parallel channels connected to inlet and outlet plenums. The analytical model (a set of equations) is described and the results compared with those of the measured transients. Hence, the objective of this report is to demonstrate the reliability of the model presented.

II. GENERAL EQUATIONS

This section contains a discussion of the general differential equations necessary to describe the dynamic behavior of a fluid flowing in a heated channel.[6] These equations also apply to the behavior of a boiling fluid flowing in a heated channel during depressurization. In Sections III and IV, these equations are to be applied to the prediction of the transient behavior of an organic-coolant flowing in an apparatus (the Flow Stability Loop[3]) during depressurization transients resulting in bulk boiling.

The general equations are as follows:*

a) Conservation of Mass

$$\frac{\partial G}{\partial L} + \frac{\partial \rho}{\partial t} = 0$$

b) Conservation of Momentum

$$\frac{\partial G}{\partial t} + \frac{\partial}{\partial L}\left(\frac{G^2}{\rho}\right) = - g\rho \frac{dz}{dL} - \frac{fG^2}{2\rho D} - g\frac{\partial P}{\partial L}$$

c) Heat Balances

1) Channel

$$(MC)_w \frac{\partial T_w}{\partial t} = Q_{in} - hA\,(T_w - T_c)$$

2) Coolant

$$(MC)_c \frac{\partial T_c}{\partial t} + M_c h_{fg} \frac{\partial x}{\partial t} = hA\,(T_w - T_c) - GA_f C_c \frac{\partial T_c}{\partial L}\,dL - GA_f h_{fg} \frac{\partial x}{\partial L}\,dL$$

*See foldout of nomenclature, Appendix B.

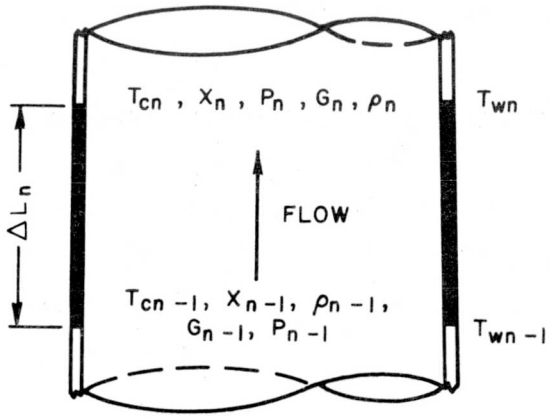

Figure 1. A Typical Section of Heated Channel Showing the Important Variables

The equations apply at each point along the channel of uniform cross sectional area and are applicable to both one- or two-phase flow. Up to this point, no assumption has been made regarding the relative velocity of the two phases or about void volumes in subcooled boiling. These effects can be taken care of separately in the relation between quality, x, and density for bulk boiling conditions, or by some other correlation for subcooled boiling.

Analog computer solution of these equations requires that they be simplified and put into a form suitable for analog programming. A multinode lumped model was chosen (see Figure 1). The simplified dynamic equations for each node are described below.

A. CONSERVATION OF MASS

$$\frac{\partial G}{\partial L} = 0 \text{ or } G_n = G_{n-1} \text{ and } \dot{G}_n = \dot{G}_{n-1} .$$

This approximation assumes that the amount of coolant in any node does not change rapidly, and does not introduce significant errors for the case of moderately slow transients like the experimental transients included in this report (where the time required to empty part of the channel because of void formation is much longer than the coolant transport time through that part of the channel).

For fast transients or transients with very low flow rate (where the time required to empty part of the channel because of void formation is of the same order or shorter than the coolant transport time through that part of the channel), the change in inventory of coolant in the channel with time must be considered. This can be done with the following equations (see Appendix A for derivation):

$$\frac{\partial G}{\partial L} = \frac{(\rho_\ell - SR\rho_v)\rho^2}{SR\rho_\ell \rho_v} \frac{\partial x}{\partial t} .$$

This equation can be approximated for analog simulation by the following expression:

$$G_n - G_{n-1} = \frac{\Delta L_n (\rho_\ell - SR\rho_v)}{SR\rho_\ell \rho_v} \rho_n \rho_{n-1} \dot{x}_n .$$

Since, in the proposed analog model the subscript refers to the outlet conditions for a particular node, n, the value of the density squared over a particular node is approximated by the density at the inlet times the density at the outlet. All the variables on the right side of the above equation are to be made available in subsequent equations. This relation must also provide information regarding the relation of $\dot{G}_n$ to $\dot{G}_{n-1}$ for use in calculating the pressure drop in each node due to a change in momentum of the coolant in that node. The simple relation, $\dot{G}_n = \dot{G}_{n-1} = \dot{G}$, is adequate in most cases. In the cases where the difference in these values is significant, bulk boiling (hence two phase flow) will only be over a small part of the heated channel and the resulting errors should be small.

B. CONSERVATION OF MOMENTUM

$$P_{n-1} - P_n = \frac{\Delta L_n}{g} \dot{G} + \frac{G_n^2}{g}\left(\frac{1}{\rho_n} - \frac{1}{\rho_{n-1}}\right)$$

$$+ \rho_n \Delta L_n - \left(\frac{dP}{dL}\right)_{\ell ss}\left(\frac{\rho_\ell}{\rho_n}\right)\left(\frac{\rho_\ell}{\rho_{n-1}}\right)\left(\frac{G_n}{G_{\ell ss}}\right)^2 \Delta L_n .$$

This is an integrated form of the previous conservation of momentum equation assuming a uniform flow area and upflow. The frictional pressure drop (the 4th term on the right side) was written in a form similar to Equation 28 in the FUGUE report[7]. It is based on the steady state liquid phase pressure drop with correction factors for increased velocity due to decreases in density accompanying partial vaporization of the coolant. Since this equation is written over a finite interval of channel length, and since there is vaporization along the channel, it is necessary to have a factor in this frictional pressure drop term which is representative of the average squared velocity. Study of this

problem has lead to the conclusion that, over short lengths of channel, the average squared velocity is best approximated by the inlet velocity multiplied by the outlet velocity. This product is proportional to the inverse of the product of the inlet and outlet densities. The other important assumption in this equation is that the frictional pressure drop for the two phase mixture is the same as for liquid flowing in the channel at the velocity of the liquid phase in the two phase mixture. This assumption is essentially in agreement with the results of Lockhart and Martinelli.[8]

C. HEAT BALANCES

1. Channel

$$(MC)_{wn} \dot{T}_{wn} = Q_n - hA_n (T_{wn} - T_{cn})$$

2. Coolant

$$\rho_n \Delta L_n \left\{ \left[x_n C_v + (1 - x_n) C_\ell \right] \dot{T}_{cn} + h_{fg} \dot{x}_n \right\} = \frac{hA_n}{A_f} (T_{wn} - T_{cn})$$

$$- h_{fg} G_n (x_n - x_{n-1})$$

$$- G_n \left\{ \left[x_n C_v + (1 - x_n) C_\ell \right] T_{cn} \right.$$

$$\left. - \left[x_{n-1} C_v + (1 - x_{n-1}) C_\ell \right] T_{cn-1} \right\}$$

These equations are solved with the following boundary conditions:

IF	THEN
$T_{cn} < T_{sn}$	$x_n = 0, \quad \dot{x}_n = 0$
$T_{cn} = T_{sn}$	$\dot{T}_{cn} = \dot{T}_{sn}$

The heat balance accounts for stored heat in the channel walls. The heat transfer coefficient, h, is variable. Boiling and nonboiling heat transfer are considered in each node as predicted from previous steady state correlations.[2]

D. PHYSICAL PROPERTIES

Since the physical properties (except the saturation temperature) are considered to be constant in the above equations, it is necessary to choose values that are representative of the average values of the properties during the transients. In most cases, the properties do not change significantly over the range of interest during the transients and can be evaluated at the initial conditions. The vapor density, however, does vary a great deal with pressure. This property was evaluated at a pressure corresponding to the vapor pressure of the coolant at the outlet of the channel.

The coolant saturation temperature, T_s, as a function of pressure can be approximated (over the pressure range of interest in the transient) by an equation of the form:

$$T_{sn} = k + k'P_n - k''/P_n \ .$$

The above equations are written for each node of the channel. The pressure drops are summed and set equal to the pump head as a function of flow. The system pressure drives the transient and is specified as a function of time for a particular point in the coolant loop.

III. UPFLOW TRANSIENT EQUATIONS

The equations written in the previous section of this report were applied to the prediction of the transient behavior of an organic coolant flowing in an apparatus (the Flow Stability Loop[3]) during depressurization transients resulting in bulk boiling of the coolant. The organic reactor coolant, Santowax-R, was used in this apparatus. Bulk boiling only occurs in the test section during the transients. The loop is arranged with a bypass line around the test section so that it is possible to maintain constant flow in the loop during test section transients. Hence, it is not necessary to write conservation of momentum equations for the loop since the momentum of the coolant in the loop does not change.

A three-node model was selected to describe the test section behavior for the upflow transient study. The nodes were chosen starting at the inlet of the channel as follows:

Node	Length (ft)	Heated	Type of Flow
1	10.67	yes	single phase
2	1.33	yes	one or two phase
3	0.67	no	one or two phase

The equations with constants evaluated for Santowax-R and upflow conditions are listed below.

A. CONSERVATION OF MOMENTUM

$$P_{in} - P_1 = 1.06\left(\frac{\dot{W}}{5}\right) + 3.82 + 2.13\left(\frac{W}{5}\right)^2 \qquad \text{(psi)}$$

$$P_1 - P_2 = 0.267\left(\frac{51.6}{\rho_2}\right)\left(\frac{W}{5}\right)^2 + 0.132\left(\frac{\dot{W}}{5}\right) + 0.885\left(\frac{W}{5}\right)^2\left(\frac{51.6}{\rho_2} - 1\right) + 0.00925\rho_2 \qquad \text{(psi)}$$

$$P_2 - P_3 = 0.133\left(\frac{51.6}{\rho_2}\right)\left(\frac{51.6}{\rho_3}\right)\left(\frac{W}{5}\right)^2 + 0.066\left(\frac{\dot{W}}{5}\right) + 0.885\left(\frac{W}{5}\right)^2\left(\frac{51.6}{\rho_3} - \frac{51.6}{\rho_2}\right)$$

$$+ 0.00463\rho_3 \qquad \text{(psi)}$$

These equations are essentially in the same form as those in Section II-B. The units were selected for convenience of scaling in the analog computer mechanization and for ease of comparison with experimental data. In most cases it was convenient to handle the two phase density as the ratio of liquid phase density to two phase density. The liquid phase density is 51.6 lb/ft^3. The mass velocity, G, was normalized with respect to the mass velocity corresponding to a liquid flow rate of 5 gpm through the test section. Hence, the factor (W/5) in these equations corresponds to the fraction of the mass velocity at a liquid flow rate of 5 gpm that exists at any time in the test section.

B. HEAT BALANCES

1. Channel

$$\dot{T}_{w1} = 1.02 \times 10^{-3} \frac{Q}{A} - 3.67\, h(T_{w1} - T_{c1}) \qquad (°F/sec)$$

$$\dot{T}_{w2} = 1.02 \times 10^{-3} \frac{Q}{A} - 3.67\, h(T_{w2} - T_{c2}) \qquad (°F/sec)$$

2. Coolant

$$\dot{T}_{c1} = 3.58\, h(T_{w1} - T_{c1}) - 0.836 \left(\frac{W}{5}\right)(T_{c1} - T_{in}) \qquad (°F/sec)$$

$$\dot{T}_{c2} + 221\dot{x}_2 = \left(\frac{51.6}{\rho_2}\right)\left[3.58h\,(T_{w2} - T_{c2}) - 6.7\left(\frac{W}{5}\right)(T_{c2} - T_{c1}) - 1480\left(\frac{W}{5}\right)x_2\right] \qquad (°F/sec)$$

Boundary Conditions:

IF	THEN
$T_{s2} > T_{c2}$	$x_2 = 0,\ \dot{x}_2 = 0$
$T_{s2} = T_{c2}$	$\dot{T}_{s2} = \dot{T}_{c2}$
$x_2 + 0.00453\,(T_{c2} - T_{s3}) \geq 0$	$x_3 = x_2 + 0.00453\,(T_{c2} - T_{s3})$
$x_2 + 0.00453\,(T_{c2} - T_{s3}) < 0$	$x_3 = 0$

These equations correspond to the equations in Section II-C evaluated for Santowax-R and the test section. The last two boundary conditions above represent the heat balance for the coolant in the 3rd node (the unheated exit end of the test section). The value 0.00453 in the boundary conditions represents the ratio of specific heat to the latent heat of vaporization for Santowax-R.

An additional assumption has been used in arriving at these equations. Since the specific heat of Santowax-R vapor is nearly the same as for the liquid, it was not necessary to have a variable specific heat for the two-phase mixture. The change in stored heat in the unheated part of the channel wall was also neglected during the transient. Neither assumption should have any significant effect on the results of the present study.

C. COOLANT DENSITY

1. Subcooled Boiling Density Ratio

$$\left(\frac{\rho_\ell}{\rho_n}\right)_a = \frac{1 - 0.013\left[\frac{Q}{A} - h_{NB}\,(T_{wn} - T_{cn})\right]}{h_{NB}^2\,(T_{sn} - T_{cn})}$$

2. Density Ratio Near Saturated Boiling

$$\left(\frac{\rho_\ell}{\rho_n}\right)_b \approx \frac{\frac{Q}{A}}{h_{NB}\,(T_{wn} - T_{cn})}$$

Note: $\rho_\ell = 51.6$ lb/A^3

In using the two equations above, the steady state power input, Q/A, was used in calculating the density ratios. This resulted in a slightly better void fraction prediction (the relation between void fraction and density is shown in Appendix A) than would have resulted if the instantaneous heat flux had been used. In the cases tested, the instantaneous heat flux was affected up to about 10% by changes in stored heat within the channel wall. There was some difficulty in predicting wall temperature during depressurization. In this situation, the

variable dissolved gas concentration affects the boiling wall-temperature in a manner which has not been correlated.[2]

3. Bulk Boiling Density Ratio

$$\left(\frac{\rho_\ell}{\rho_n}\right)_C = 1.0 + 54.4 x_n \quad .$$

This equation assumes a slip ratio of 3.0 (the ratio of vapor to liquid velocity in two phase flow). This approximation is in good agreement with experimental data[2] and predictions using the Lockhart-Martinelli method[8] for quality, x, above 3% which is the main area of interest. The pressure at which the vapor density was evaluated was taken to be 20 psia, the approximate pressure during experimental transients.

These density equations were obtained from experimentally verified void fraction correlations[2] for Santowax-R in this pressure range. The following criteria are used to choose the appropriate density equation:

IF	THEN
$\left(\frac{\rho_\ell}{\rho_n}\right)_a < \left(\frac{\rho_\ell}{\rho_n}\right)_b$	$\left(\frac{\rho_\ell}{\rho_n}\right) = \left(\frac{\rho_\ell}{\rho_n}\right)_a$
$\left(\frac{\rho_\ell}{\rho_n}\right)_a > \left(\frac{\rho_\ell}{\rho_n}\right)_b$	$\left(\frac{\rho_\ell}{\rho_n}\right) = \left(\frac{\rho_\ell}{\rho_n}\right)_b$
$\left(\frac{\rho_\ell}{\rho_n}\right)_b > \left(\frac{\rho_\ell}{\rho_n}\right)_C$	$\left(\frac{\rho_\ell}{\rho_n}\right) = \left(\frac{\rho_\ell}{\rho_n}\right)_b$
$\left(\frac{\rho_\ell}{\rho_n}\right)_b < \left(\frac{\rho_\ell}{\rho_n}\right)_C$	$\left(\frac{\rho_\ell}{\rho_n}\right) = \left(\frac{\rho_\ell}{\rho_n}\right)_C$

Note: $\rho_\ell = 51.6$ lb/ft^3

D. HEAT TRANSFER

1. Forced Convection Heat Transfer[3]

$$\left(\frac{Q}{A}\right)_{NB} = h_{NB}\,(T_{wn} - T_{cn}) \approx 0.253\left(\frac{W}{5}\right)(T_{wn} - T_{cn}) \qquad (\text{Btu/sec-ft}^2)$$

2. Nucleate Boiling Heat Transfer[2]

$$\left(\frac{Q}{A}\right)_{B} \approx 9.25 \times 10^{-5}\,(T_{wn} - T_{sn})^3 \qquad (\text{Btu/sec-ft}^2)$$

These heat fluxes are used with the following criteria:

IF	THEN
$\left(\frac{Q}{A}\right)_{NB} > \left(\frac{Q}{A}\right)_{B}$	$\left(\frac{Q}{A}\right) = \left(\frac{Q}{A}\right)_{NB}$
$\left(\frac{Q}{A}\right)_{NB} < \left(\frac{Q}{A}\right)_{B}$	$\left(\frac{Q}{A}\right) = \left(\frac{Q}{A}\right)_{B}$

E. SATURATION TEMPERATURE

$$T_{sn} = 721 + 2.7\,P_n - \frac{1110}{P_n} \qquad (^\circ\text{F})$$

This equation closely approximates the vapor pressure curve for the Santowax-R and isopropyldiphenyl mixture used in the Flow Stability Loop during the upflow pressure transient experiments.

F. TEST SECTION PRESSURE AND PRESSURE DROP

1. Outlet Pressure

$$P_3 = P_{ss} + \Delta P\, e^{-t/\tau} \qquad \text{(psia)}$$

where P_{ss}, ΔP, and τ are chosen to conform to the experimental conditions.

This is an empirical equation which was used to approximate the experimentally measured outlet pressure curves for the transients that were to be duplicated analytically.

2. Test Section Pressure Drop

$$\Delta P_T = (P_{in} - P_1) + (P_1 - P_2) + (P_2 - P_3) = \Delta P_{bp} \qquad \text{(psi)}$$

3. Bypass Line Pressure Drop

a. Fixed Bypass Valve

$$\Delta P_{bp} = C' \left[1 - 2 \left(\frac{W}{W_T} \right) + \left(\frac{W}{W_T} \right)^2 \right] + \Delta P_s \qquad \text{(psi)}$$

where

C' = constant depending on valve position,

W_T = total test section plus bypass flow, and

ΔP_s = static head difference across bypass line = 4.53 psi.

The pressure drop across the bypass line was set equal to a constant times the bypass line flow squared plus the static head difference from inlet to outlet.

b. Controlled Bypass Valve

$$\Delta P_{bp} = \text{constant}$$

For some of the experiments, the bypass valve was controlled to maintain constant pressure drop across the test section (also across the bypass line).

The above equations were solved simultaneously as a function of time for the conditions of the experimental tests on an analog computer at the Atomic International analog computer installation.

IV. DOWNFLOW TRANSIENT EQUATIONS

During the period between the upflow and downflow tests, the experimental flow measuring capability was improved to permit quantitative flow measurement down to 25% of the original flow rate. This, in turn, warranted the use of a more detailed analog model to check the advanced stages of the downflow transients. Two major changes were made in the simulation. First, another boiling node was added, making the model applicable over a slightly longer portion of the transient. Secondly, the prediction of void fraction was improved by using one correlating equation for the entire range of subcooling. If no changes were made in the model, the only changes required in the equations going from upflow to downflow would be to change the sign of the static head terms in the conservation of momentum equations and in the equation for pressure drop in the bypass line.

A four-node model was selected to describe the test section behavior for the downflow transient study. The nodes were chosen starting at the inlet of the channel as follows:

Node	Length (ft)	Heated	Type of Flow
1	8.0	yes	single phase
2	2.67	yes	one or two-phase
3	1.33	yes	one or two-phase
4	0.67	no	one or two-phase

The equations with constants evaluated for Santowax-R and downflow conditions were as follows:

A. CONSERVATION OF MOMENTUM

$$P_{in} - P_1 = 1.60\left(\frac{W}{5}\right)^2 + 0.794\left(\frac{\dot{W}}{5}\right) - 2.86 \qquad \text{(psi)}$$

$$P_1 - P_2 = 0.533\left(\frac{51.6}{\rho_2}\right)\left(\frac{W}{5}\right)^2 + 0.264\left(\frac{\dot{W}}{5}\right) + 0.885\left(\frac{W}{5}\right)^2\left[\left(\frac{51.6}{\rho_2}\right) - 1\right] - 0.0185\rho_2 \qquad \text{(psi)}$$

$$P_2 - P_3 = 0.267\left(\frac{51.6}{\rho_3}\right)\left(\frac{51.6}{\rho_2}\right)\left(\frac{W}{5}\right)^2 + 0.132\left(\frac{\dot{W}}{5}\right)$$

$$+ 0.885\left(\frac{W}{5}\right)^2\left[\left(\frac{51.6}{\rho_3}\right) - \left(\frac{51.6}{\rho_2}\right)\right] - 0.00925\rho_3 \quad \text{(psi)}$$

$$P_3 - P_4 = 0.133\left(\frac{51.6}{\rho_4}\right)\left(\frac{51.6}{\rho_3}\right)\left(\frac{W}{5}\right)^2 + 0.066\left(\frac{\dot{W}}{5}\right)$$

$$+ 0.885\left(\frac{W}{5}\right)^2\left[\left(\frac{51.6}{\rho_4}\right) - \left(\frac{51.6}{\rho_3}\right)\right] - 0.00463\rho_4 \quad \text{(psi)}$$

These equations are essentially of the same form as those in Section II-B. The units were chosen for convenience of scaling in the analog computer mechanization and for ease of comparison with experimental data. In most cases, it was convenient to normalize the two-phase density as the ratio of liquid phase density to two-phase density. The mass velocity, G, was normalized with respect to that mass velocity which corresponds to a liquid flow rate of 5 gpm through the test section. Hence, the factor (W/5) in these equations corresponds to the fraction of the mass velocity at a liquid flow rate of 5 gpm that exists at any time in the test section.

B. HEAT BALANCES

1. Channel

$$\dot{T}_{w1} = 1.02 \times 10^{-3}\frac{Q}{A} - 3.67\, h(T_{w1} - T_{c1}) \quad (^\circ F/sec)$$

$$\dot{T}_{w2} = 1.02 \times 10^{-3}\frac{Q}{A} - 3.67\, h(T_{w2} - T_{c2}) \quad (^\circ F/sec)$$

$$\dot{T}_{w3} = 1.02 \times 10^{-3}\frac{Q}{A} - 3.67\, h(T_{w3} - T_{c3}) \quad (^\circ F/sec)$$

2. Coolant

$$\dot{T}_{c1} = 3.58\, h(T_{w1} - T_{c1}) - 1.113 \left(\frac{W}{5}\right)(T_{c1} - T_{in}) \quad (^{\circ}F/sec)$$

$$\dot{T}_{c2} + 221\, \dot{x}_2 = \left(\frac{51.6}{\rho_2}\right)\Bigg[3.58\, h(T_{w2} - T_{c2}) - 3.33 \left(\frac{W}{5}\right)(T_{c2} - T_{c1}) - 740 \left(\frac{W}{5}\right) x_2\Bigg] \quad (^{\circ}F/sec)$$

$$\dot{T}_{c3} + 221\, \dot{x}_3 = \left(\frac{51.6}{\rho_3}\right)\Bigg[3.58\, h(T_{w3} - T_{c3}) - 6.7 \left(\frac{W}{5}\right)(T_{c3} - T_{c2}) - 1480 \left(\frac{W}{5}\right)(x_3 - x_2)\Bigg] \quad (^{\circ}F/sec)$$

Boundary Conditions:

IF	THEN
$T_{s2} > T_{c2}$	$x_2 = 0,\ \dot{x}_2 = 0$
$T_{s2} = T_{c2}$	$\dot{T}_{s2} = \dot{T}_{c2}$
$T_{s3} > T_{c3}$	$x_3 = 0,\ \dot{x}_3 = 0$
$T_{s3} = T_{c3}$	$\dot{T}_{s3} = \dot{T}_{c3}$
$x_3 + 0.00453\,(T_{c3} - T_{s4}) \geq 0$	$x_4 = x_3 + 0.00453\,(T_{c3} - T_{s4})$
$x_3 + 0.00453\,(T_{c3} - T_{s4}) < 0$	$x_4 = 0$

For a discussion of the assumptions in these equations see Section III-B.

C. COOLANT DENSITY

1. Subcooled Boiling Density Ratio

$$\left(\frac{\rho_\ell}{\rho_n}\right)_a = \frac{1}{1 - \dfrac{0.0371\left[\dfrac{Q}{A} - h_{NB}\,(T_{wn} - T_{cn})\right]}{h_{NB}^2\left[(T_{sn} - T_{cn}) + 20\right]}}$$

Note: $\rho_\ell = 51.6$ lb/ft^3

This equation is based on the subcooled boiling correlation of Reference 2, modified to approximate the density over the entire subcooling range.

2. Bulk Boiling Density Ratio

$$\left(\frac{\rho_\ell}{\rho_n}\right)_C = 1.0 + 54.4\,x_n$$

This equation assumes a slip ratio of 3.0 (the ratio of vapor to liquid velocity in two-phase flow). This approximation is in good agreement with experimental data[2] and predictions using the Lockhart-Martinelli method[8] for quality, x, above 0.03 which is the main area of interest. The pressure at which the vapor density was evaluated was taken to be 20 psia. This pressure corresponds to that at which most of the action takes place during experimental transients.

Boundary Conditions:

IF	THEN
$\left(\frac{\rho_\ell}{\rho_n}\right)_a > \left(\frac{\rho_\ell}{\rho_n}\right)_C$	$\left(\frac{\rho_\ell}{\rho_n}\right) = \left(\frac{\rho_\ell}{\rho_n}\right)_a$
$\left(\frac{\rho_\ell}{\rho_n}\right)_a < \left(\frac{\rho_\ell}{\rho_n}\right)_C$	$\left(\frac{\rho_\ell}{\rho_n}\right) = \left(\frac{\rho_\ell}{\rho_n}\right)_C$

Note: $\rho_\ell = 51.6$ lb/ft^3

D. HEAT TRANSFER

These equations are the same as for upflow as written in Section III-D.

E. SATURATION TEMPERATURE

$$T_{sn} = 738 + 2.7\,P_n - \frac{1110}{P_n} \qquad (^\circ F)$$

This equation closely approximates the vapor pressure for the Santowax-R used in the Flow Stability Loop during the downflow transients.

F. TEST SECTION PRESSURE AND PRESSURE DROP

1. Outlet Pressure

$$P_4 = P_{ss} - \Delta P\, e^{-t/\tau} \quad \text{(psia)}$$

where P_{ss}, P, and τ are chosen to conform to the experimental conditions.

This empirical equation was used to approximate the experimentally measured outlet pressure curves for the transients to be duplicated analytically.

2. Test Section Pressure Drop

$$\Delta P_T = (P_{in} - P_1) + (P_1 - P_2) + (P_2 - P_3) + (P_3 - P_4) = \Delta P_{bp} \quad \text{(psi)}$$

3. Bypass Line Pressure Drop

a. Fixed Bypass Valve

$$\Delta P_{bp} = C' \left[1 - 2\left(\frac{W}{W_T}\right) + \left(\frac{W}{W_T}\right)^2\right] + \Delta P_s \quad \text{(psi)}$$

where

C' = constant depending on valve position,

W_T = total test section plus bypass flow, and

ΔP_s = static head difference across bypass line = - 4.53 psi.

The bypass line pressure drop was approximated by a friction term proportional to the bypass flow squared, plus the static head difference from inlet to outlet.

b. Controlled Bypass Valve

$$\Delta P_{bp} = \text{Constant}$$

In some of the experiments, the bypass valve was controlled to maintain constant pressure drop across the test section.

V. EXPERIMENTAL FACILITIES AND METHOD

The experimental facilities consist essentially of a closed loop where the circulating coolant undergoes a heating and cooling cycle at controlled conditions of flow, temperature, and pressure. A schematic of the test loop is presented in Figure 2. The loop flow is split between the test section and a bypass line. During tests, the loop flow rate is constant but the ratio of test section to bypass flow changes depending on the two-phase flow resistance of the test section. A control valve is also provided in the bypass line. This valve is used to establish the initial ratio of test section to bypass flow and can also be controlled to maintain constant test section pressure drop. A detailed description of the experimental facilities and related instrumentation is presented in Reference 3.

A. TEST SECTION

The test section (see Figure 3) consists of a seamless nickel tubing 9/16 inches OD with a 0.042 in. close tolerance wall thickness. It is electrically heated with dc power. The terminals are connected directly to the test section. The heated length is 12 ft and the total length is 13 ft. The test section is oriented vertically and the loop piping arrangement provides for either upflow or downflow of the circulating coolant.

B. BASIC INSTRUMENTATION

The instrumentation provided for the test section (see Figure 4) measures and records:

1. Void fraction,
2. Coolant and wall temperatures,
3. System pressure and pressure drops,
4. Coolant flowrate, and
5. Power input.

The instrumentation is suitable for both steady-state and transient phases of the experimental program. Measured variables are recorded by a multichannel direct-recording oscillograph on an 8-in. chart.

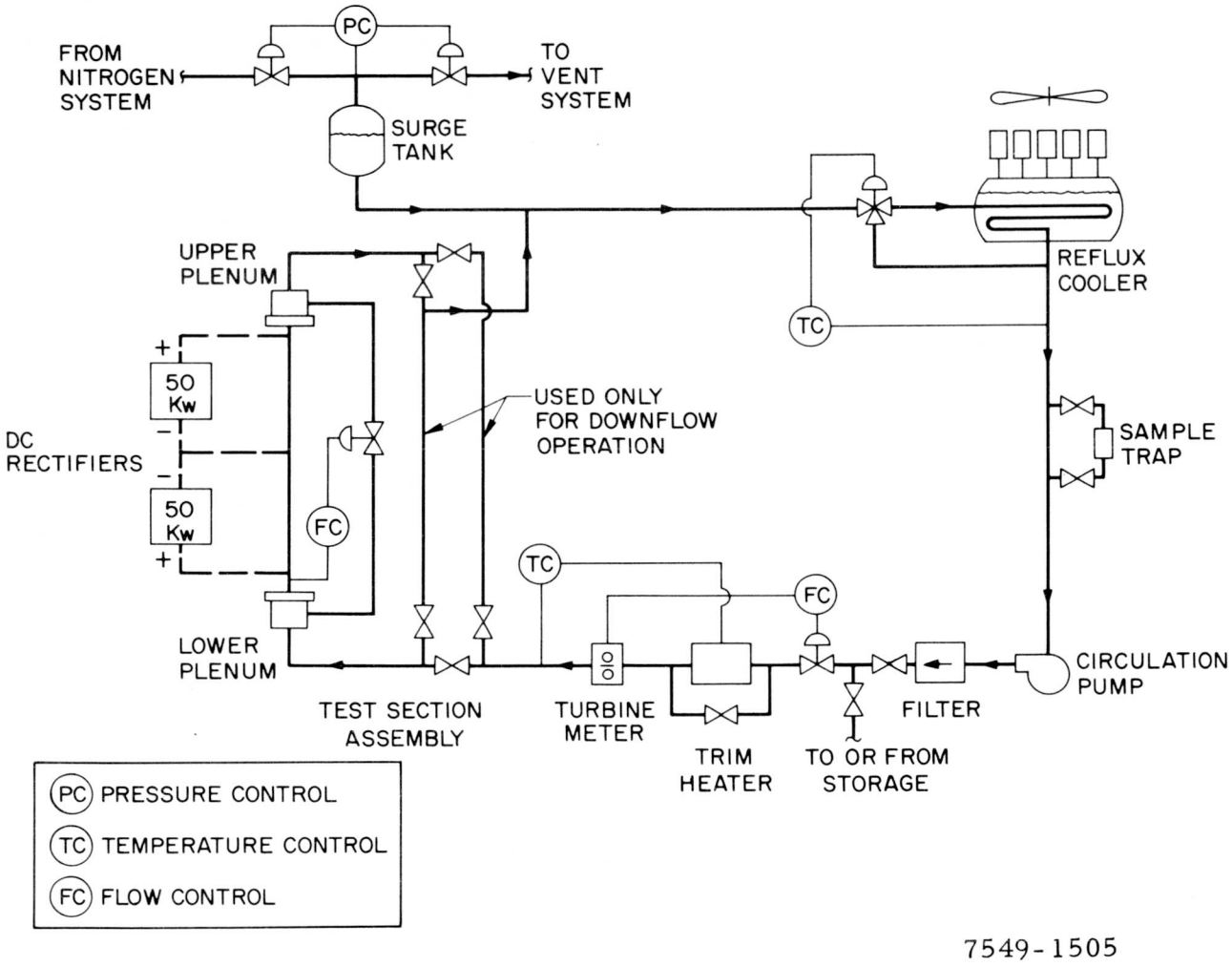

Figure 2. Schematic of Flow Stability Test Loop

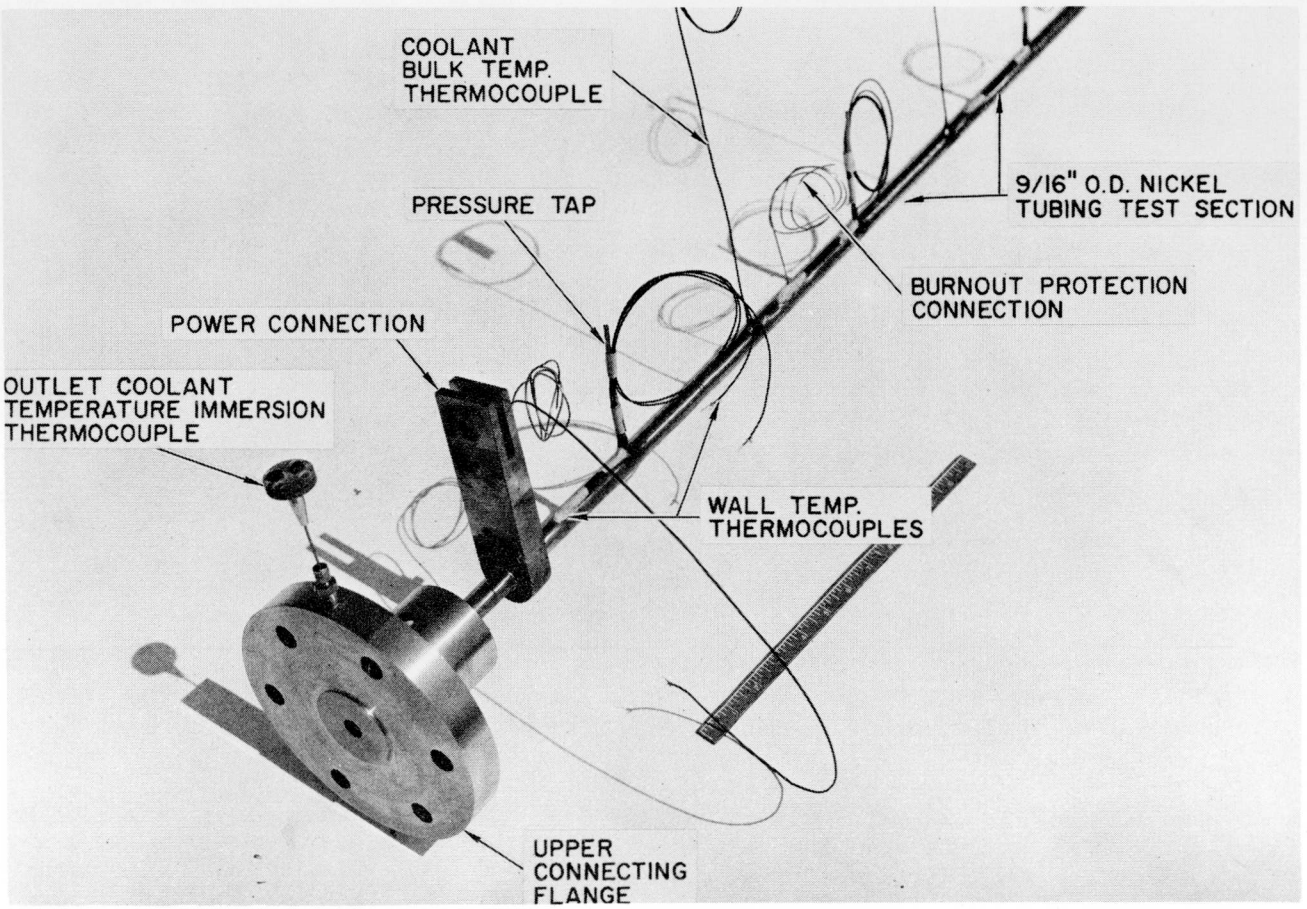

7549-5414

Figure 3. Flow Stability Loop Test Section

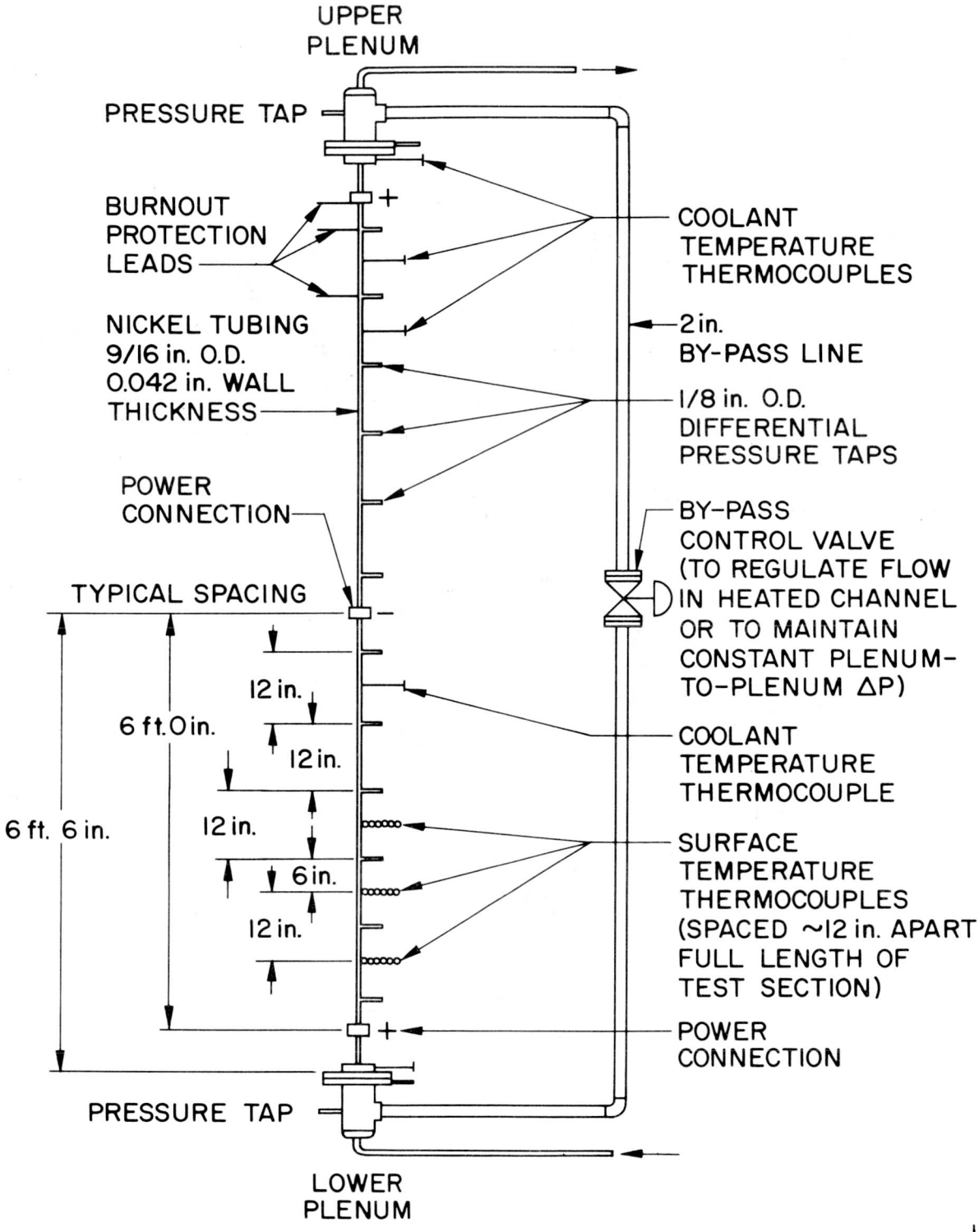

Figure 4. Sketch of Test Section Assembly

1. Void Fraction Measurement

The volume fraction of the organic coolant vapor at any preselected point along the test section is measured by a system consisting of a 150 kv x-ray machine, collimators, and two detectors. The x-ray beam is split and collimated into two beams. One beam is transmitted through a "dummy" test section, through another collimator, into a scintillation detector. The other beam is collimated in a like manner, and passes through the test section to another collimated detector. The output of each detector goes into a differential amplifier which subtracts the reference detector signal from the void detector signal. The output signal from the differential amplifier drives a high speed galvanometer calibrated in "void fraction". A complete description of the void fraction measuring system, including its calibration and accuracy, is reported in Reference 9.

2. Temperature Measurements

Chromel-constantan thermocouples are used for measurement of coolant and wall temperatures. Thermocouples which measure test section wall temperature are attached to the wall with pure silver to minimize the voltage pickup from the dc heated tube. Thermocouples which measure coolant bulk temperature are inserted directly in the coolant stream and are insulated from the test section wall. Coolant and wall thermocouples are located along the length of the test section at intervals to provide comprehensive temperature profiles of the system for heat transfer analysis.

3. Pressure Measurements

Absolute and differential pressures are measured with variable reluctance transducers. These transducers consist of a pressure sensing diaphragm of magnetic material, the deflection of which controls the gap in each of two magnetic circuits. The gaps change in opposite directions and produce corresponding changes in the inductance of two pick-off coils. This effect is utilized in an ac bridge circuit to produce an output voltage proportional to the applied pressure.

Absolute pressure is measured at the inlet and outlet of the test section. Differential pressure measurements are made between various pressure taps along the test section to determine the pressure profile for the test section.

4. Flow Measurement

The coolant flow rate through the test section is measured by means of the test section inlet differential pressure transducer calibrated in terms of flow rate.

5. Power Input Measurement

The power input to the test section, from which the heat flux is determined, is measured by recording watt-meters. The voltage drop and current through the test section are also measured by precision voltmeters and ammeters, respectively.

C. EXPERIMENTAL METHOD

The Flow Stability Loop was used to obtain experimental pressure transients. These are depressurization experiments which result in bulk boiling at the outlet of a heated channel (the test section). The tests covered in this investigation were conducted at preselected conditions of initial pressure, initial flow rate, heat flux, and coolant inlet temperature. The heat flux, coolant inlet temperature, and total loop flow rate were maintained constant during the transients. In order to make sure bulk boiling would occur during the transient, the initial conditions were selected with an initial coolant outlet temperature equal to the saturation temperature of the coolant at a pressure lower than the initial outlet pressure but greater than the final outlet pressure of the system. Pressure transients are produced by venting the pressurized nitrogen gas from the surge tank to the atmosphere. The rate of depressurization is adjusted by varying the coolant level in the surge tank which establishes the amount of nitrogen gas to be vented. The ranges of variables investigated are representative of the ranges considered in loss-of-pressure accidents for organic-cooled reactors.

The measurements of temperature and power input were used to check the heat balance on the system for the initial conditions of the transients. The temperature measurements were also used to check the heat transfer during the transients. The departure from nucleate boiling was observed by a rapid rate of increase of wall temperature. Outlet pressure was measured during the transients. The incremental pressure drops along the test section were used to check the two-phase pressure deop as predicted by the equations and to establish the pressure profile along the test section during the experiments. The experimental outlet pressure curves were closely approximated by exponentials (as plotted in the illustration for each experiment) for use on the analog computer in duplicating the transients. By direct comparison of analog and experimental transients, the applicability of the analytical model for pressure transients was established.

VI. RESULTS

An analytical model has been established that can be used to make predictions of the heat transfer and hydraulic effects of reactor loss-of-pressure accidents resulting in bulk boiling of the coolant. Predictions made by use of these equations have been verified by direct comparison with transients measured in the experimental apparatus (the Flow Stability Loop) using the organic reactor coolant, Santowax-R. The range of experimental verification (not necessarily the range of usefulness) is shown in Table 1.

TABLE 1

RANGE OF EXPERIMENTAL VERIFICATION

Heat flux (Btu/hr ft^2)	40,000 to 100,000
Inlet temperature (°F)	600 to 670
Initial outlet temperature* (°F)	705 to 780
Rate of depressurization** at beginning of bulk boiling (psi/sec)	0.05 to 2.5
Mass velocity at beginning of transients (lb/sec ft^2)	260 to 460
Mass velocity at time transients were stopped (lb/sec ft^2)	0 to 230
Direction of flow	up and down

*The saturation temperature of the coolant at atmospheric pressure is approximately 700°F.

**This corresponds to a flashing rate of 0.1 to 6% quality/sec

Initial conditions for the transients are shown in Tables 2 and 3.

The depressurization rates tested are representative of the range considered in organic cooled reactor loss-of-pressure accident. The rate of depressurization for a pressurized reactor is a function of the initial pressure and the mechanism of depressurization. The important parameter which determines the speed of the transients to be investigated is the rate of depressurization at the time bulk boiling begins. For reactors operating with a coolant outlet temperature slightly above the saturation temperature at atmospheric pressure (this can be the case for future organic-cooled reactors), the rate of depressurization when bulk boiling is reached may be more than an order of magnitude lower than the initial rate.

TABLE 2

INITIAL CONDITIONS FOR THE UPFLOW EXPERIMENTS

Transient No.	T Inlet (°F)	Heat Flux (BTU/hr-ft^2)	Initial Flow (gpm)		Test Section Pressure Drop
			Channel	Bypass	
1	652	42,300	4.0	4.0	uncontrolled
2	652	53,100	4.6	3.4	uncontrolled
3	607	63,900	4.0	4.0	uncontrolled
4	605	74,000	4.2	3.8	uncontrolled
5	603	84,600	4.0	4.0	uncontrolled
6	604	52,300	3.1	2.9	uncontrolled
7	605	78,200	3.8	4.2	uncontrolled
8	655	54,600	5.0	3.0	uncontrolled
9	654	60,200	4.8	3.2	uncontrolled
10	600	90,000	4.0	4.0	uncontrolled
11	602	63,200	3.0	3.0	uncontrolled
12	651	51,300	3.0	3.0	uncontrolled
13	606	62,700	3.1	2.9	uncontrolled
14	603	97,800	5.0	1.0	uncontrolled
15	650	42,300	4.0	4.0	uncontrolled
16	603	45,000	2.9	3.1	uncontrolled
17	605	87,300	5.0	5.0	uncontrolled
18	650	33,900	3.1	2.9	constant
19	656	50,800	4.0	2.0	constant
20	654	57,000	5.0	3.0	constant
21	650	50,500	5.0	1.0	constant
22	651	64,900	4.8	3.2	constant
23	604	61,000	3.9	2.1	constant
24	620	76,300	4.0	2.0	constant
25	605	80,000	4.0	4.0	constant
26	605	61,200	3.0	3.0	constant
27	605	90,000	3.8	4.2	constant
28	650	42,000	3.1	2.9	constant
29	602	80,000	4.0	4.0	constant

TABLE 3

INITIAL CONDITIONS FOR THE DOWNFLOW EXPERIMENTS

Transient No.	T Inlet (°F)	Heat Flux (BTU/hr-ft^2)	Initial Flow (gpm)		Test Section Pressure Drop
			Channel	Bypass	
30	645	41,700	3.1	2.9	uncontrolled
31	652	40,500	3.0	3.0	uncontrolled
32	660	49,700	2.9	3.1	uncontrolled
33	663	48,800	2.9	3.1	uncontrolled
34	660	63,300	3.9	4.1	uncontrolled
35	658	62,700	4.0	4.0	uncontrolled
36	645	42,600	3.0	3.0	constant
37	663	40,200	2.9	3.1	constant
38	665	48,300	2.9	3.1	constant
39	663	49,500	2.9	3.1	constant
40	667	63,500	4.1	3.9	constant
41	663	63,500	4.0	4.0	constant

Comparisons of analog and experimental pressure transients are shown in Appendix C. The upflow transients are shown in Figures C-1 through C-29; the downflow transients are shown in Figures C-30 through C-41. Experiments in which the channel pressure drop varies depending on a fixed bypass valve arrangement are shown in Figures C-1 through C17 and C-30 through C-35. Figures C-18 through C-29 and C-36 through C-41 show transients in which the bypass valve is controlled to provide constant channel pressure drop.

Depressurization did not affect flow, temperatures, or void fraction until boiling began; therefore, the transients included in the illustrations are shown only from the point where changes in flow or void fraction occurred. The transients with constant pressure drop are faster than the others, as is shown in Figure 5. In the case of the transients for which a fixed bypass valve is used, the pressure drop across the test section builds up which tends to maintain flow. Figure 5 also indicates that downflow transients are slightly faster than upflow transients. This is due to changes in static head, during the formation of voids, which aid upflow while hindering downflow.

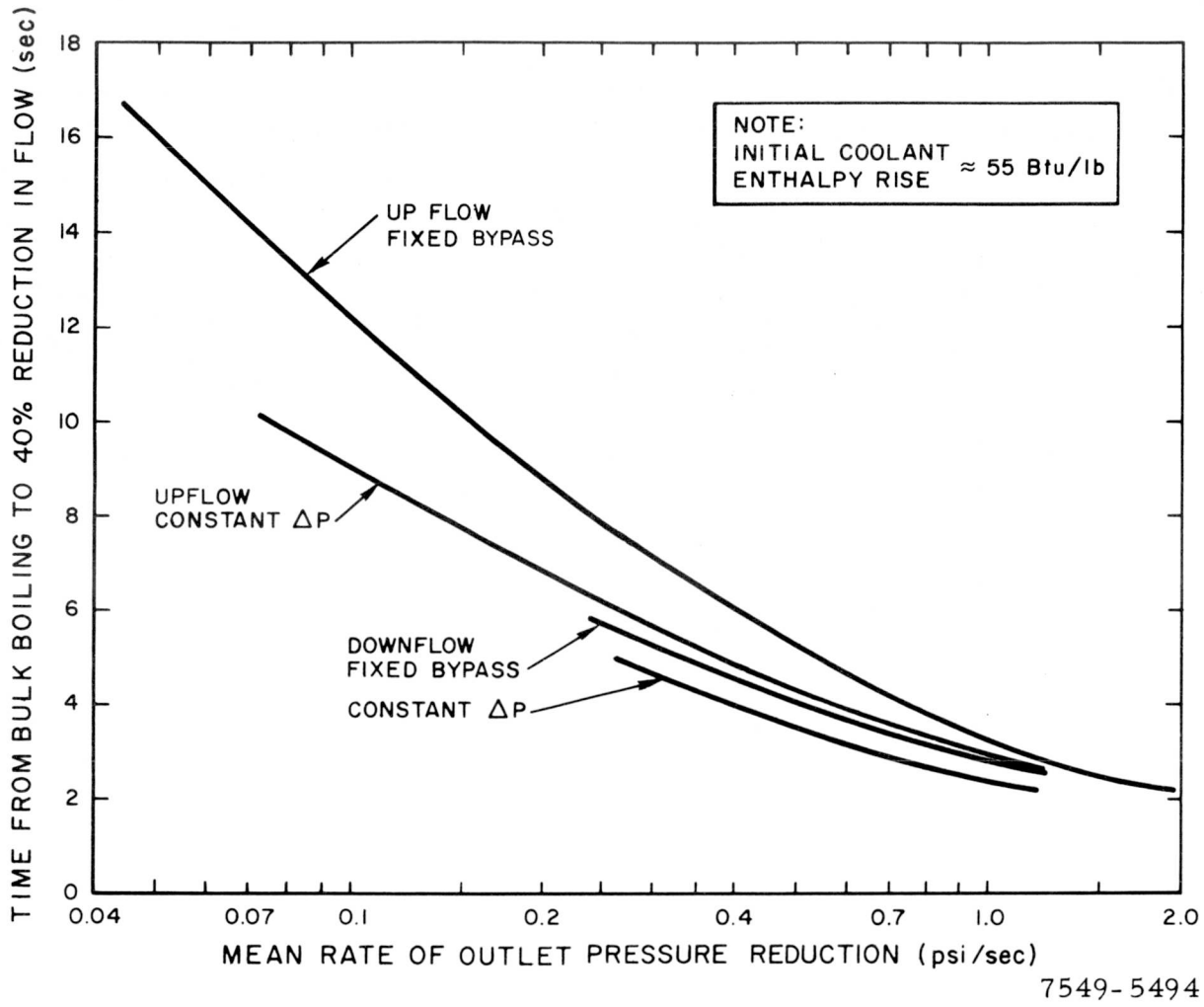

Figure 5. The Effect of Depressurization Rate on the Initial Rate of Flow Reduction for Pressure Transients in the Flow Stability Loop

The illustrations show experimental test section outlet pressure, flow, and void fraction, and show approximated test section outlet pressure, and analog computer predictions of flow and void fraction. The test section outlet pressure is used to "drive" the experimental transients and the approximated test section outlet pressure (shown in the illustrations) is used to "drive" the analog computer transients. Experimental and predicted flow rates agree within 10 to 15% during the transient. The void fraction (measured near the end of the heated section of the channel) for the experimental and predicted results are in qualitative agreement. The void fractions agree within 20% voids for most of the experiments. The wall temperatures (not shown in the illustrations) were predicted within 20°F up to the point of film boiling. Film boiling began during the experimental transients about the time the void fraction reached 95%.

VII. DISCUSSION

The pressure transient study has verified the suitability of an analytical model for use in evaluating heat transfer and hydraulic effects of organic-cooled reactor loss-of-pressure accidents resulting in bulk boiling. The experiments have shown a reasonable indication of the time when film boiling begins at the outlet of the heated channel. Hence, a method has been established to evaluate the heat transfer and hydraulic effects of loss-of-pressure accidents from the initiation of the incident to the time when fuel melting begins.

The upflow analog transients were determined with a model which considers bulk boiling over the last two feet of a channel having a heated length of twelve feet. Bulk boiling began to occur over a length greater than two feet, during the transients, approximately when flow was reduced to 50%. This was roughly the time at which the experimental transients were stopped in an effort to preserve the test section. Therefore, it was not necessary to extend the analog model for comparison with experimental data. This does, however, cause nonconservative extrapolations below 50% flow. The extrapolations of analog results indicate that the flow decreases at a relatively constant rate. However, in reality the flow is reduced at an accelerating rate and decreases very rapidly below 50% flow. At the same time, the experimental flow indication had limited accuracy in this range.

Prior to the downflow transients, the experimental flow measuring capability was improved allowing quantitative flow measurement to about 25% of the original flow rate. This warranted the use of a more detailed analog model to study these effects. The allowable boiling zone in the analog simulation used for the downflow tests was extended by the addition of another boiling region. This extension made it possible to get a better overall view of the transient with respect to flow choking due to bulk boiling.

The prediction of void fraction for the upflow transients was divided into three regions based on coolant subcooling. This procedure is similar to a previously reported method for correlating void fraction.[2,5] The regions are essentially: subcooled, nearly saturated, and bulk boiling zones. The net effect of this method is to produce a jog in the analog void fraction curves as observed in Figures C-1 through C-29. For the downflow void fraction predictions, the first two regions were combined and described by one equation. This resulted in a

substantial improvement in void fraction prediction as shown in Figures C-30 through C-41. The importance of void fraction data in this work is mainly for determining the velocity of the two-phase mixture. The velocity is inversely proportional to $1 - \alpha$. Hence, errors in void fraction at low void fractions will not affect velocity as much as when the void fraction is high.

The void fraction prediction method is sufficiently accurate to be of value in calculating void reactivity effects accompanying these bulk boiling depressurization transients in organic-cooled reactors. The method presented for calculation of flow, pressure drop, and heat transfer effects is also applicable for calculation of void fraction at various points along the channel. The high two-phase pressure drop causes most of the voids to appear near the outlet of the channel and the economics of the hydraulic calculation (at least using an analog computer) suggest concentrating the effort of calculating voids where they are most likely to occur. This does not present a problem except that of choosing the number and location of the axial regions within the reactor to be considered. The void reactivity worth in each region can be calculated and used to evaluate the void coefficient of reactivity for each region. The overall problem of accounting for void reactivity effects is not significantly more difficult than accounting for spatial temperature induced reactivity effects within the core.

VIII. REFERENCES

1. Annual Technical Progress Report - Fiscal Year 1962, "Pressure Transients and Flow Stability Project," NAA-SR-7400, August 1962
2. Bergonzoli, F. and Halfen, F. J., "Heat Transfer and Void Formation During Forced Circulation Boiling of Organic Coolants," NAA-SR-8906, June 1964
3. Bergonzoli, F., et al., "Flow Stability Test Loop, "NAA-SR-8610," March 1964
4. Kunkel, W. P., "A Survey of the Assumptions and Areas of Uncertainty in OMR Hazards Evaluations," NAA-SR-TDR-6006, January 1961
5. Maurer, G. W., "A Method of Predicting Steady-State Boiling Vapor Fractions in Reactor Coolant Channels," Bettis Technical Review, WAPD-BT-19, June 1960
6. Meyer, J. E., et al., "Art – A Program for the Treatment of Reactor Thermal Transients on the IBM-704," WAPD-TM-156, November 1959
7. Noyes, R. C., Bergonzoli, F., and Gingrich, J.E., "FUGUE – A Non-dimensional Method for Digital Computer Calculation of Steady State Temperature, Pressure, and Void Fraction in Pipe Flow With or Without Boiling," NAA-SR-5958, May 1961
8. Lockhart, R. W. and Martinelli, R. C., "Proposed Correlation of Data for Isothermal Two-Phase, Two-Component Flow in Pipes," Chem. Engr. Progress, Volume 45, 39 (1949)
9. Kendron, J. H., Stoner, E. E., and Taylor, G. M., "Dynamic Void Fraction Measurement System," NAA-SR-7875, May 1963

APPENDIX A
DENSITY RELATIONSHIPS

RELATION BETWEEN DENSITY AND QUALITY

The specific volume of the two-phase mixture flowing through a pipe is equal to the sum of the volume occupied by the liquid and the apparent volume occupied by the vapor;
hence,

$$\frac{1}{\rho} = \frac{1 - x}{\rho_\ell} + \frac{x}{SR\rho_v} ,$$

or

$$\frac{1}{\rho} = \frac{1}{\rho_\ell} + \frac{(\rho_\ell - SR\rho_v)}{SR\rho_v\rho_\ell} x .$$

DERIVATIVE OF DENSITY WITH RESPECT TO TIME

From the above equation, the derivative of density with respect to time is as follows:

$$\frac{\partial\rho}{\partial t} = - \frac{\rho^2 (\rho_\ell - SR\rho_v)}{SR\rho_v\rho_\ell} \frac{\partial x}{\partial t} ;$$

hence, the equation for conservation of mass in Section II-A can be written:

$$\frac{\partial G}{\partial t} = \frac{(\rho_\ell - SR\rho_v)}{SR\rho_v\rho_\ell} \rho^2 \frac{\partial x}{\partial t} .$$

RELATION BETWEEN DENSITY AND VOID FRACTION

The relation between density and void fraction is:

$$\alpha = 1 - \frac{\rho - \rho_v}{\rho_\ell - \rho_v} .$$

If the vapor density is small in comparison to the liquid density, the vapor density can be neglected in the above equation. This is particularly true if the equation is only used to calculate void fraction with an accuracy of several percent. Hence, in most cases the equation can be approximated as follows:

$$\alpha = 1 - \frac{\rho}{\rho_{\ell}} .$$

APPENDIX B
NOMENCLATURE

A = Heat transfer area (ft^2)

A_f = Flow area (ft^2)

C = Specific heat (Btu/lb-°F)

D = Channel equivalent diameter (ft)

f = Friction factor

G = Mass velocity (lb/ft^2-sec)

g = Gravitational acceleration (ft/sec^2)

h = Heat transfer coefficient (Btu/sec-ft^2-°F)

h_{fg} = Latent heat of vaporization (Btu/lb)

k,k',k'' = Constants in approximate saturation temperature equation

L = Distance along channel (ft)

M = Mass of material (lb)

P = Absolute pressure (psia)

Q = Heat transfer rate (Btu/sec)

SR = Ratio of vapor velocity to liquid velocity

T = Temperature (°F)

t = Time (sec)

W = Liquid flow rate (gpm)

x = Vapor quality

z = Elevation above a reference (ft)

α = Void fraction

ρ = Density (lb/ft^3)

τ = Time constant in approximate pressure equation (sec)

Subscripts

1,2,3 = At node (points) 1,2,3

a = Subcooled boiling

B = Boiling

b = Near saturated boiling

C = Bulk boiling

c = Coolant

in = At channel inlet

ℓ = Liquid phase

ℓ_{ss} = Liquid steady state

n = At node n

NB = Nonboiling

s = Saturation

T = Total

w = Channel wall

v = Vapor phase

APPENDIX C
PRESSURE TRANSIENTS

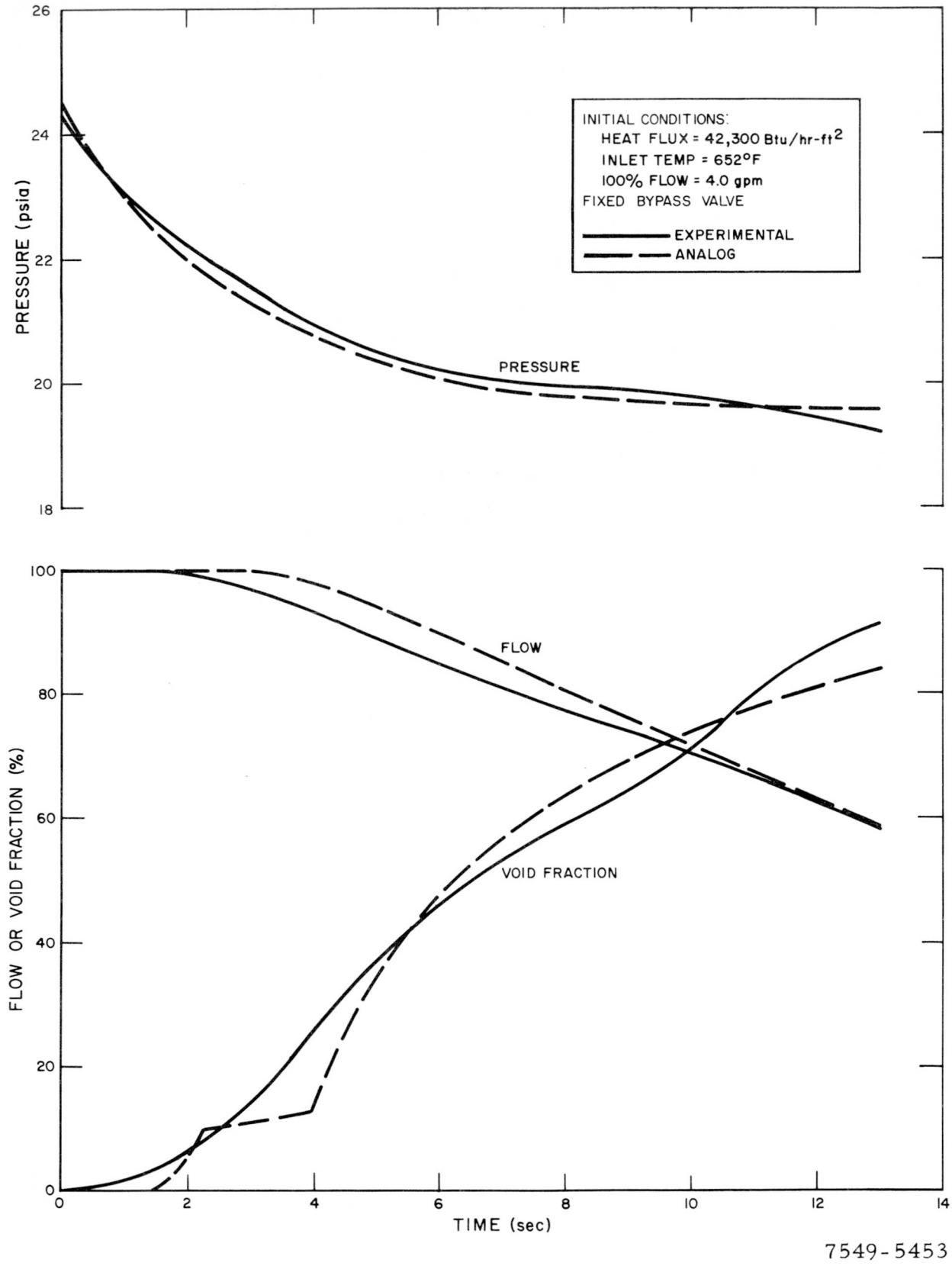

Figure C-1. Pressure Transient No. 1.
Upflow, Uncontrolled Pressure Drop

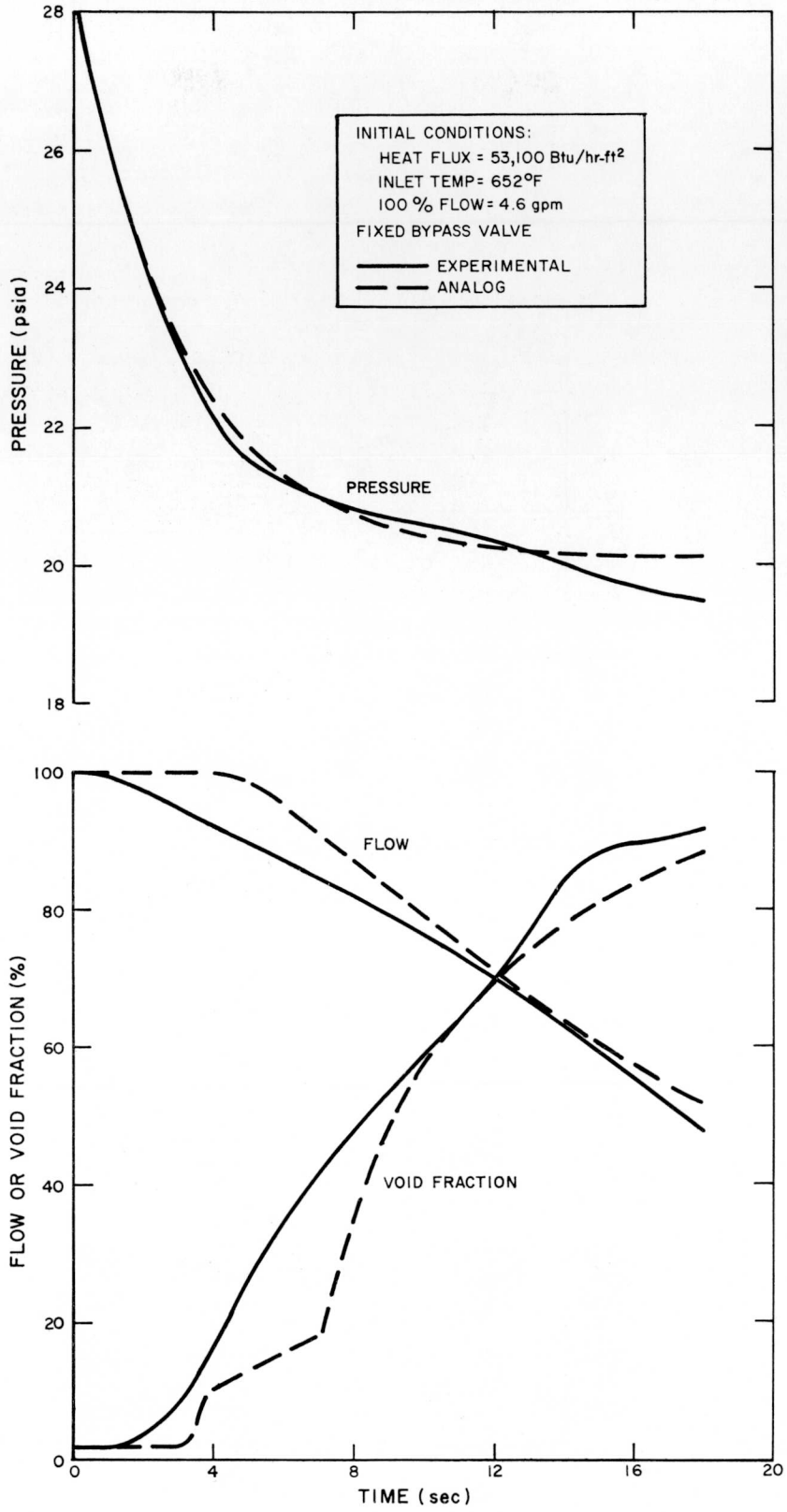

7549-5454

Figure C-2. Pressure Transient No. 2.
Upflow, Uncontrolled Pressure Drop

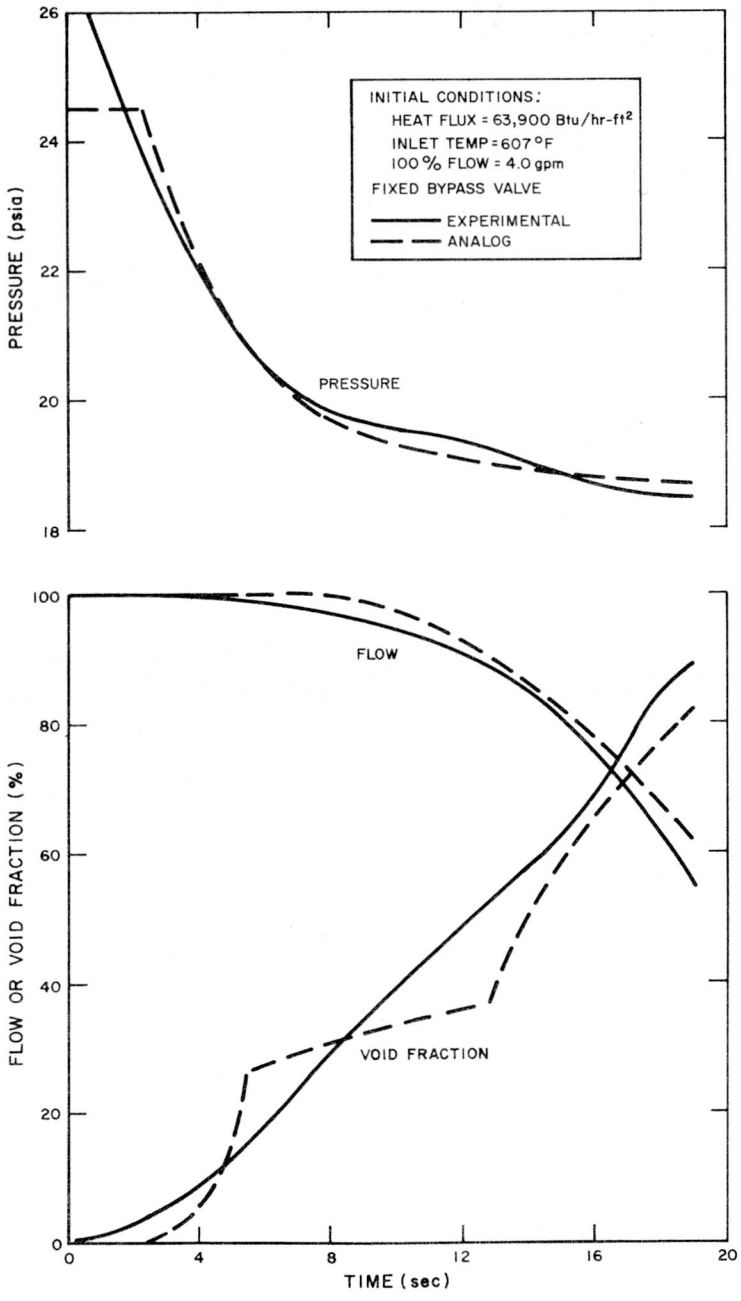

Figure C-3. Pressure Transient No. 3.
Upflow, Uncontrolled Pressure Drop

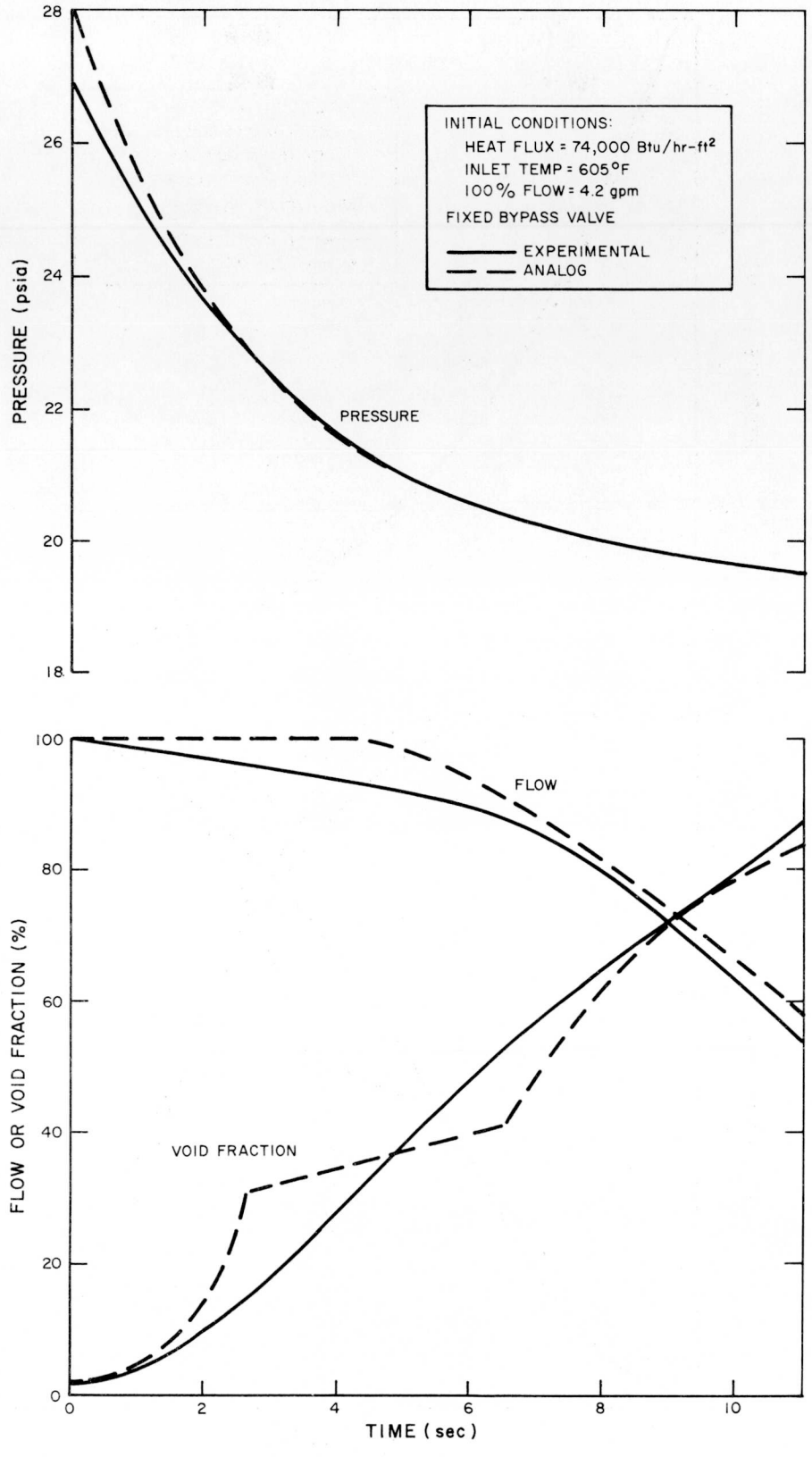

7549-5456

Figure C-4. Pressure Transient No. 4.
Upflow, Uncontrolled Pressure Drop

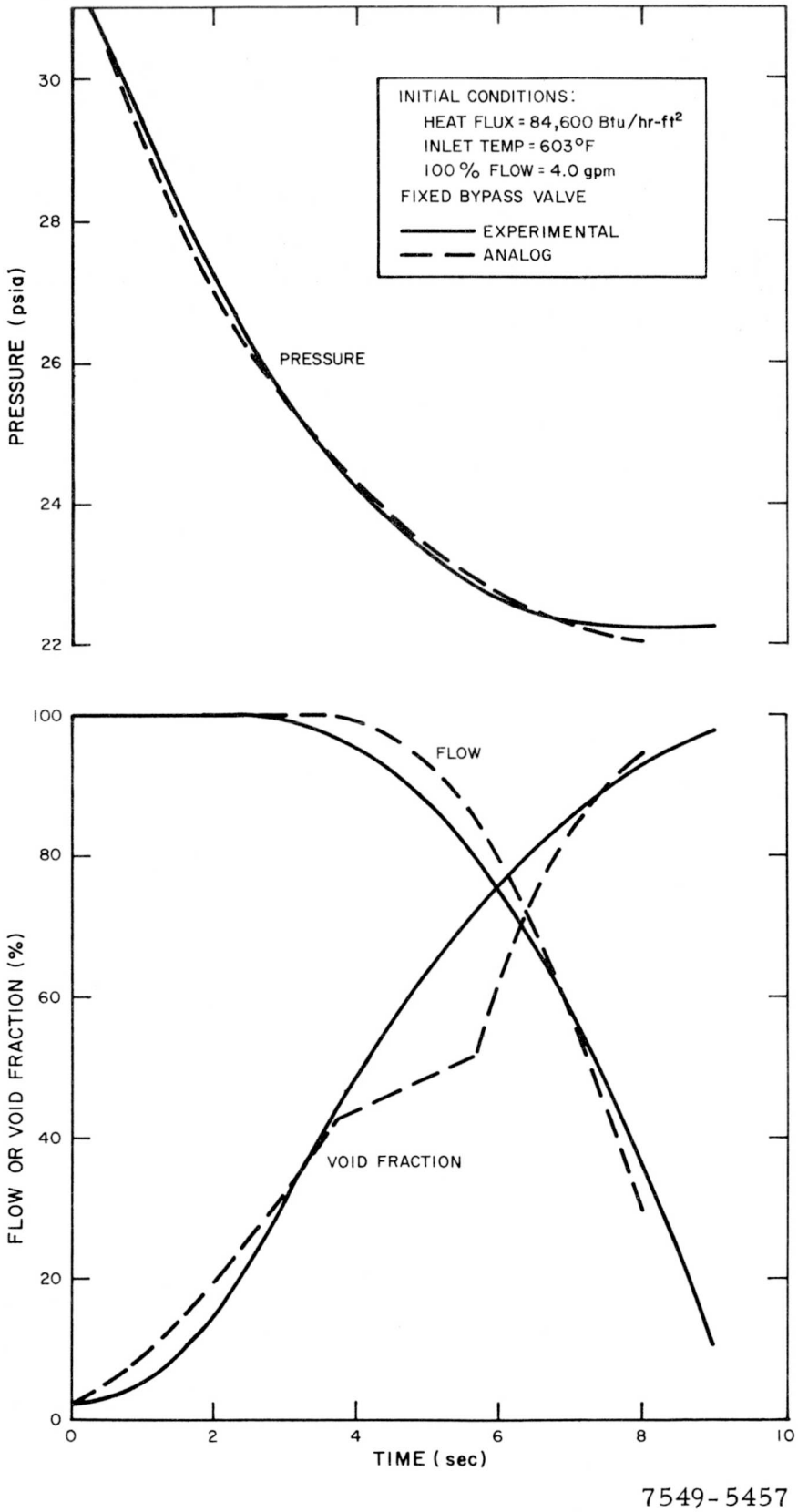

Figure C-5. Pressure Transient No. 5.
Upflow, Uncontrolled Pressure Drop

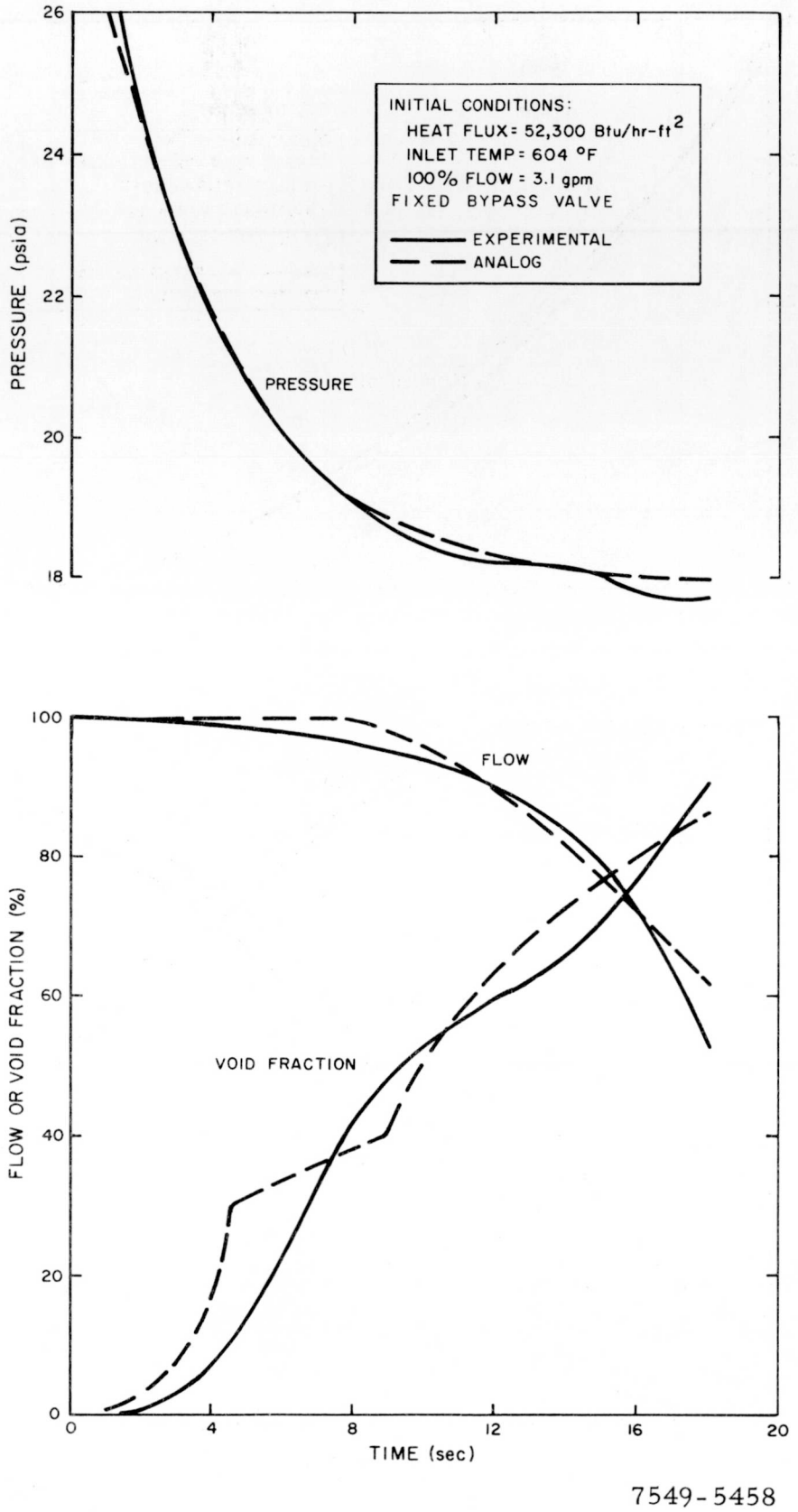

Figure C-6. Pressure Transient No. 6.
Upflow, Uncontrolled Pressure Drop

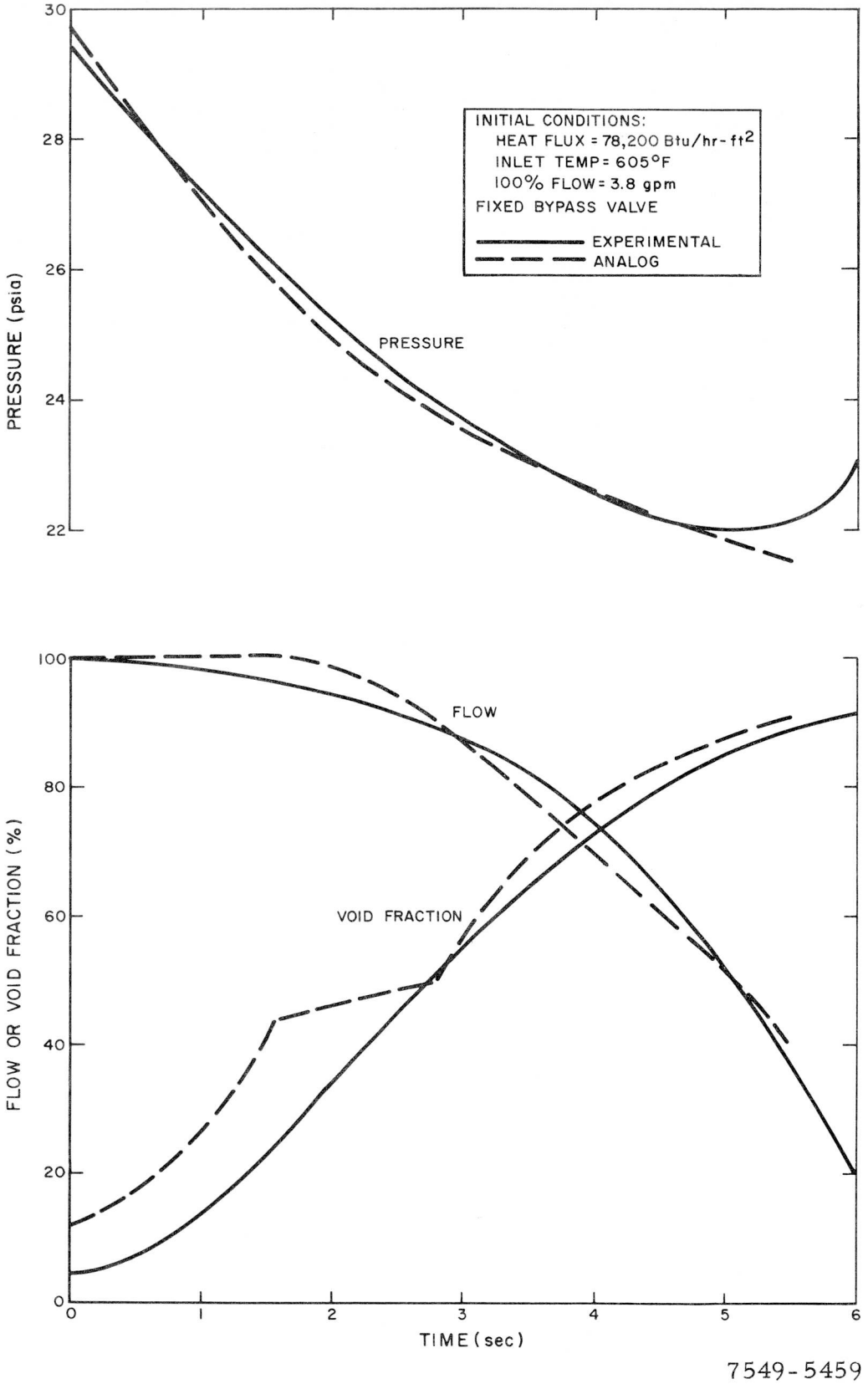

Figure C-7. Pressure Transient No. 7.
Upflow, Uncontrolled Pressure Drop

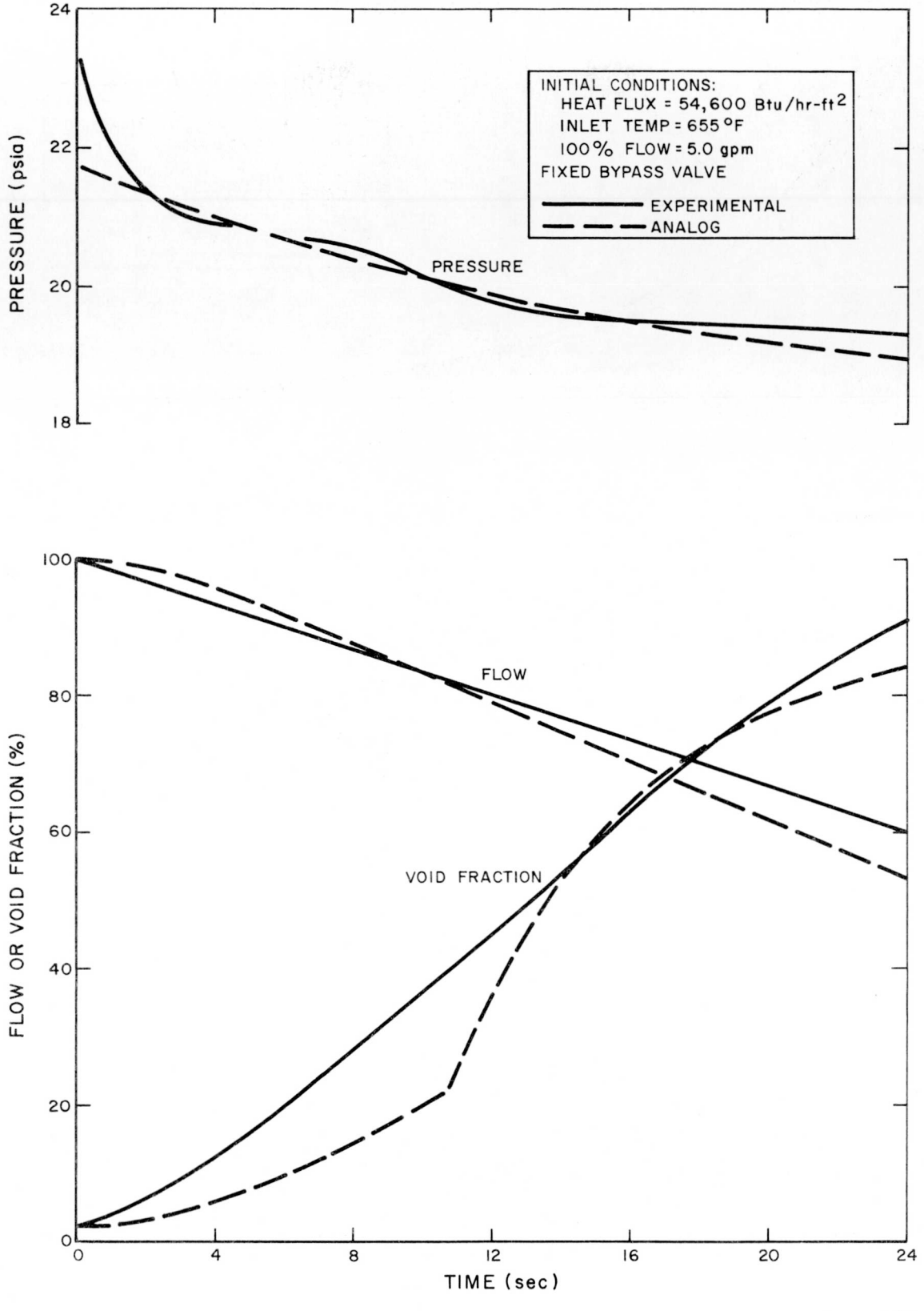

Figure C-8. Pressure Transient No. 8.
Upflow, Uncontrolled Pressure Drop

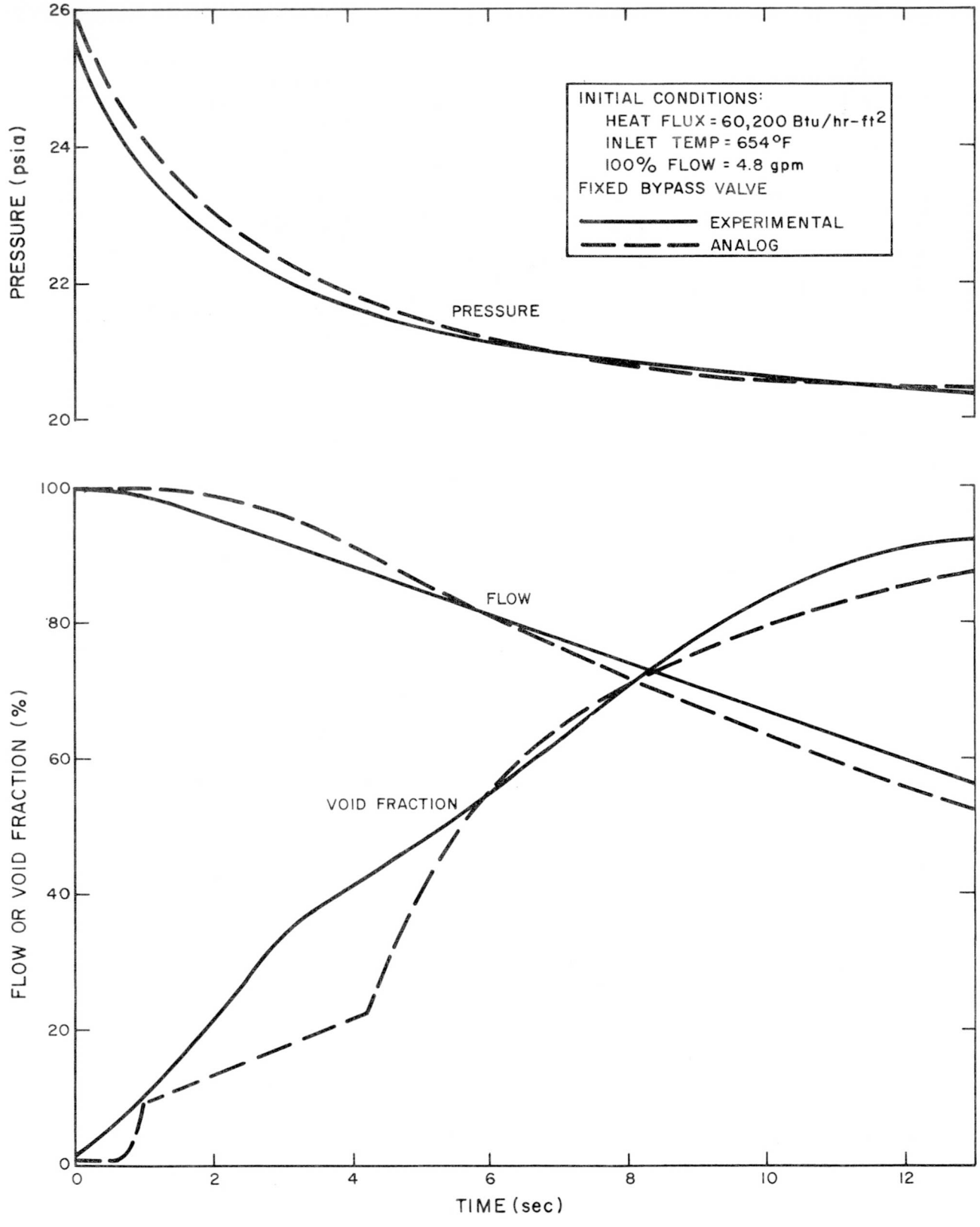

Figure C-9. Pressure Transient No. 9.
Upflow, Uncontrolled Pressure Drop

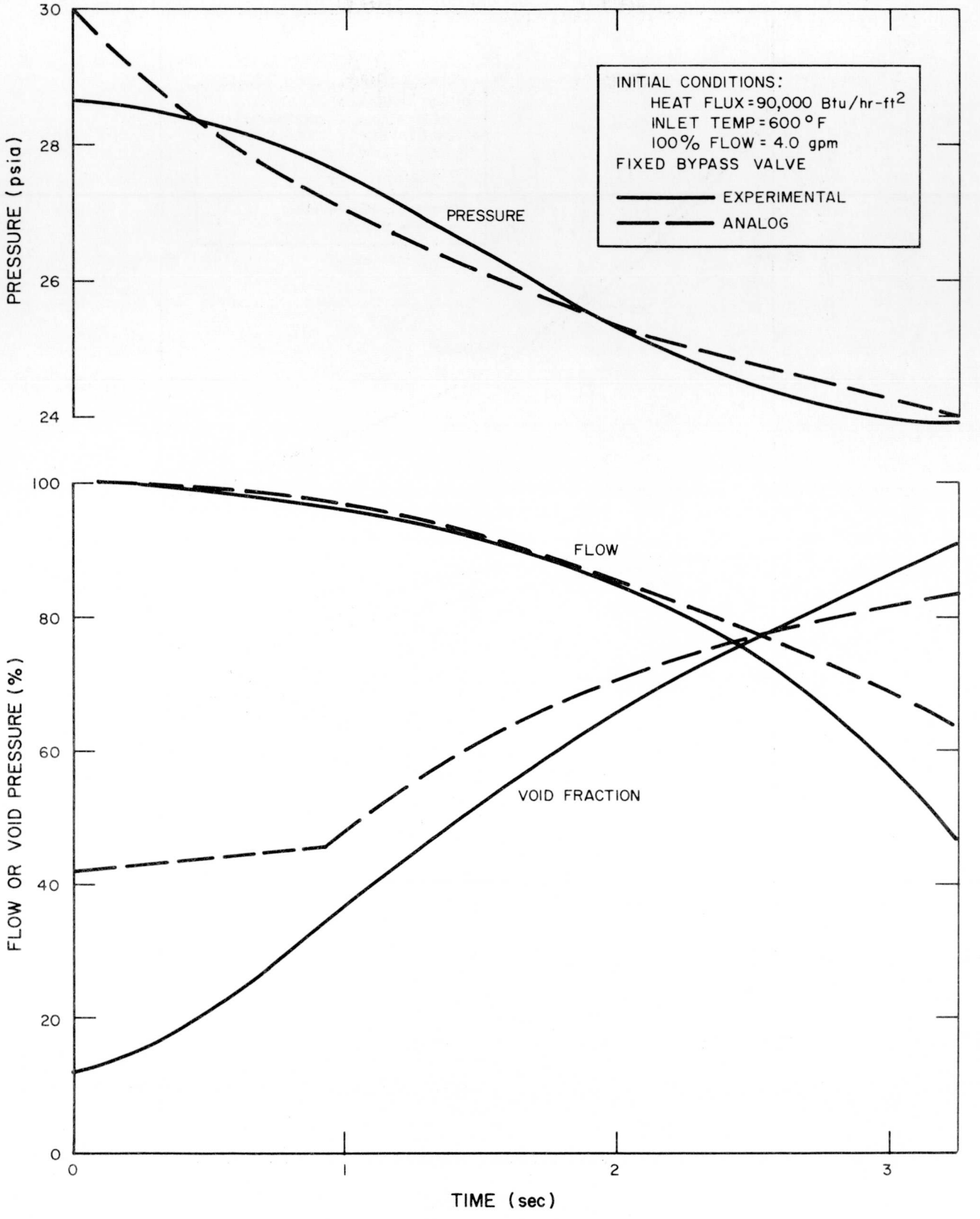

7549-5462

Figure C-10. Pressure Transient No. 10.
Upflow, Uncontrolled Pressure Drop

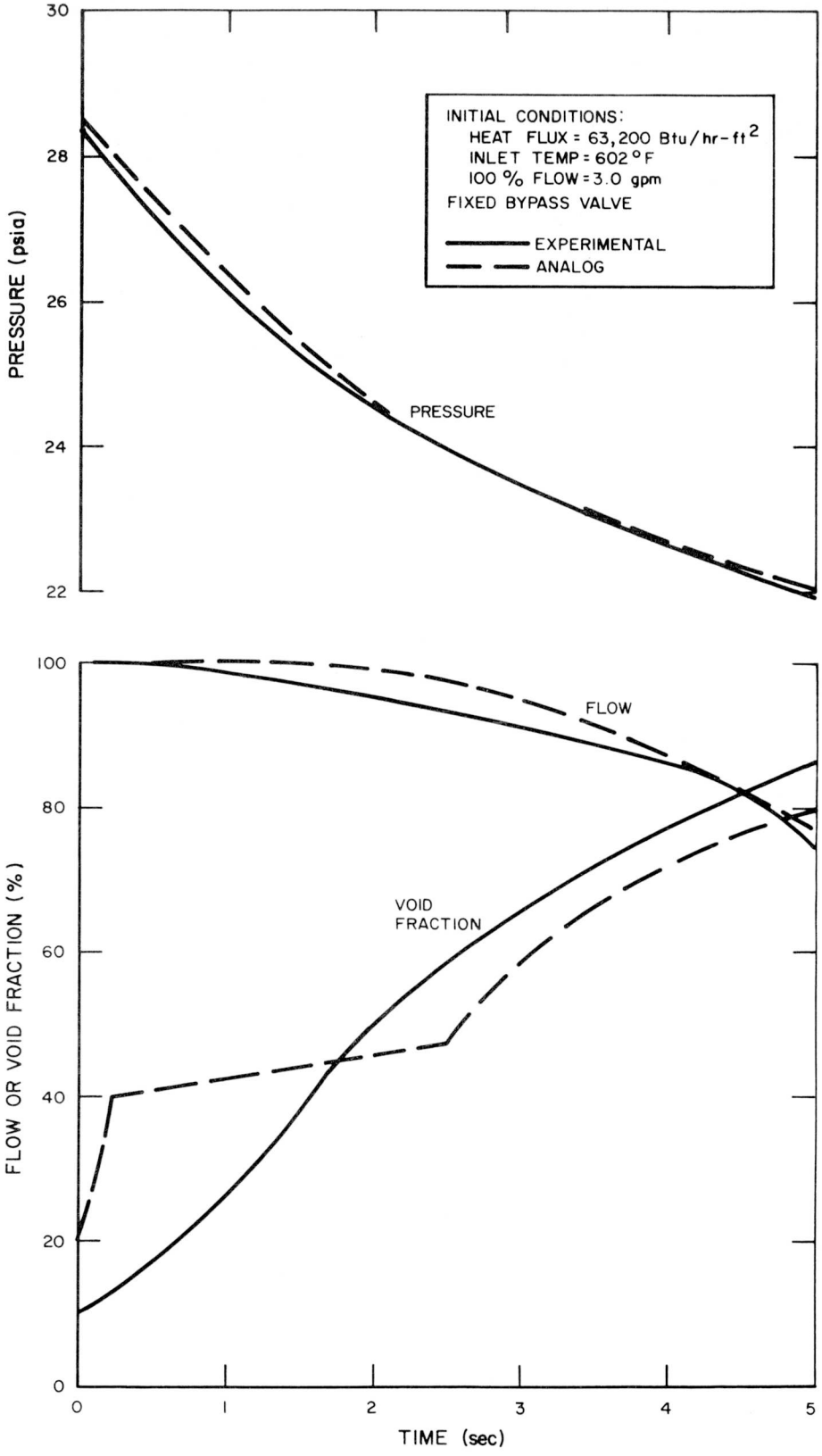

7549-5463

Figure C-11. Pressure Transient No. 11. Upflow, Uncontrolled Pressure Drop

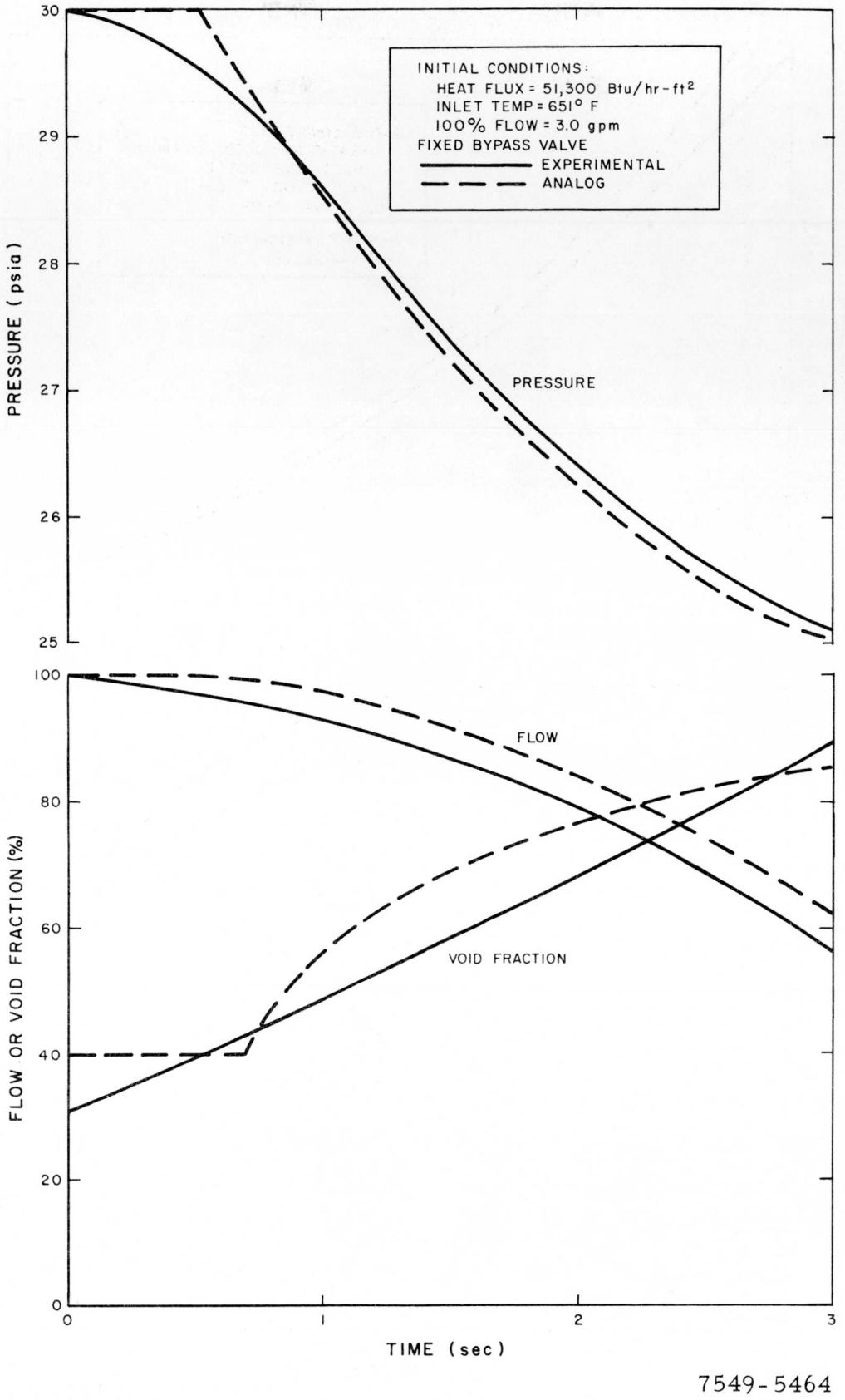

Figure C-12. Pressure Transient No. 12.
Upflow, Uncontrolled Pressure Drop

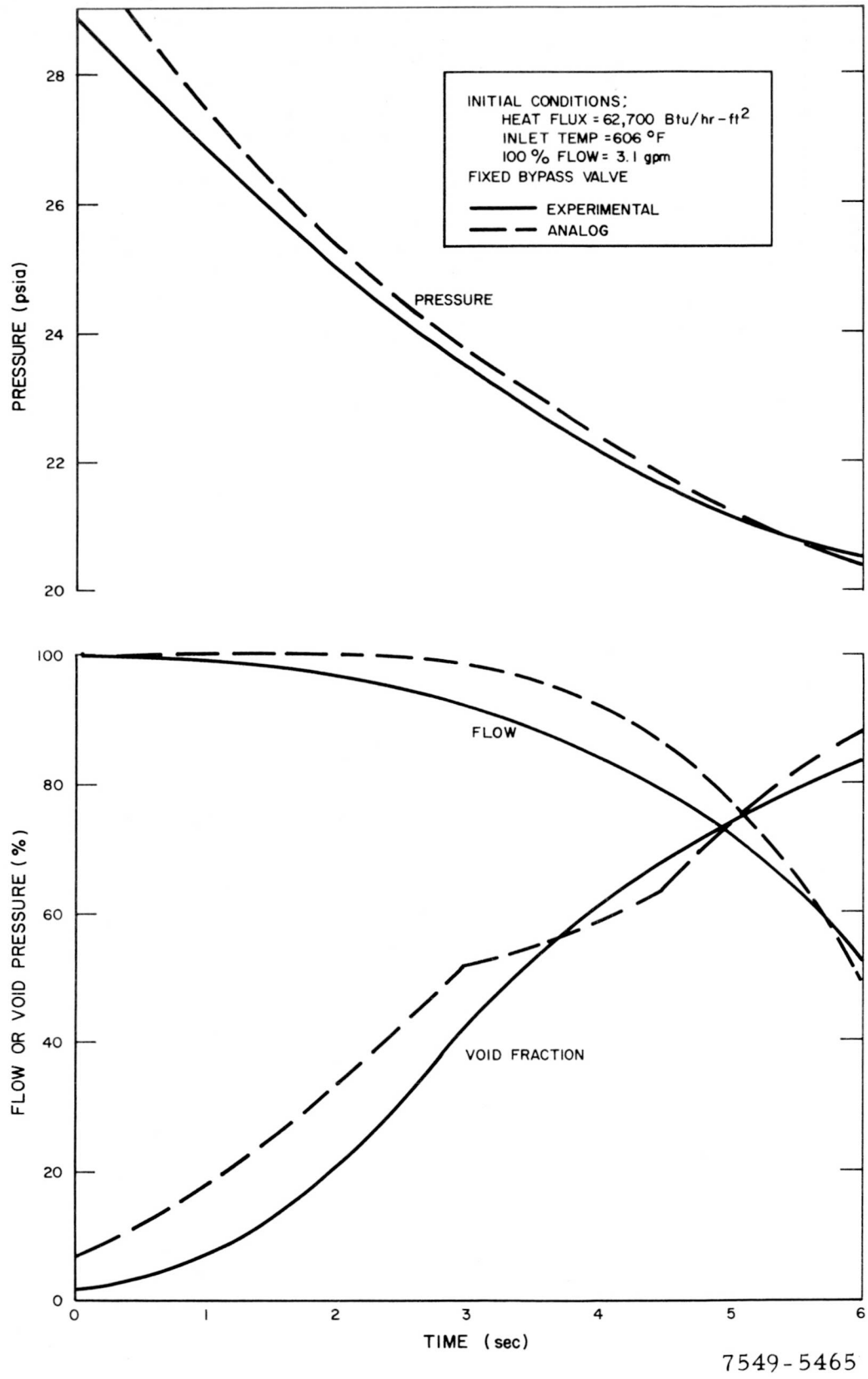

Figure C-13. Pressure Transient No. 13.
Upflow, Uncontrolled Pressure Drop

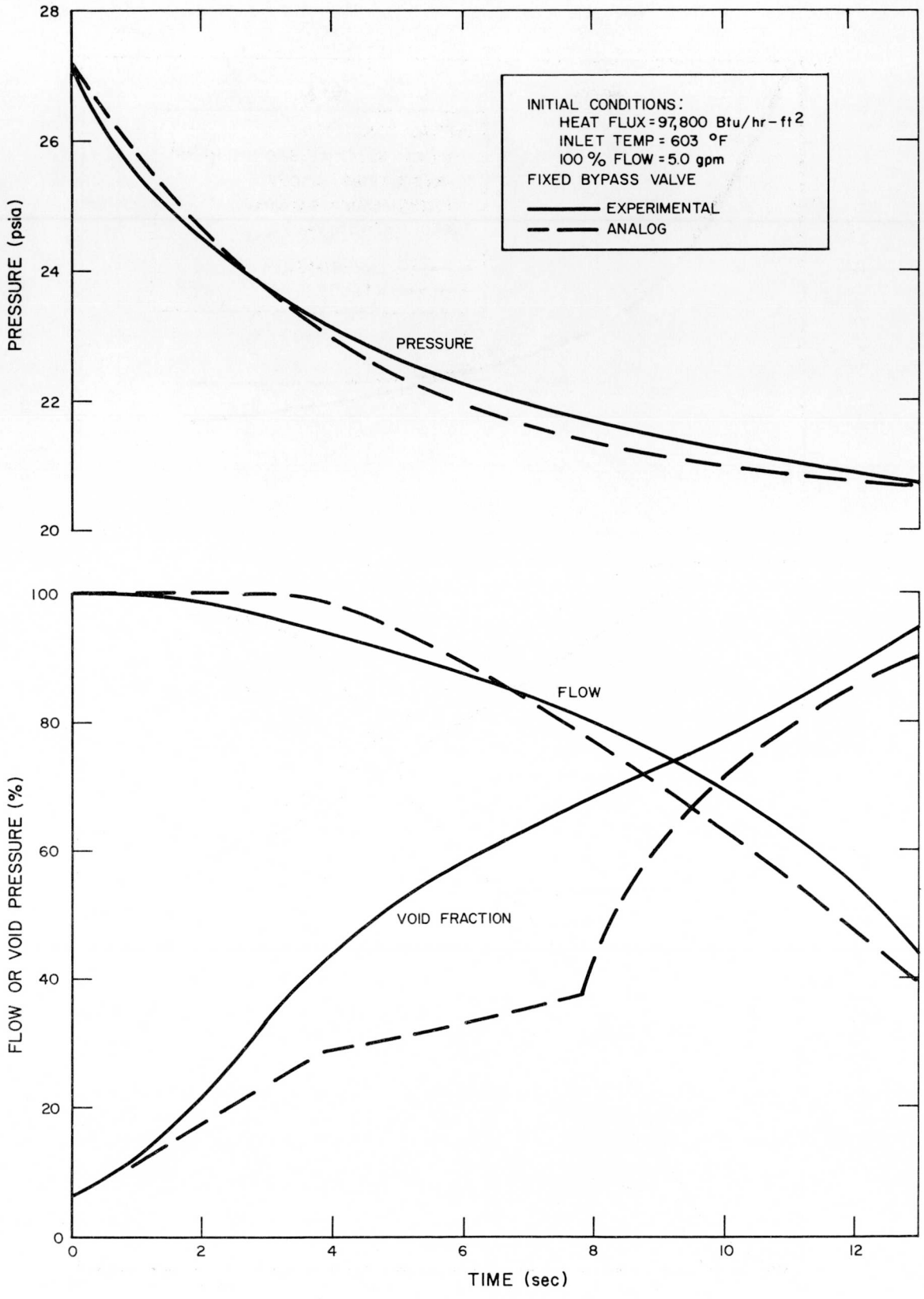

Figure C-14. Pressure Transient No. 14.
Upflow, Uncontrolled Pressure Drop

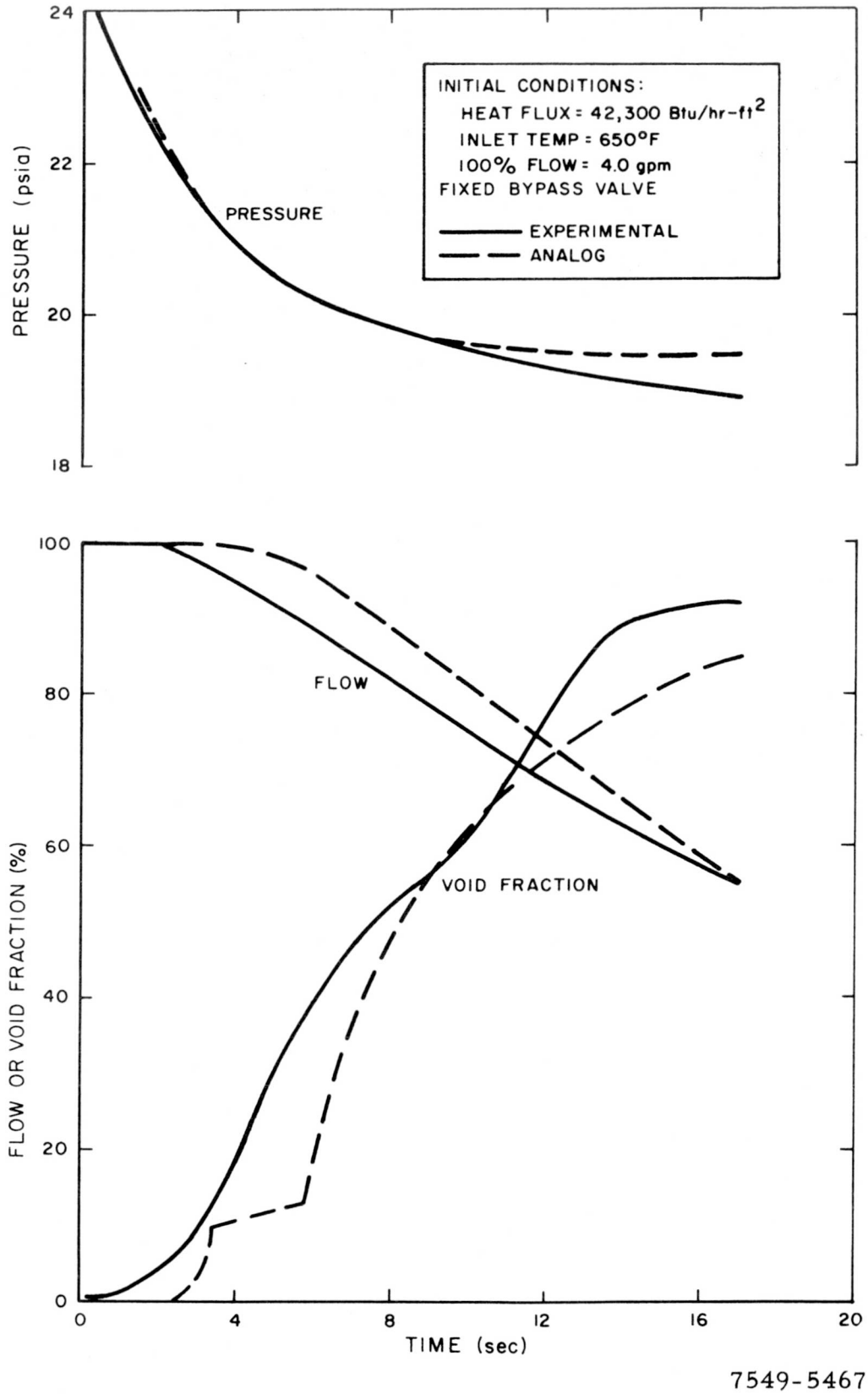

Figure C-15. Pressure Transient No. 15.
Upflow, Uncontrolled Pressure Drop

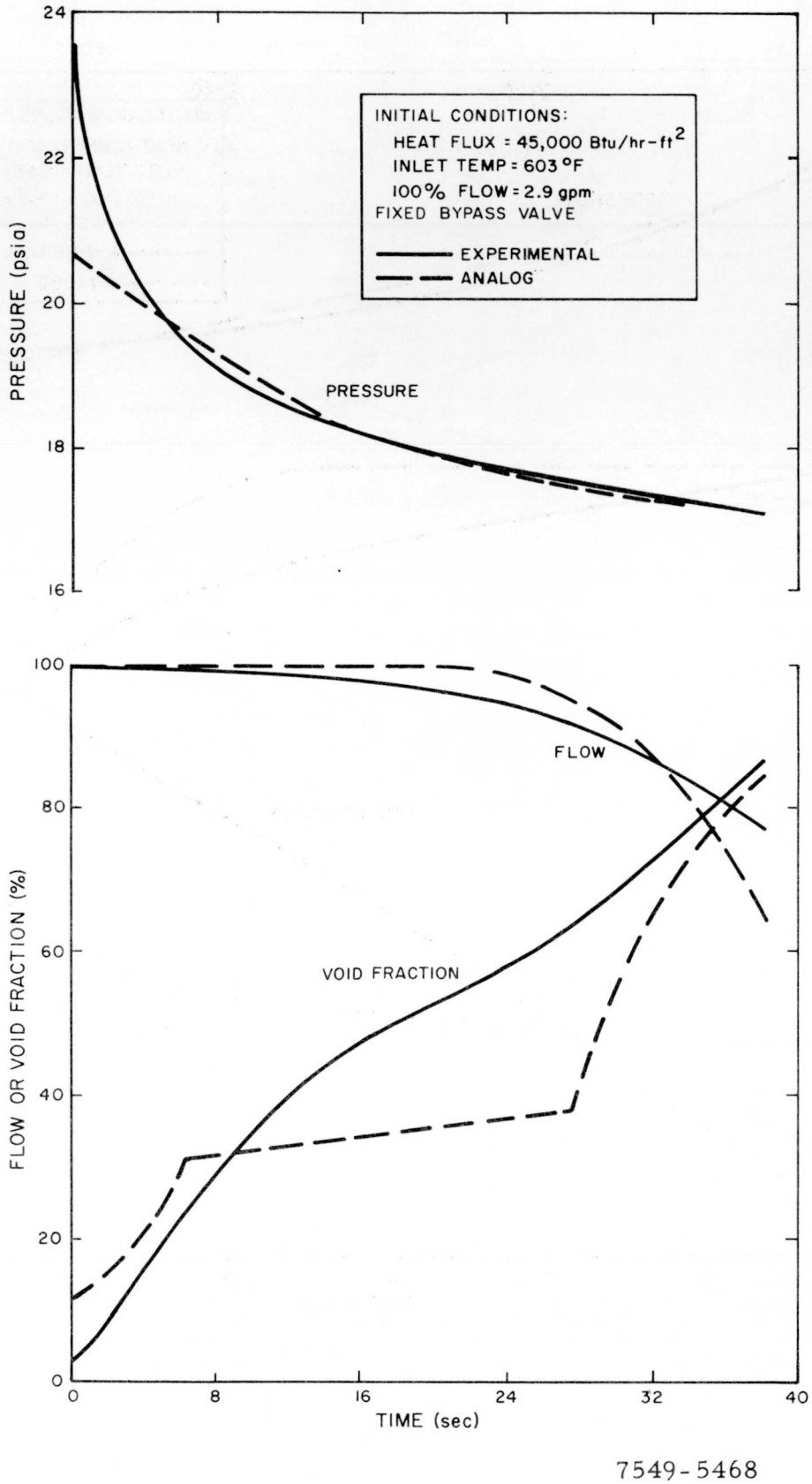

Figure C-16. Pressure Transient No. 16.
Upflow, Uncontrolled Pressure Drop

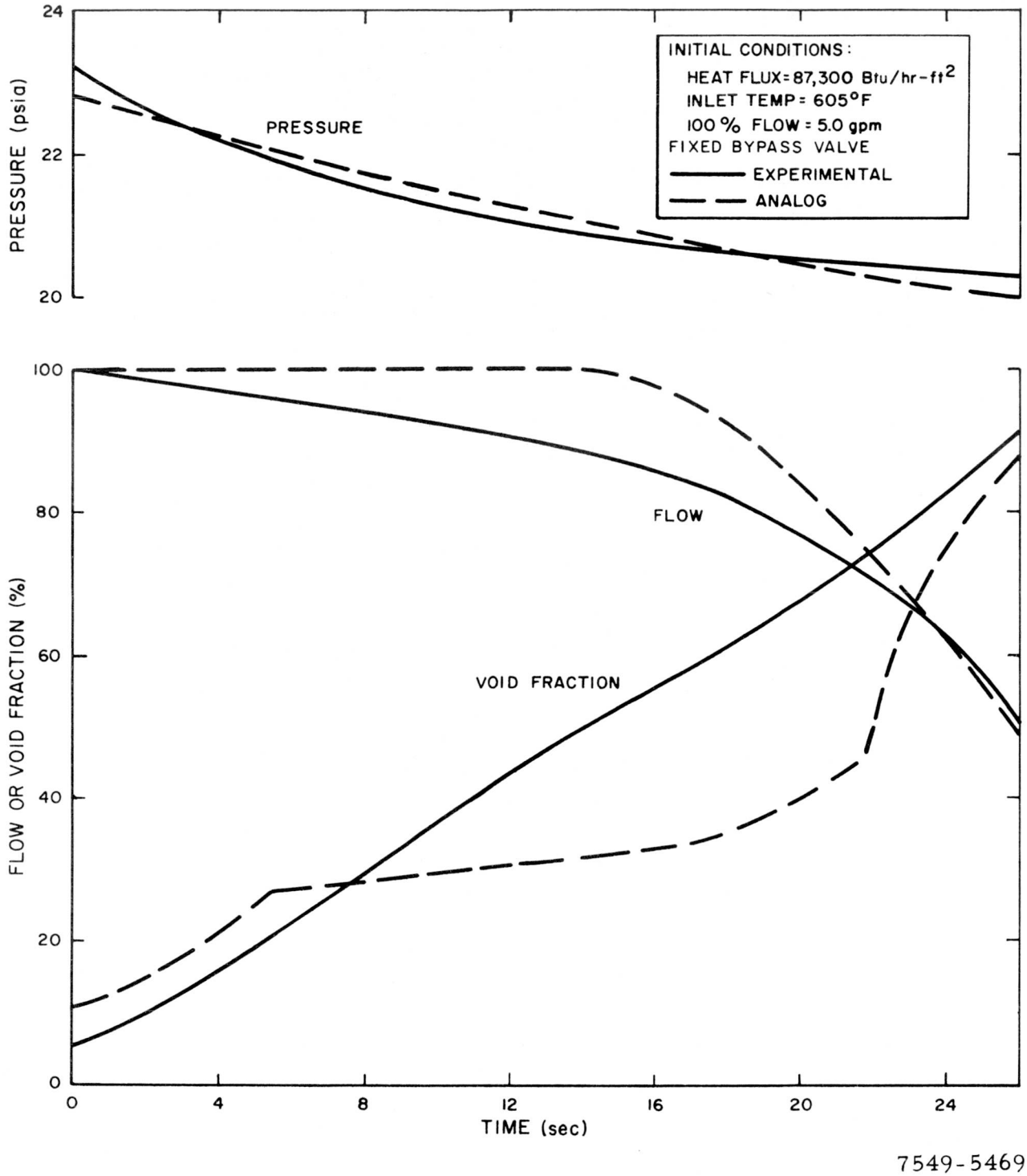

Figure C-17. Pressure Transient No. 17.
Upflow, Uncontrolled Pressure Drop

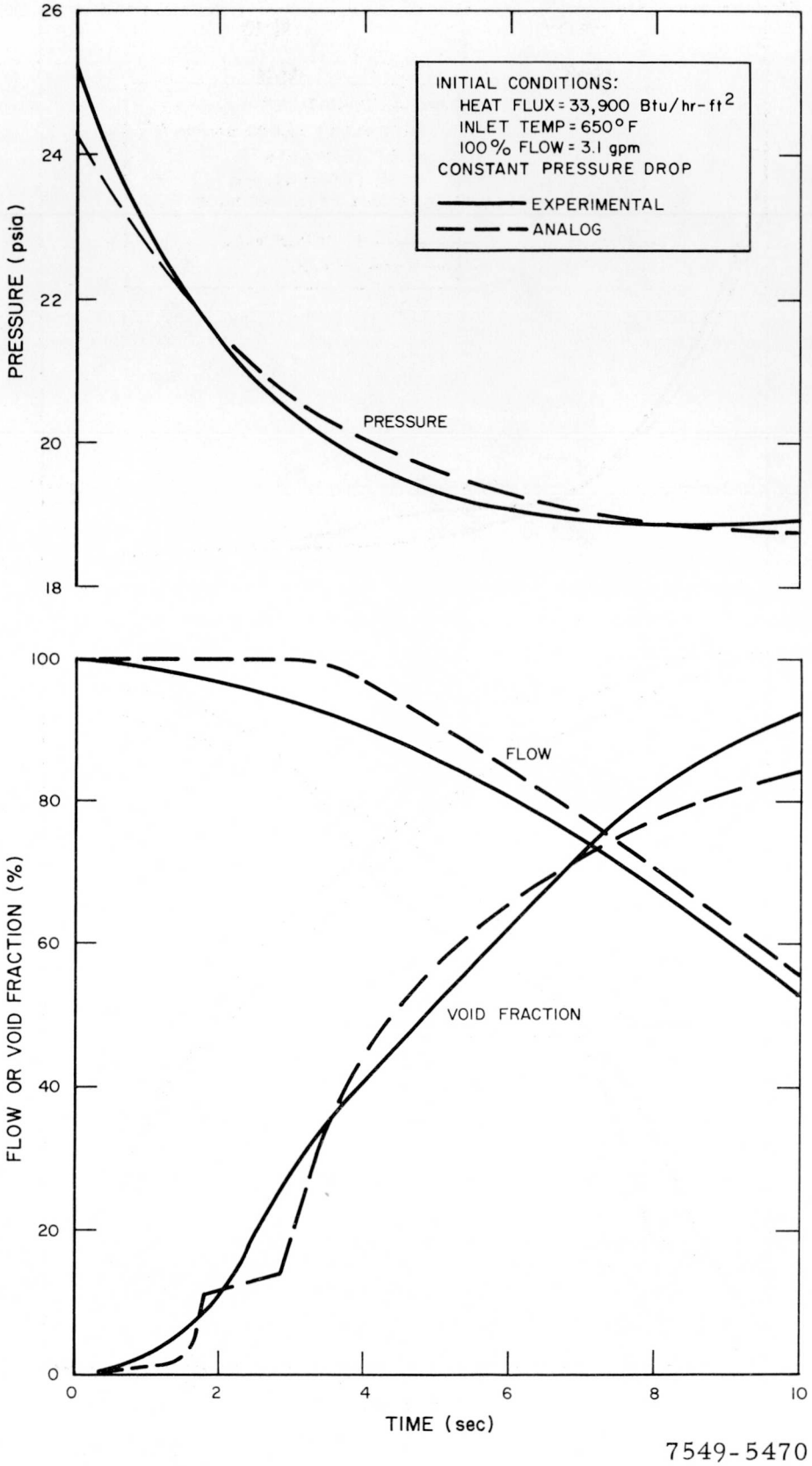

Figure C-18. Pressure Transient No. 18.
Upflow, Constant Pressure Drop

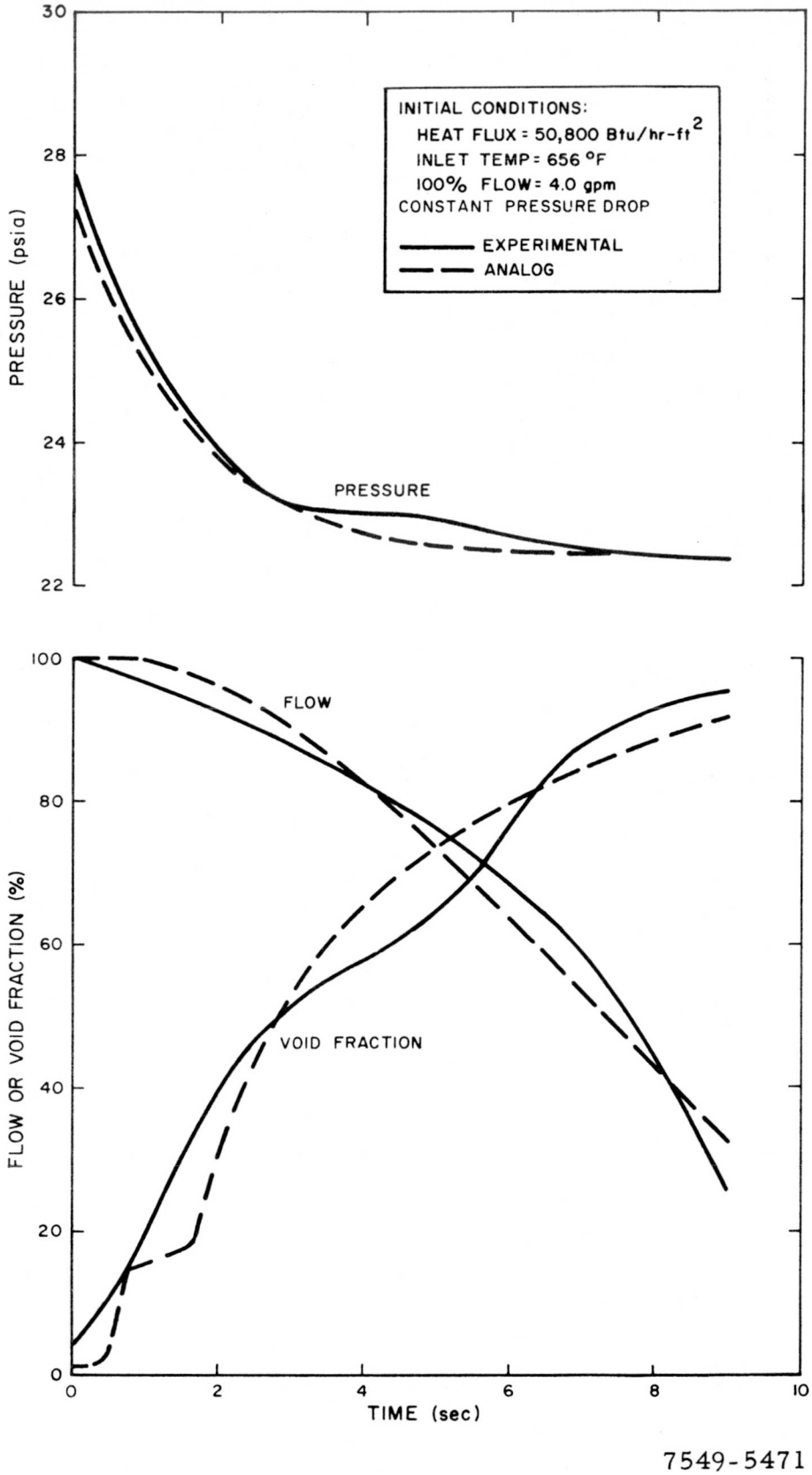

Figure C-19. Pressure Transient No. 19.
Upflow, Constant Pressure Drop

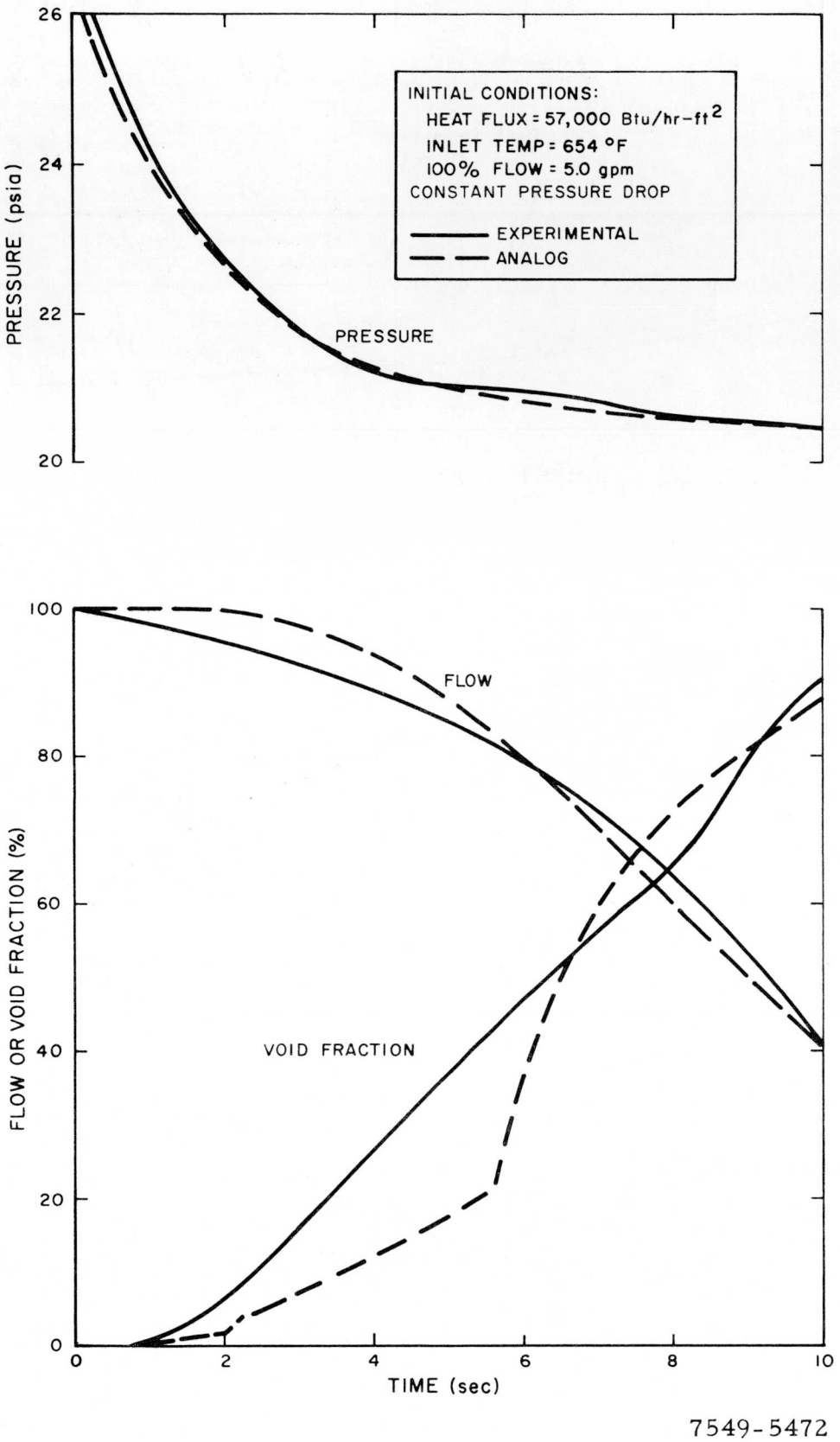

Figure C-20. Pressure Transient No. 20.
Upflow, Constant Pressure Drop

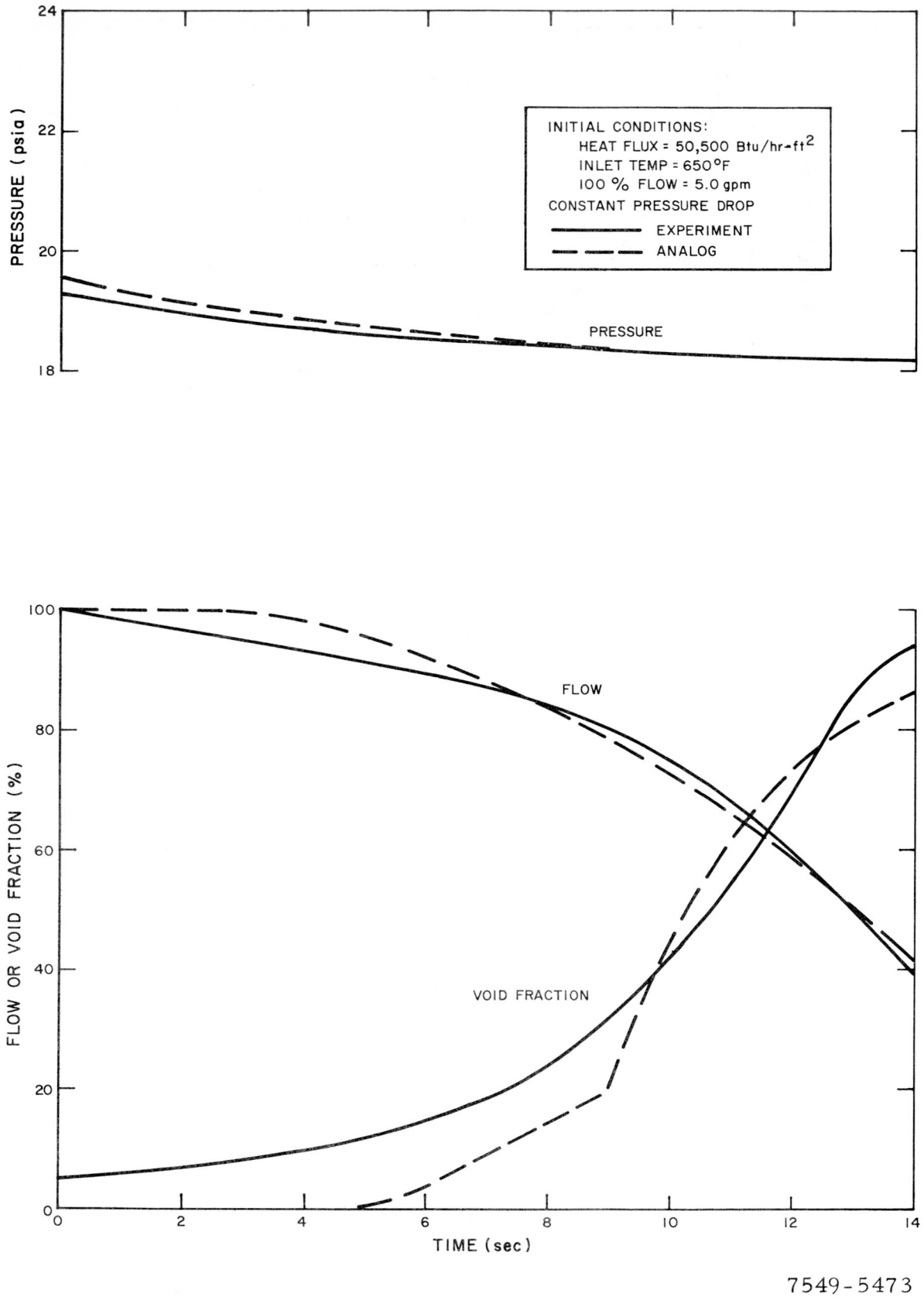

Figure C-21. Pressure Transient No. 21.
Upflow, Constant Pressure Drop

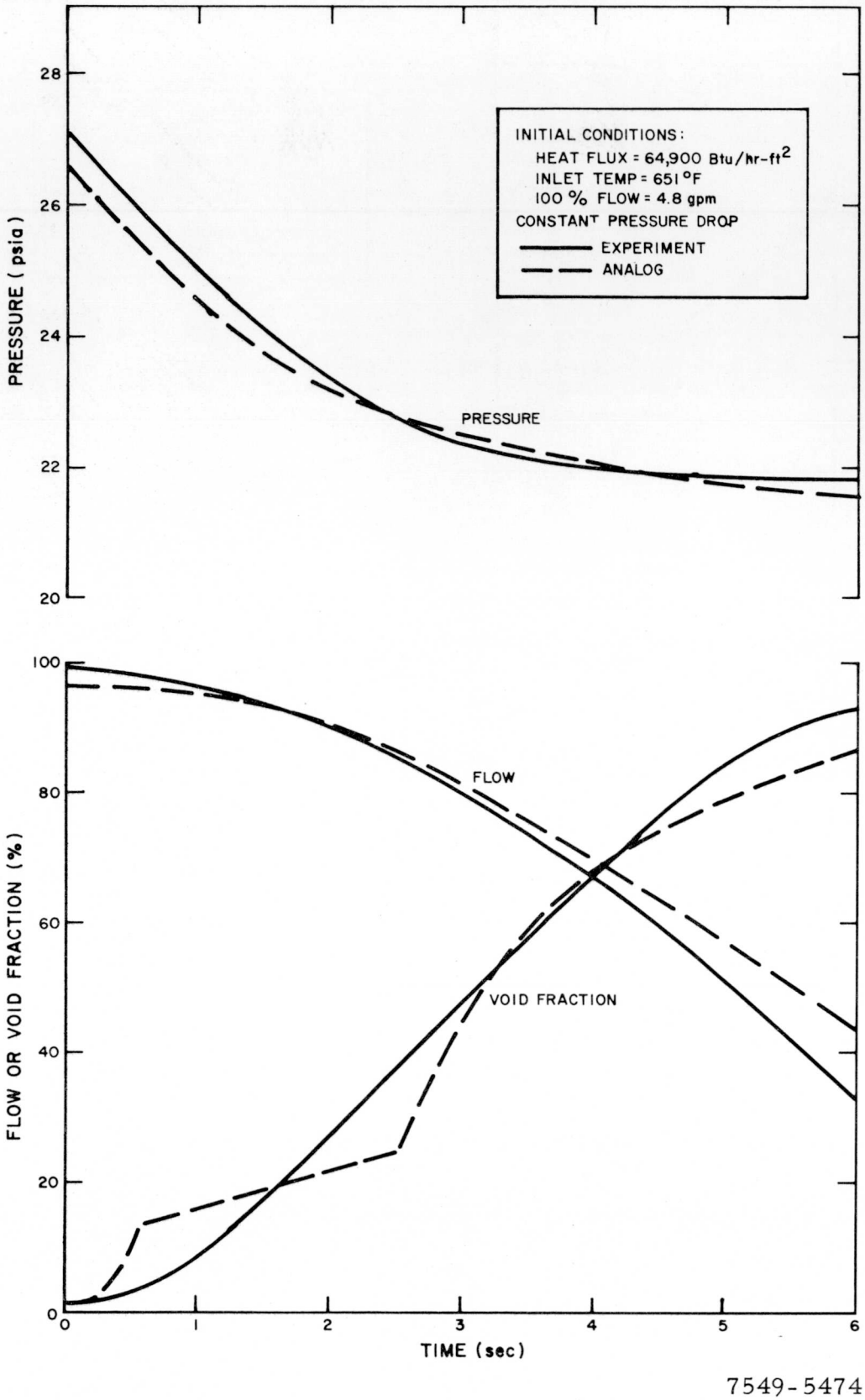

Figure C-22. Pressure Transient No. 22.
Upflow, Constant Pressure Drop

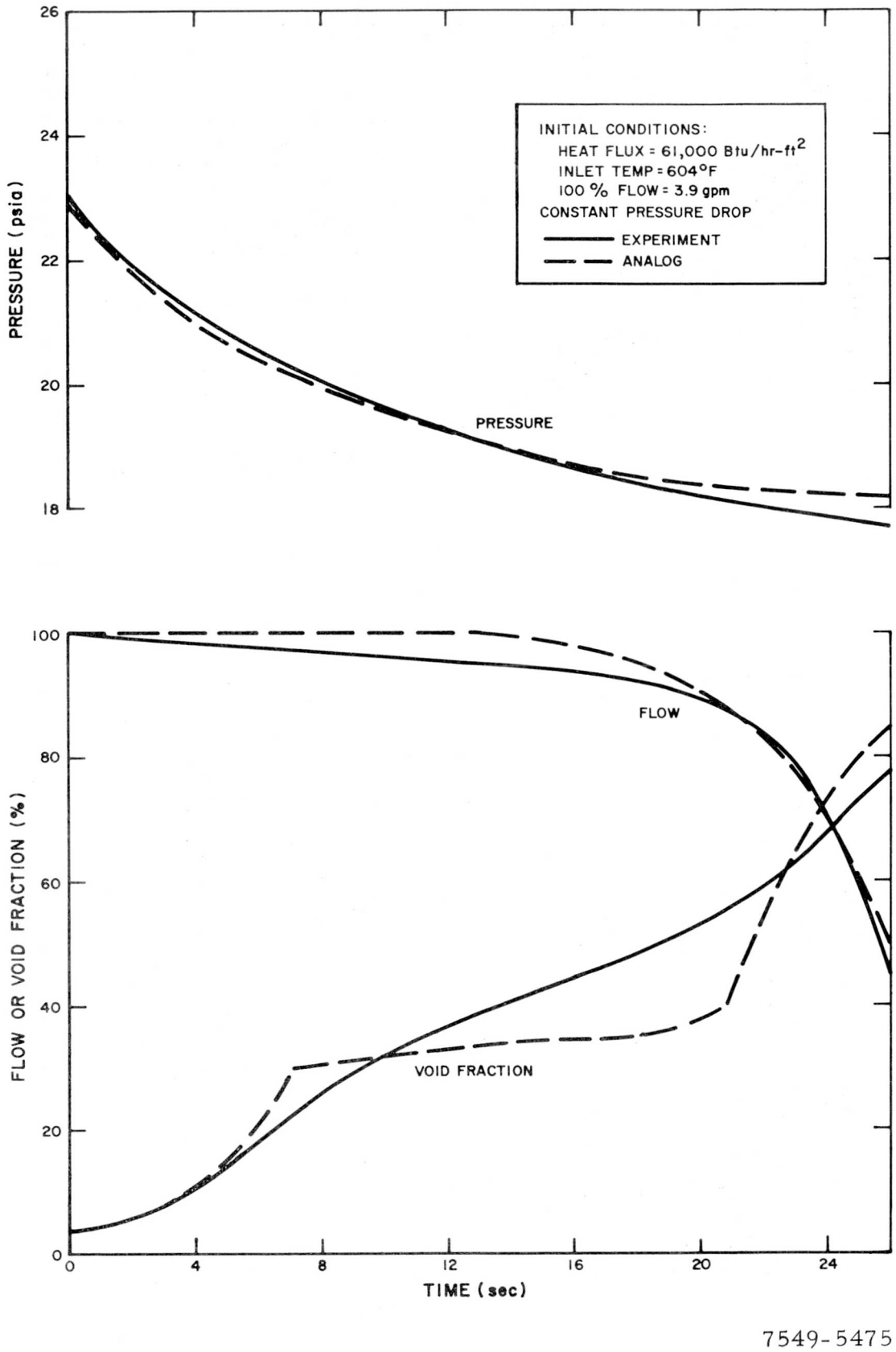

Figure C-23. Pressure Transient No. 23.
Upflow, Constant Pressure Drop

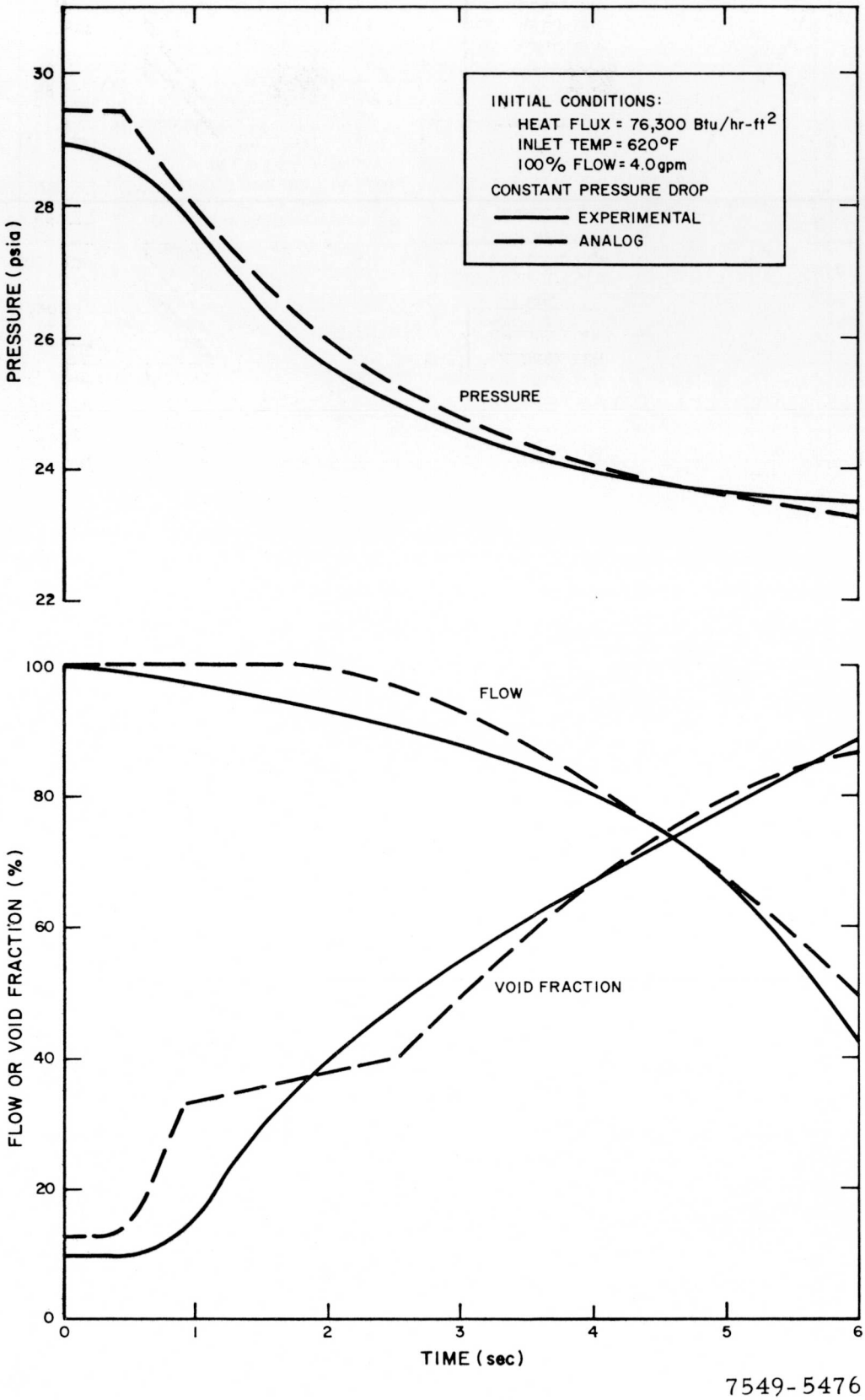

Figure C-24. Pressure Transient No. 24.
Upflow, Constant Pressure Drop

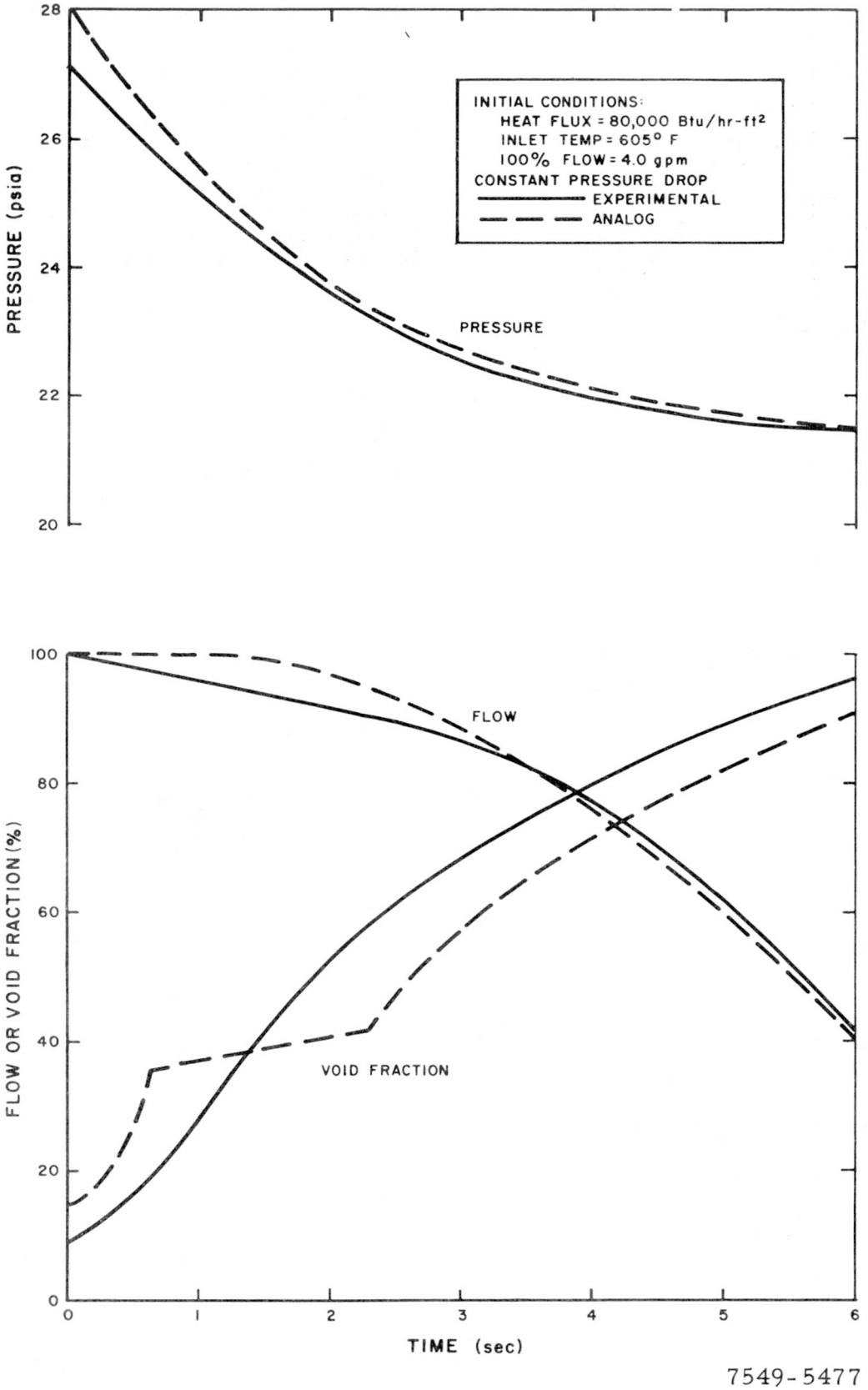

Figure C-25. Pressure Transient No. 25.
Upflow, Constant Pressure Drop

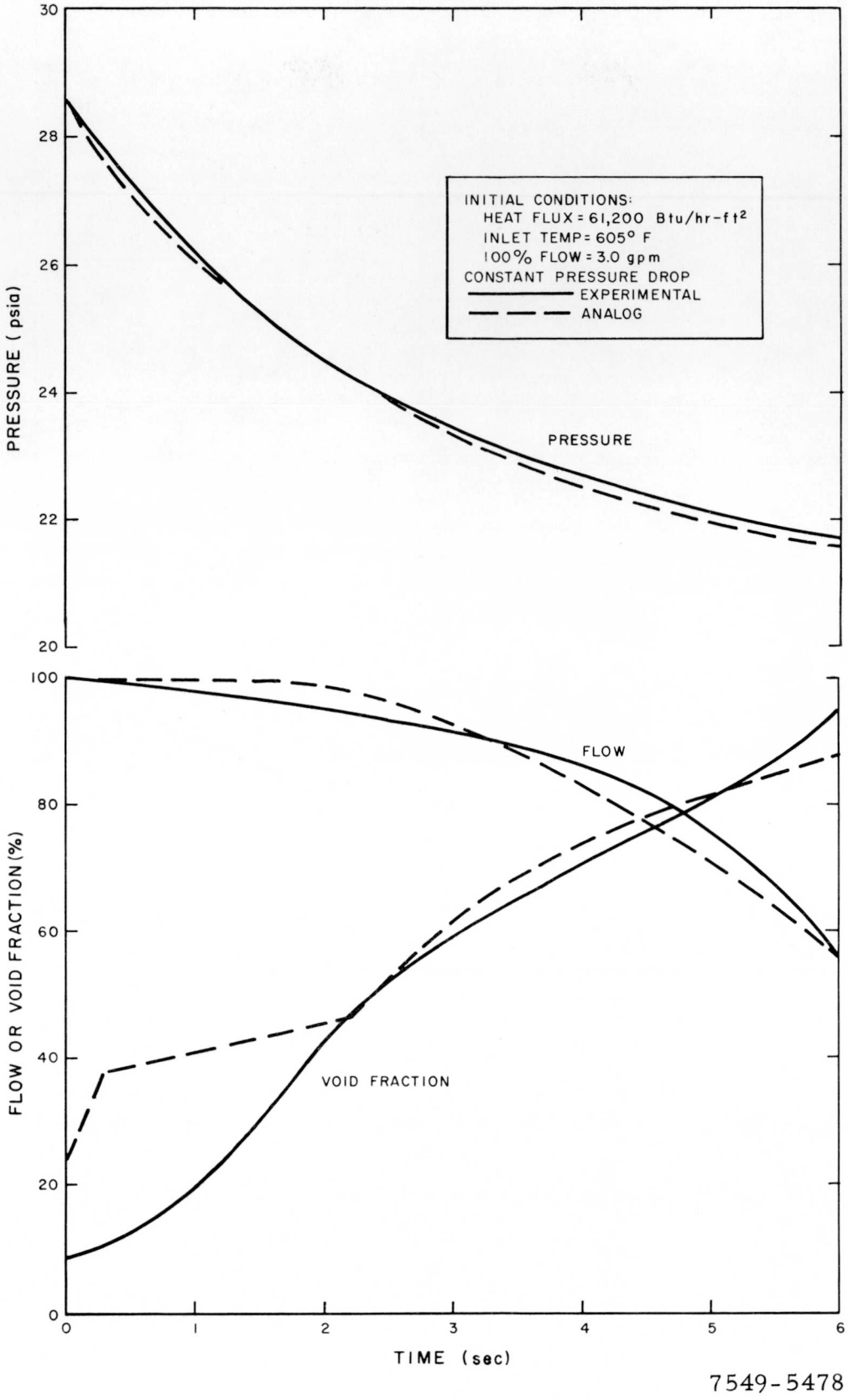

Figure C-26. Pressure Transient No. 26.
Upflow, Constant Pressure Drop

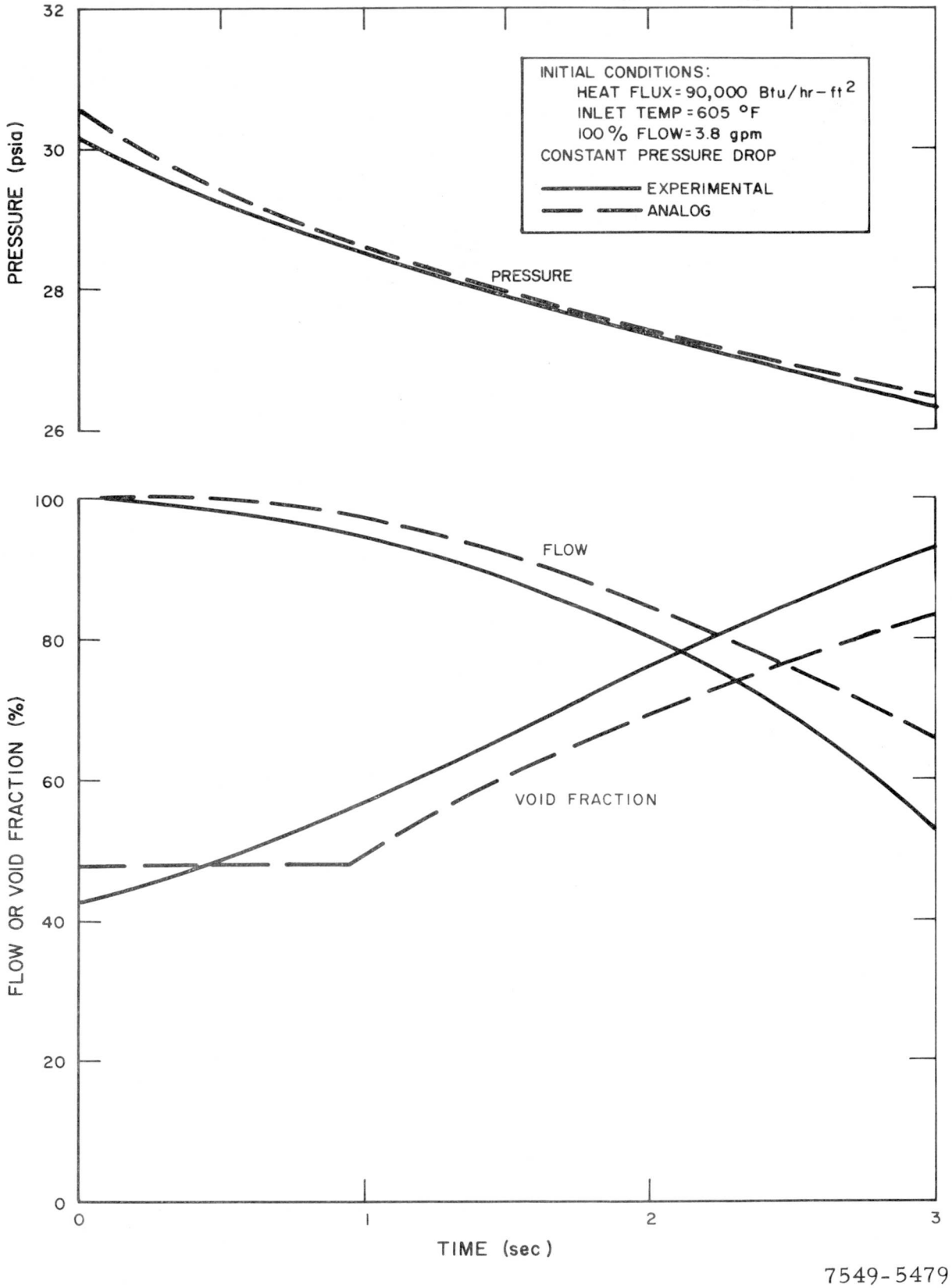

Figure C-27. Pressure Transient No. 27.
Upflow, Constant Pressure Drop

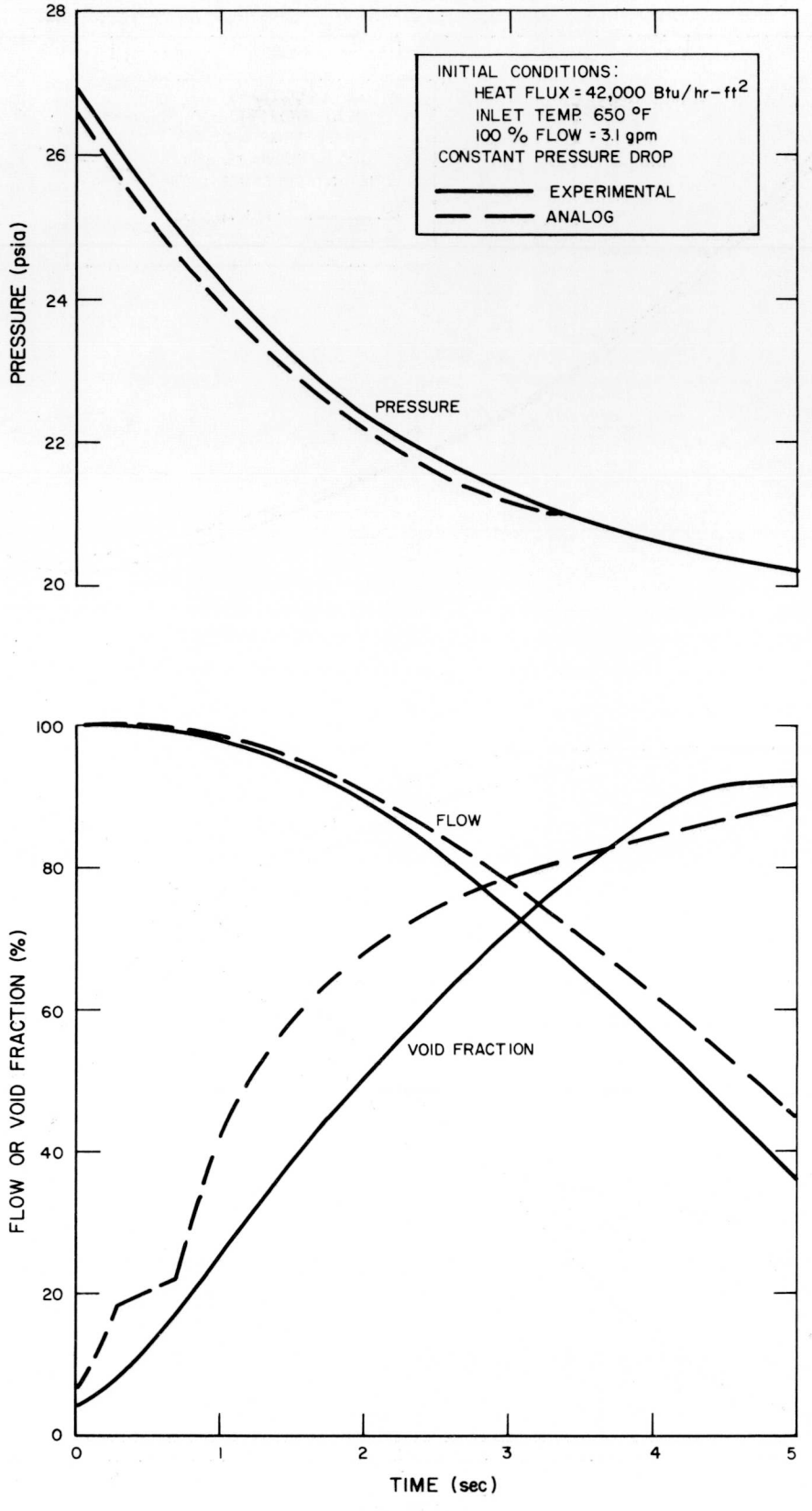

Figure C-28. Pressure Transient No. 28.
Upflow, Constant Pressure Drop

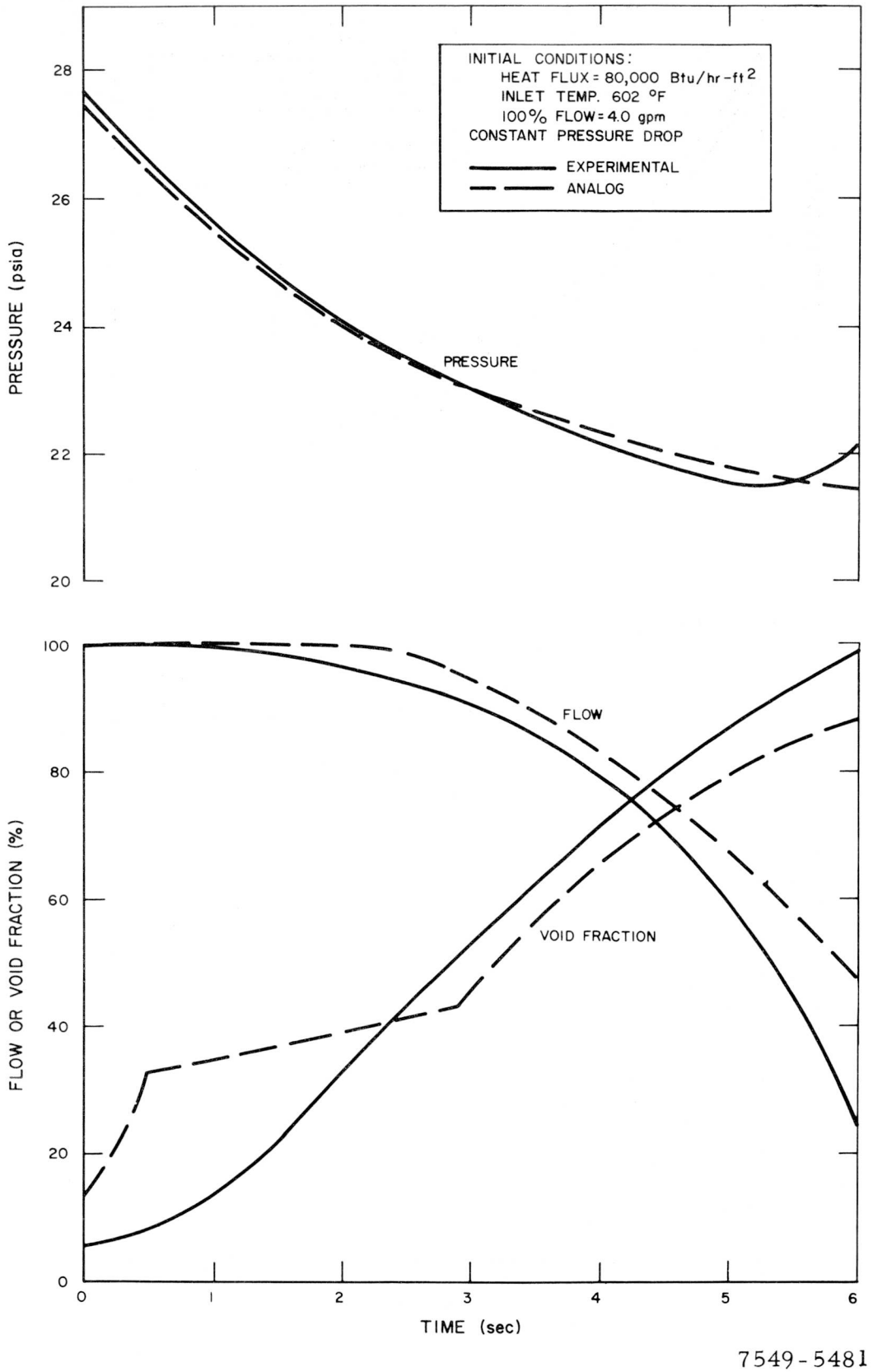

Figure C-29. Pressure Transient No. 29.
Upflow, Constant Pressure Drop

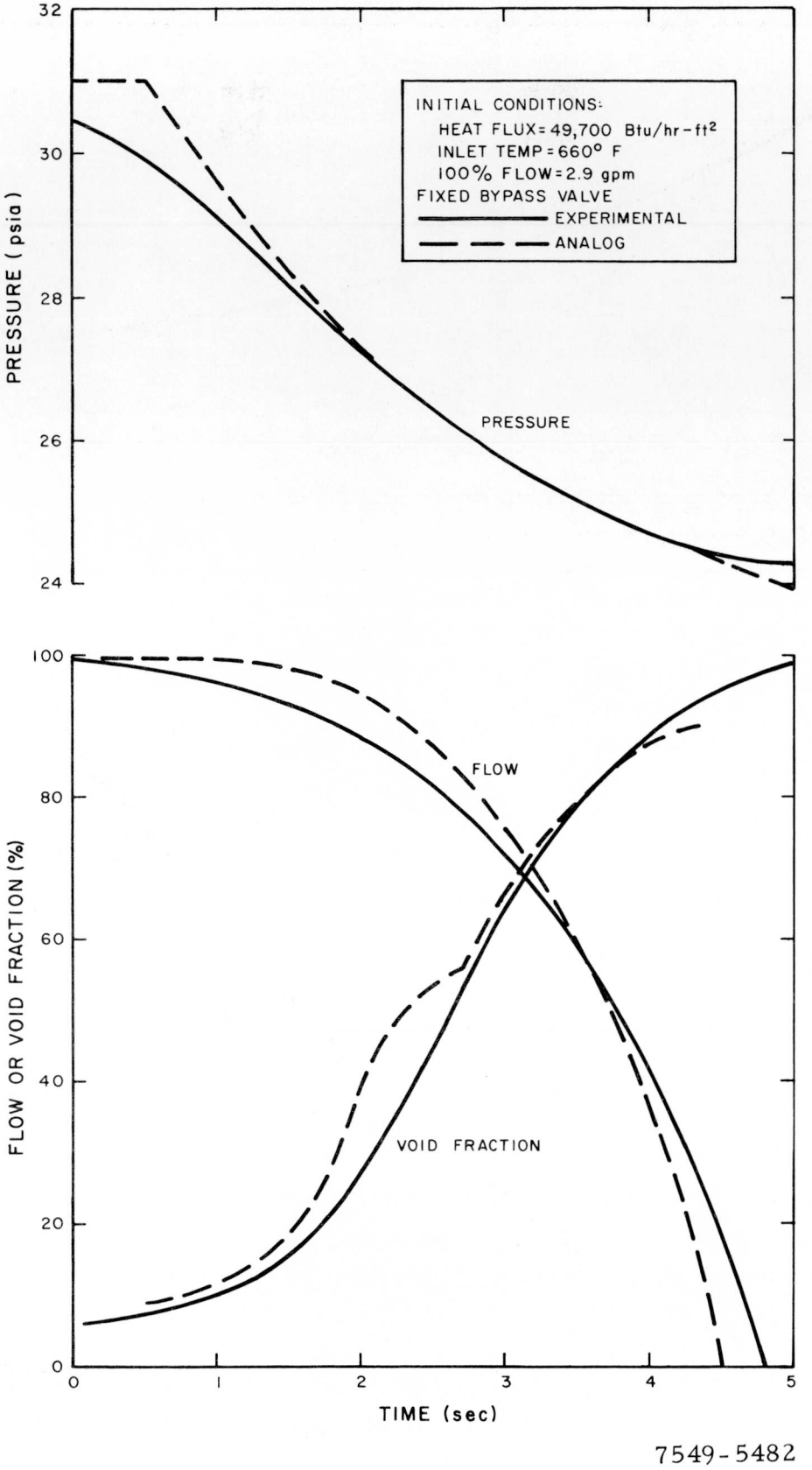

Figure C-30. Pressure Transient No. 30.
Downflow, Uncontrolled Pressure Drop

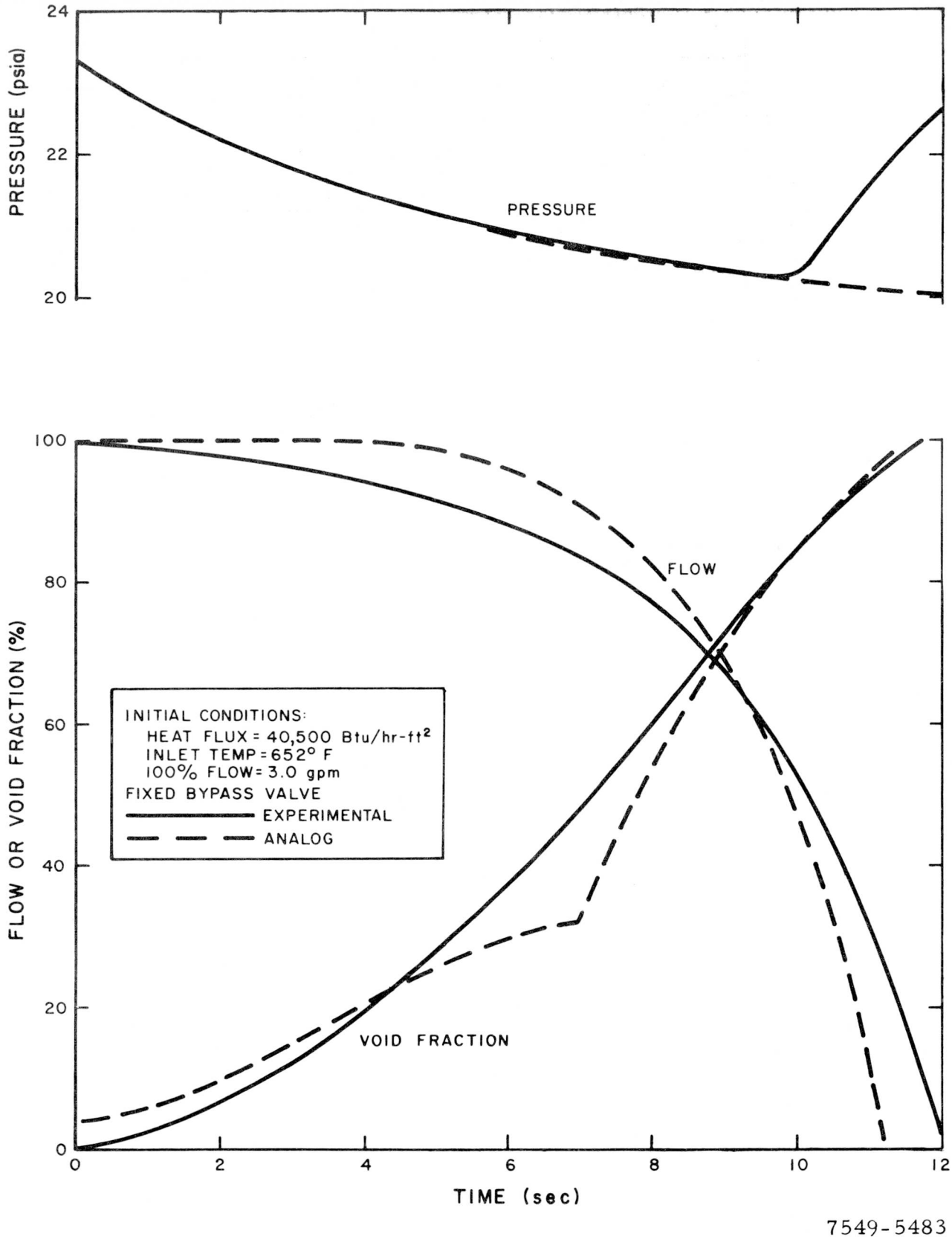

Figure C-31. Pressure Transient No. 31.
Downflow, Uncontrolled Pressure Drop

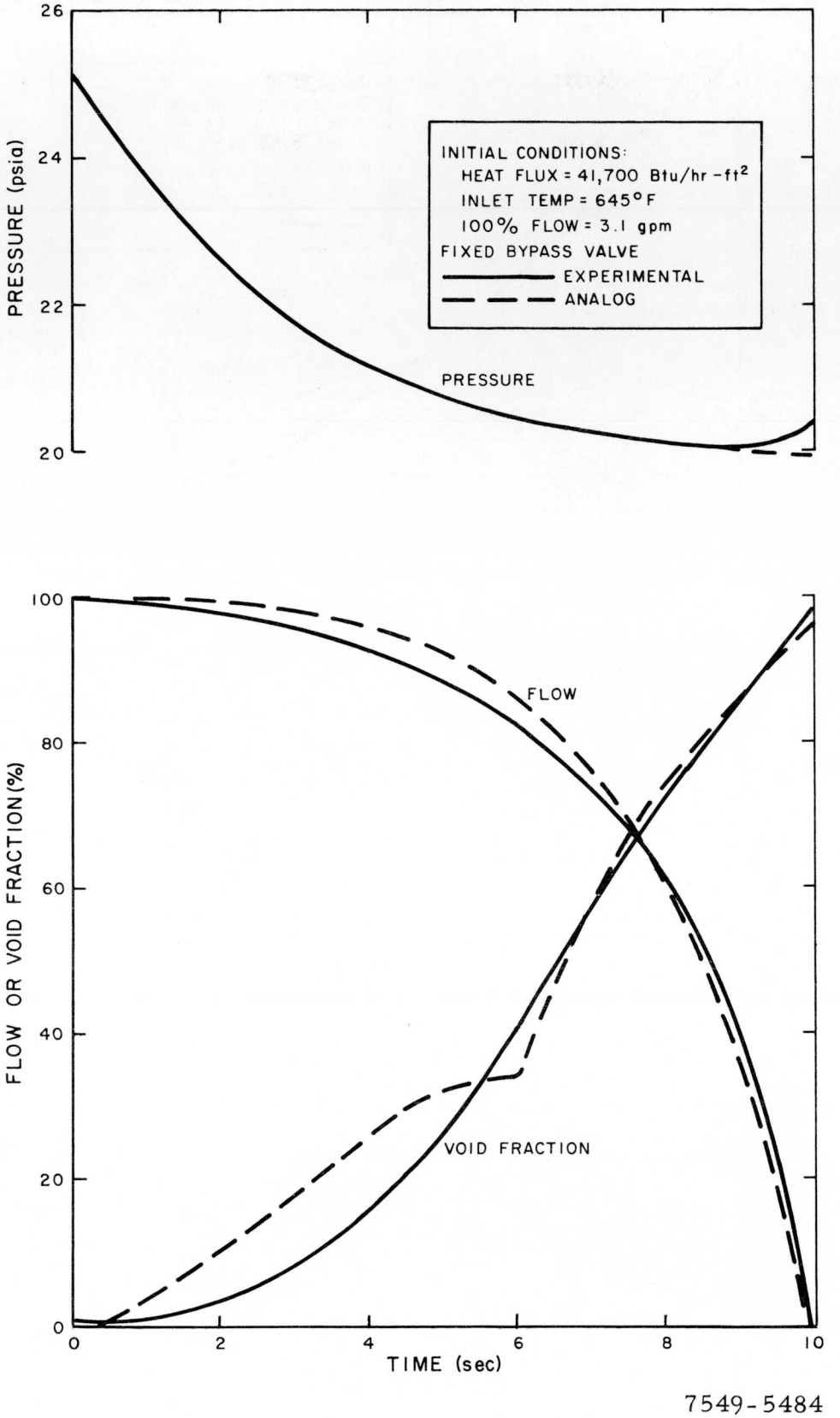

Figure C-32. Pressure Transient No. 32.
Downflow, Uncontrolled Pressure Drop

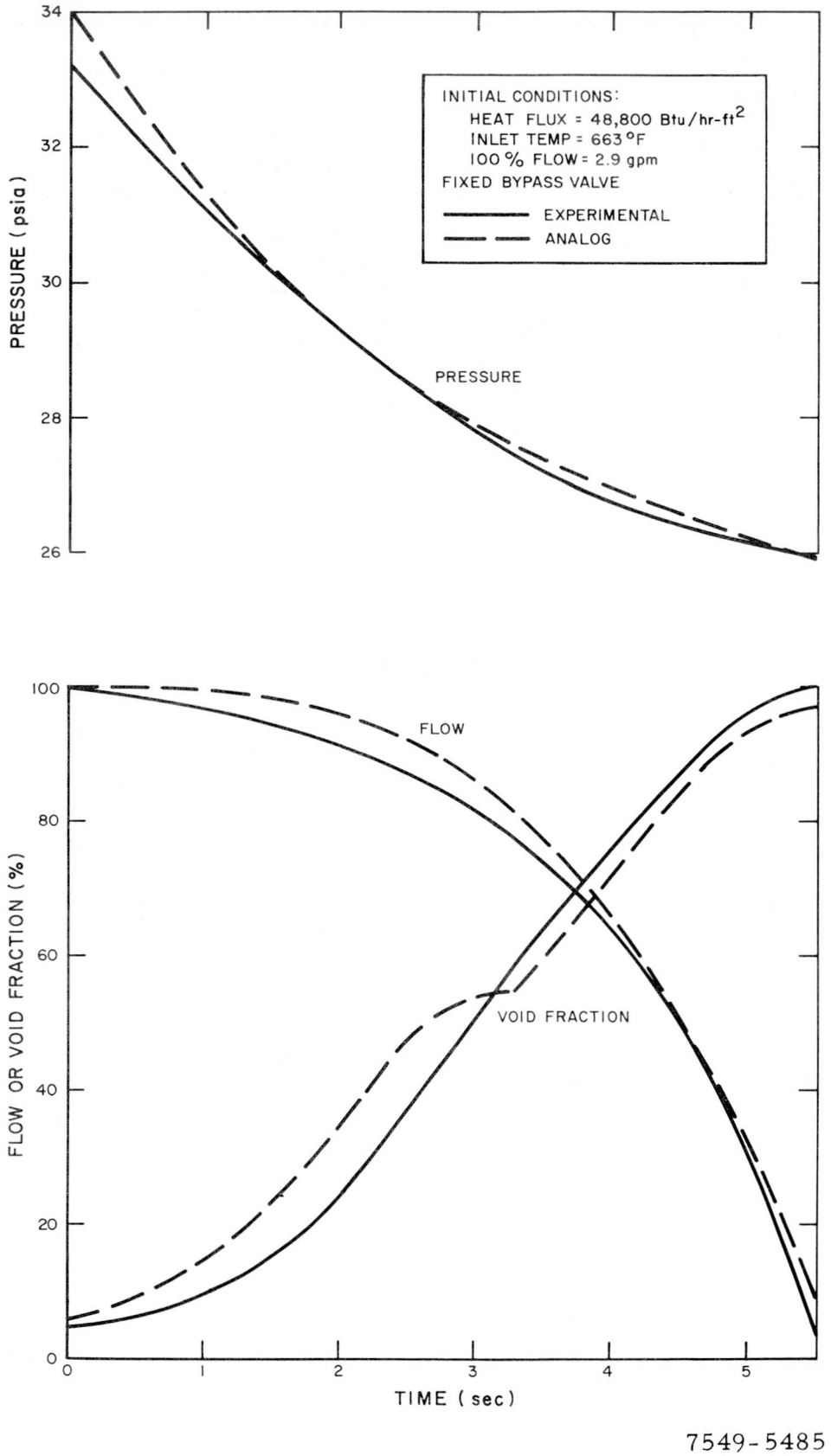

Figure C-33. Pressure Transient No. 33.
Downflow, Uncontrolled Pressure Drop

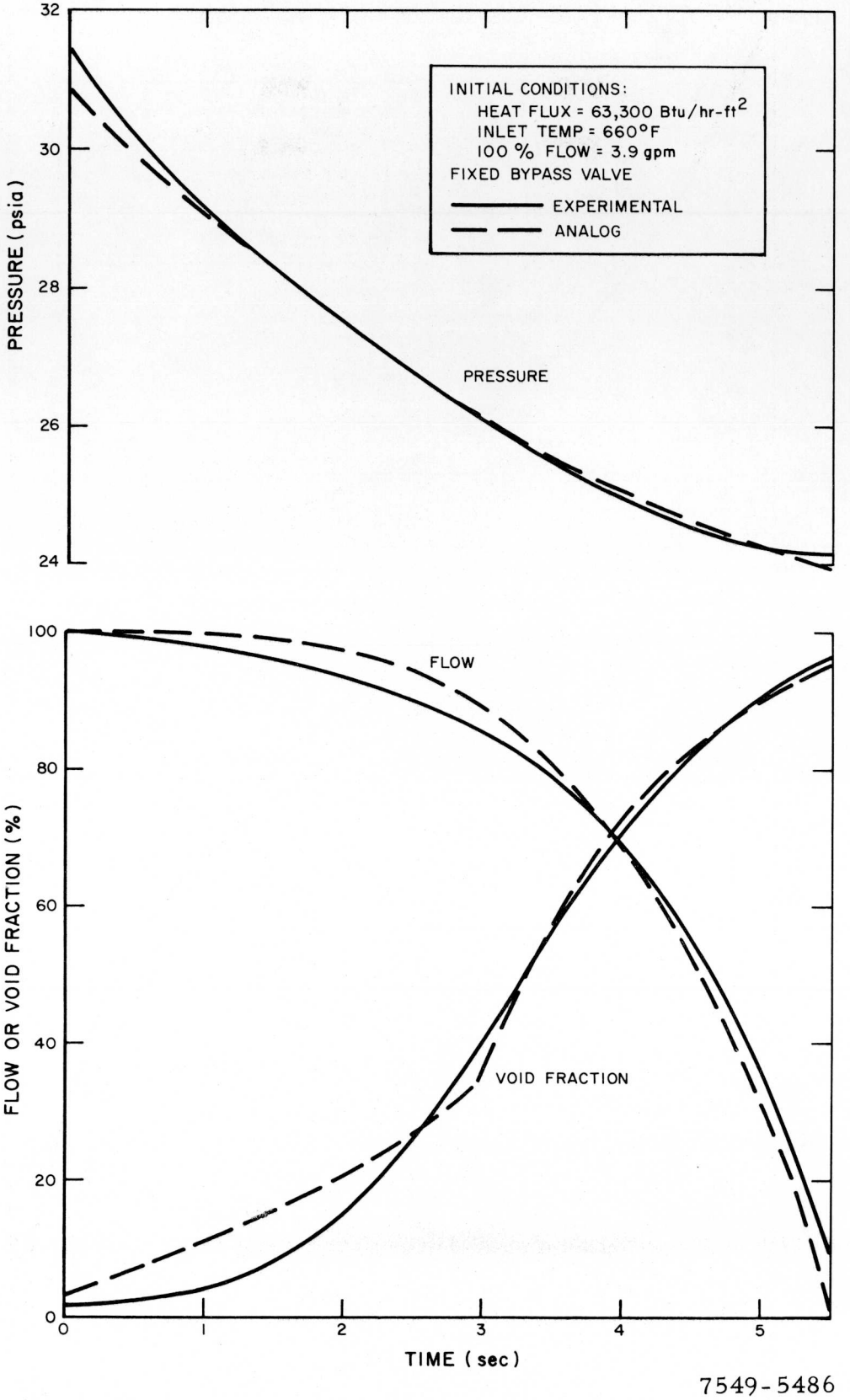

Figure C-34. Pressure Transient No. 34.
Downflow, Uncontrolled Pressure Drop

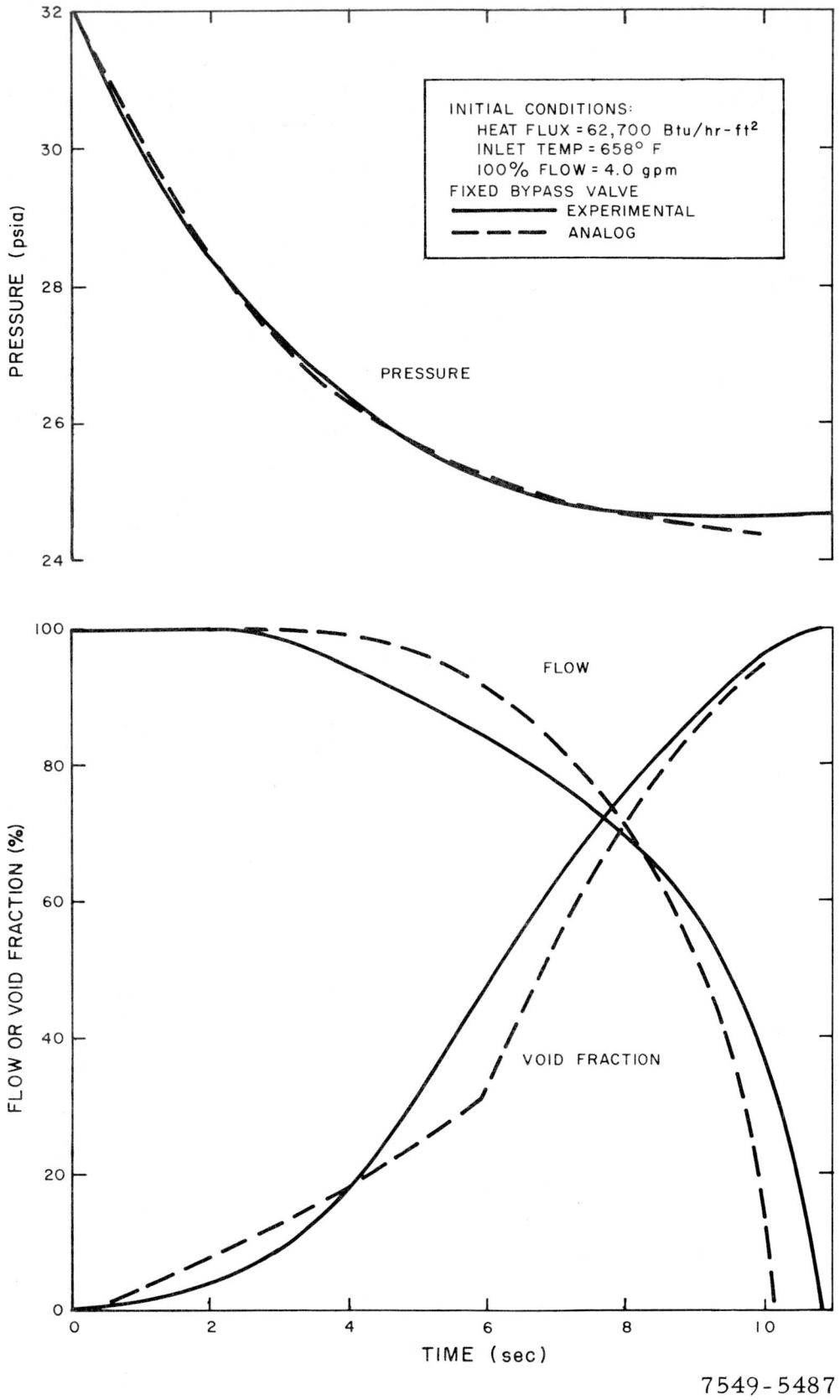

Figure C-35. Pressure Transient No. 35.
Downflow, Uncontrolled Pressure Drop

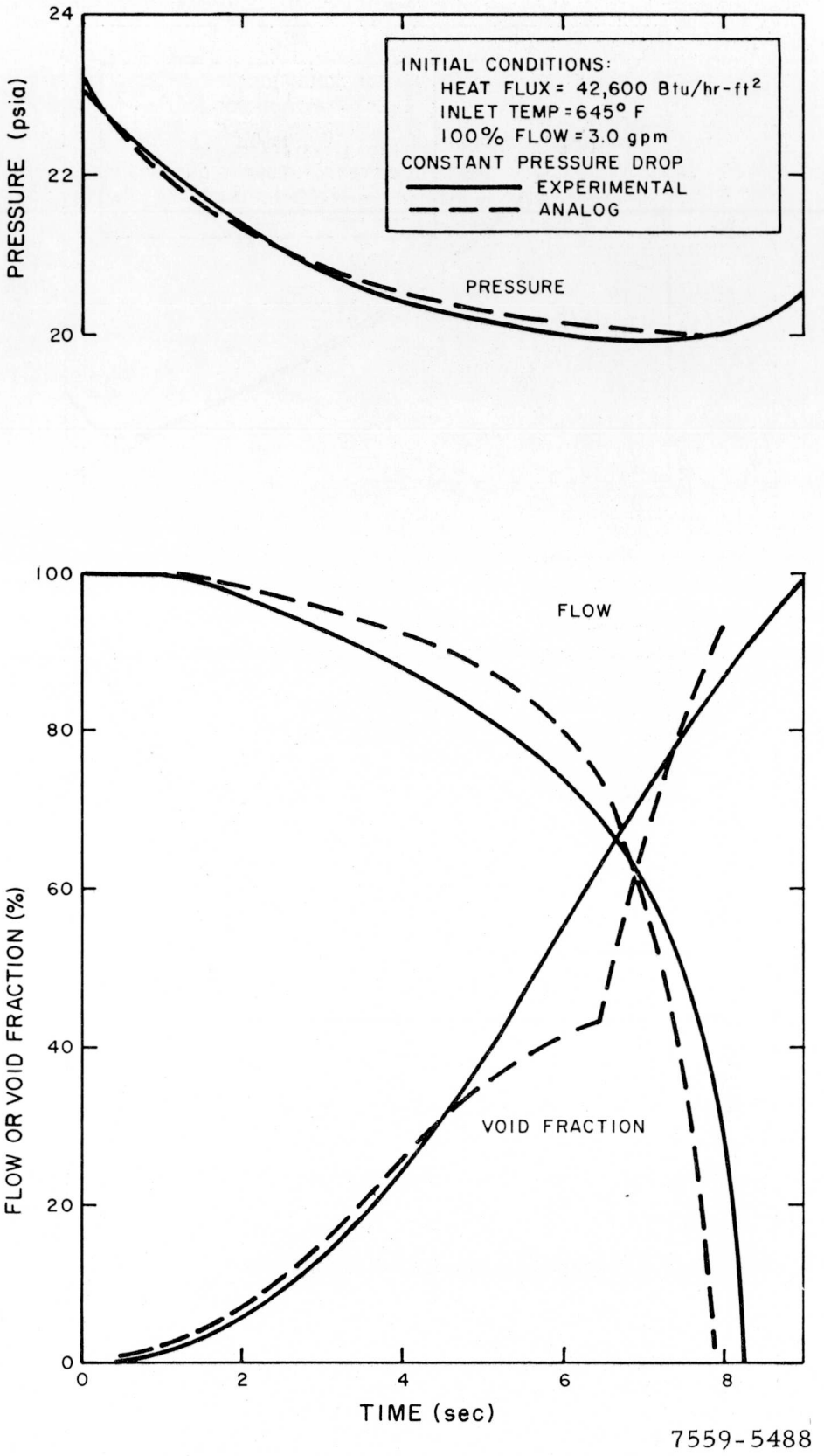

Figure C-36. Pressure Transient No. 36.
Downflow, Constant Pressure Drop

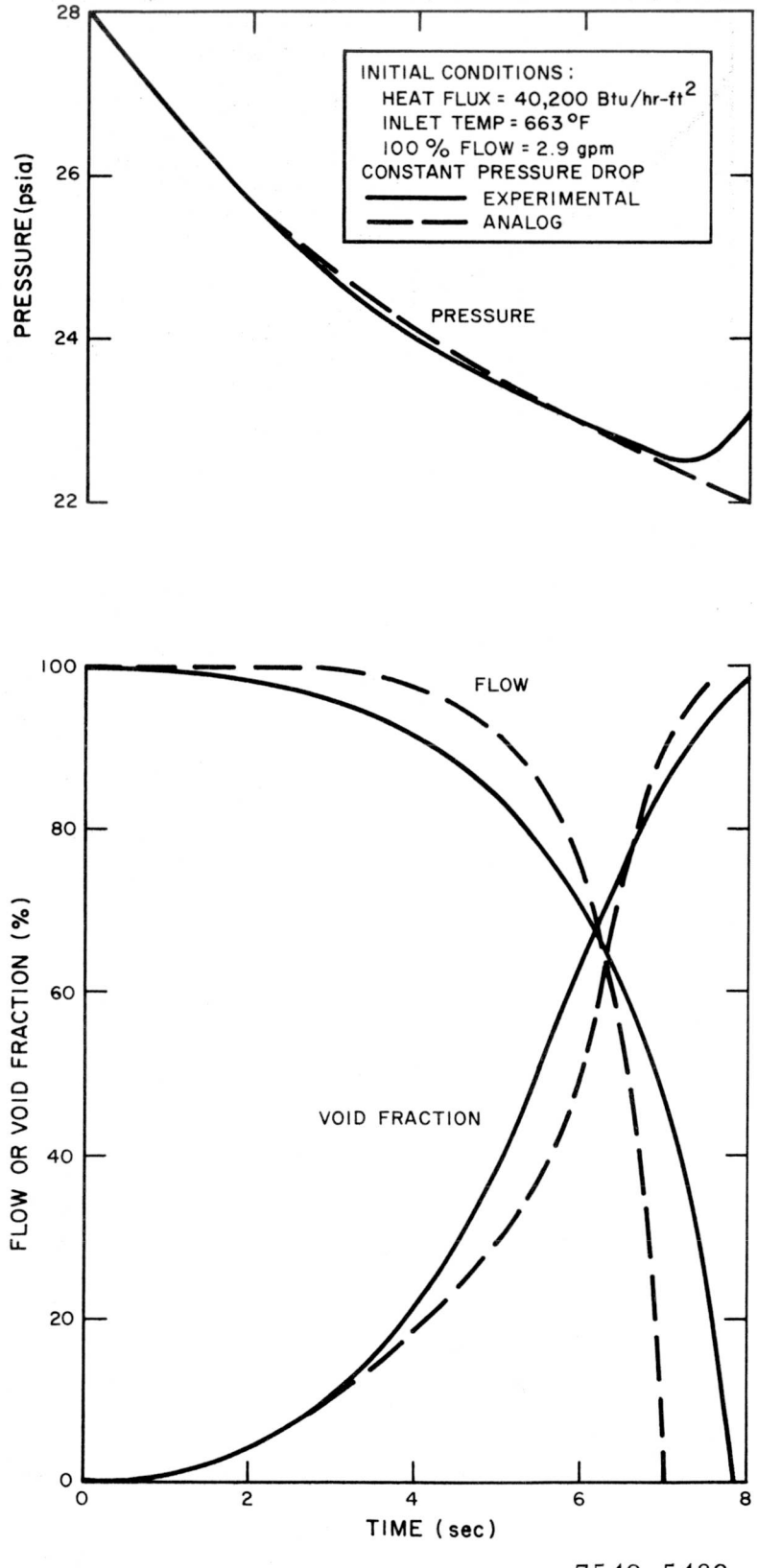

Figure C-37. Pressure Transient No. 37. Downflow, Constant Pressure Drop

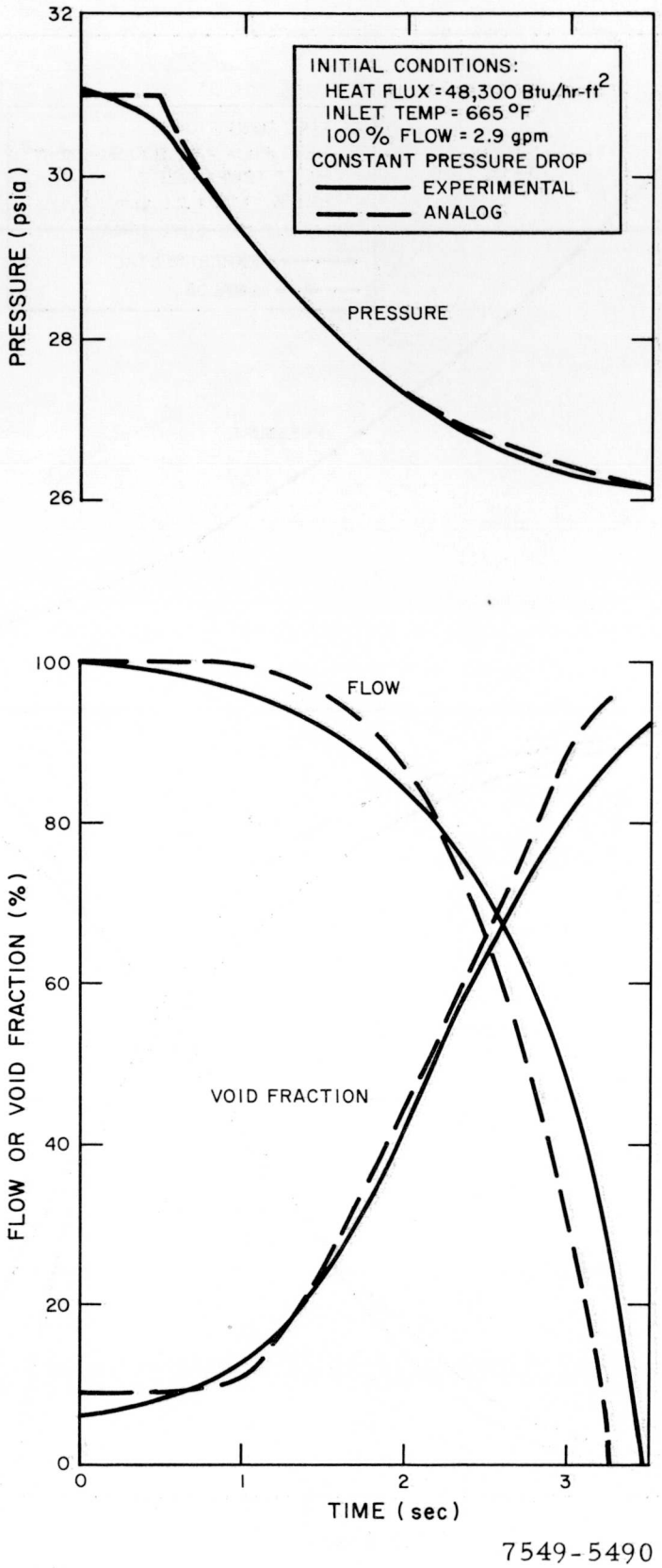

Figure C-38. Pressure Transient No. 38. Downflow, Constant Pressure Drop

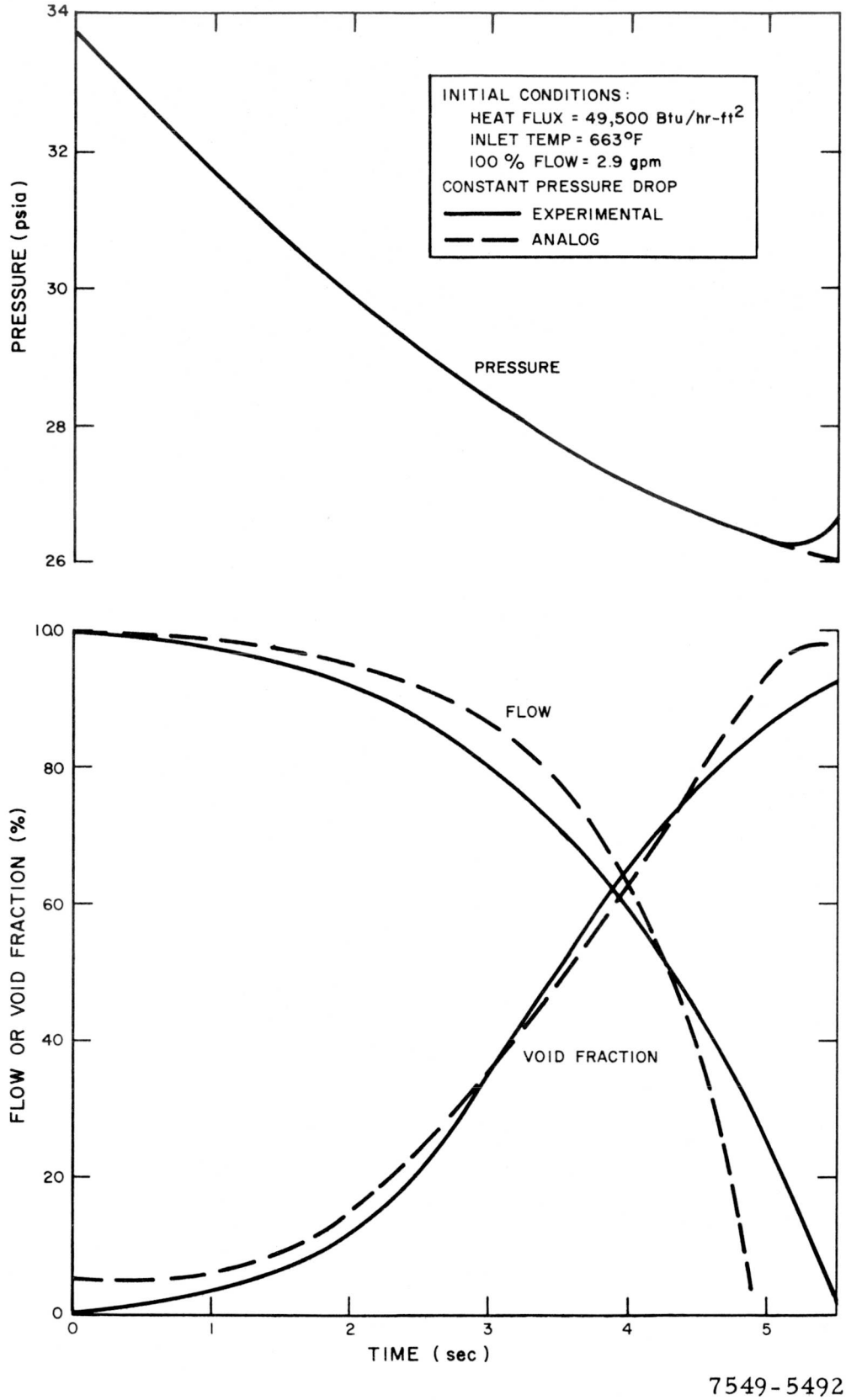

Figure C-39. Pressure Transient No. 39.
Downflow, Constant Pressure Drop

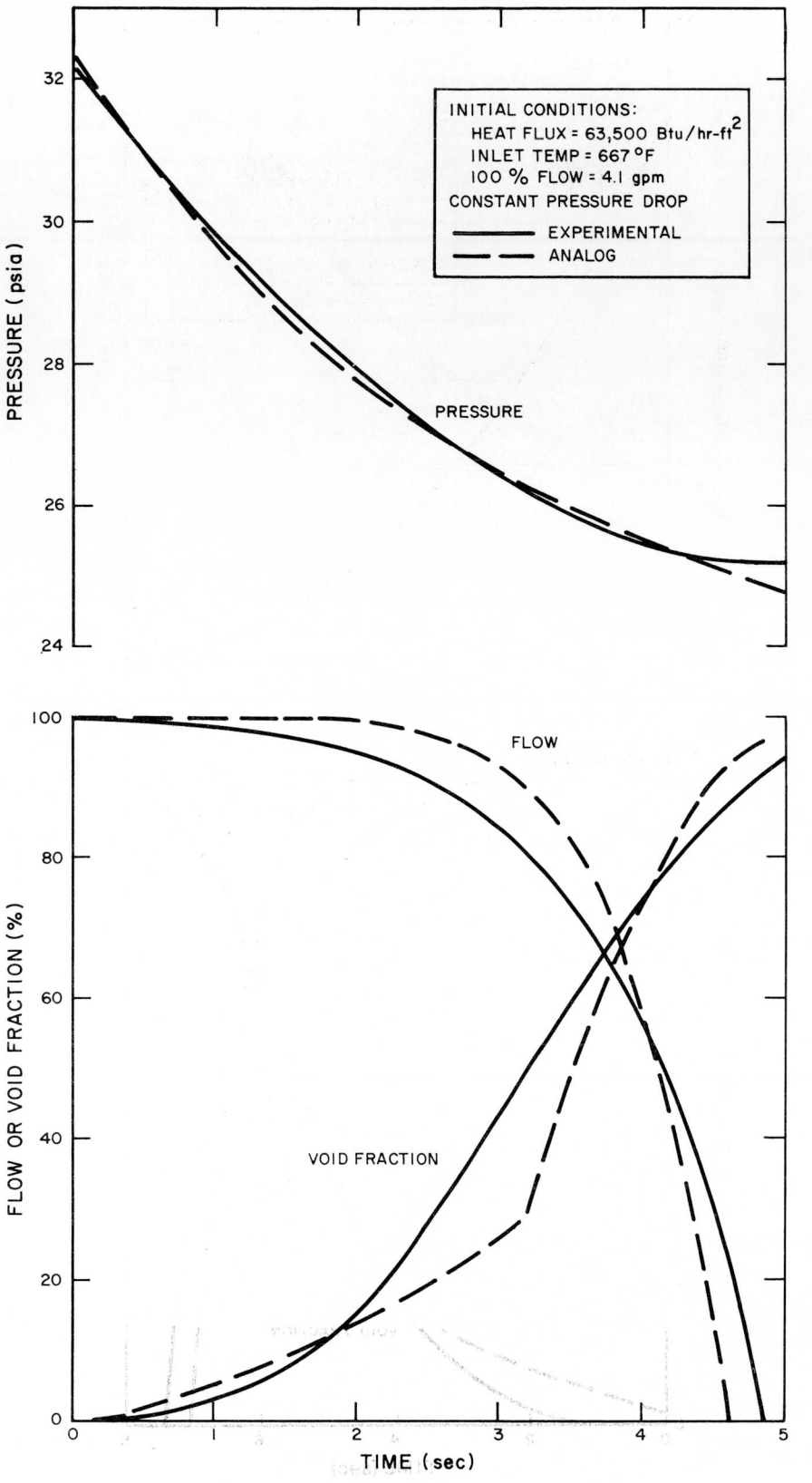

Figure C-40. Pressure Transient No. 40. Downflow, Constant Pressure Drop

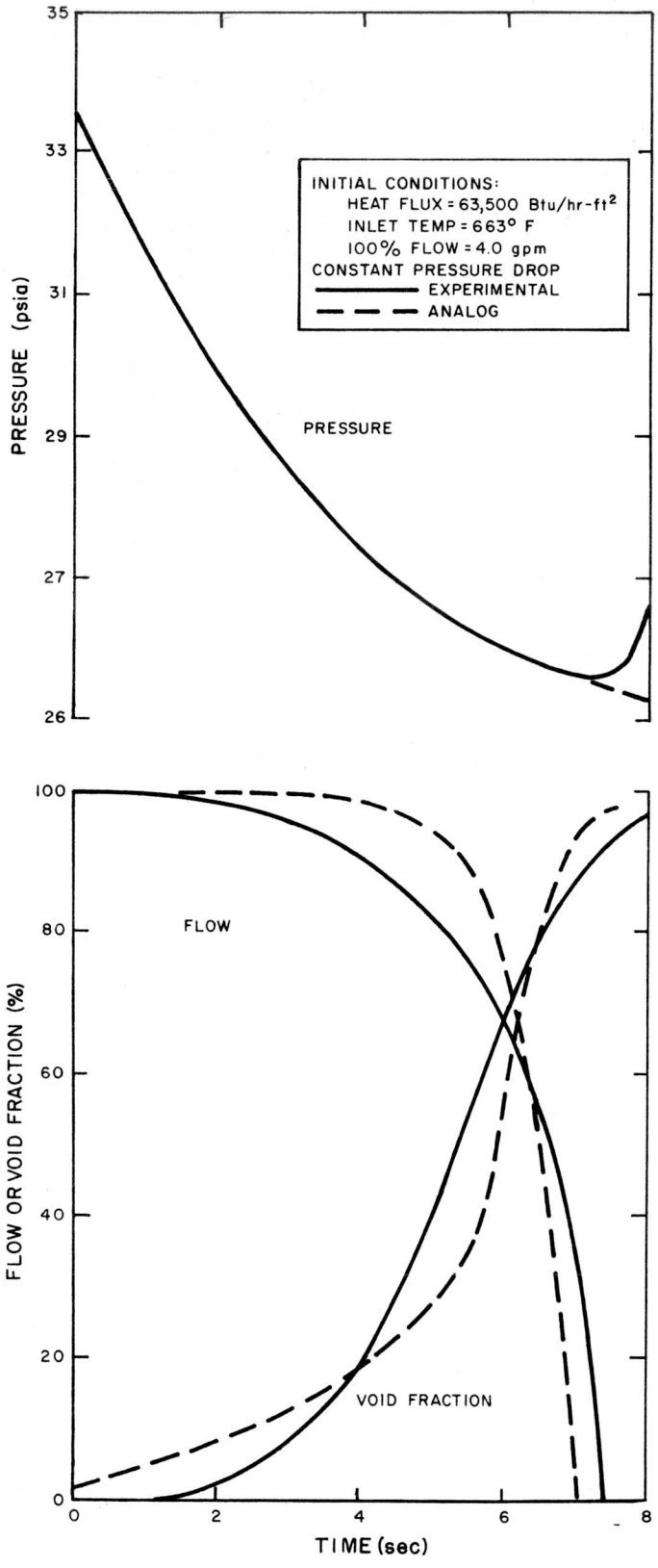

Figure C-41. Pressure Transient No. 41. Downflow, Constant Pressure Drop